Electronic Supplementary Material (ESI) for Polymer Chemistry.

Supporting Information for:

Post-polymerization 'click' end-capping of polyglyoxylate self-immolative polymers

Peter G. Maschmeyer,[a] Xiaoli Liang,[b] Allison Hung,[b] Oksana Ahmadzai,[a] Annmaree L. Kenny,[a] Yuan C. Luong,[a] Timothy N. Forder,[a] Haoxiang Zeng,[a] Elizabeth R. Gillies,*[b,c] Derrick A. Roberts*[a,d]

[a]Key Centre for Polymers and Colloids, School of Chemistry, The University of Sydney, Sydney NSW 2006, Australia

[b]Department of Chemistry and the Centre for Advanced Materials and Biomaterials Research, 1151 Richmond St., London, Canada, N6A 5B7

[c]Department of Chemical and Biochemical Engineering, The University of Western Ontario, 1151 Richmond St., London, Canada N6A 5B9

[d]Sydney Nano Institute, The University of Sydney, Sydney NSW 2006, Australia

*E-mails: egillie@uwo.ca, derrick.roberts@sydney.edu.au

Table of Contents

S1. Materials and Methods

All commercial solvents and reagents were used without further purification unless specified otherwise. Ethyl glyoxylate was purified by distillation as previously reported.[1] Standard purification procedures were sourced from *Purification of Laboratory Chemicals, 6th Edition*.[2] Azide linker **A** was synthesized according to a previously reported method.[3]

Reaction manipulation, analysis, and purification

Anhydrous reactions were carried out in glassware dried (a) for >5 h in an oven at 130 °C or (b) under vacuum using heat supplied from a heat gun (~250 °C), then cooled under an inert atmosphere of N_2 provided by a double manifold. Reaction flasks were sealed with dye-free natural rubber septa, and gases/liquids were introduced/removed by needle/syringe or cannula transfer. All reactions were stirred with Teflon-coated magnetic followers. Room temperature is taken as 293 K. Brine refers to a saturated aqueous solution of sodium chloride, and 10% $NaHCO_3$ refers to a saturated aqueous solution of sodium hydrogen carbonate.

Distillations under reduced pressure were heated using a heat gun with vacuum supplied by a rotary vane high vacuum pump with a nitrogen bleed valve to control the pressure. Vacuum seals between ground glass joints were maintained using Glindemann PTFE sealing rings.

TLC analyses were performed on Merck TLC silica gel 60 F254 aluminium-backed plates. Product spots were visualized under UV light (λ_{max} = 254 nm) and/or by staining with potassium permanganate. Flash column chromatography was performed using silica gel 60 (0.040-0.063 mm particle size, Merck).

S2. Analytical methods and instrumentation

NMR Spectroscopy

NMR spectra were recorded at the University of Sydney using Bruker AVIII 400 MHz (variable temperature/kinetics, DOSY and high-resolution characterization) and Bruker NEO 300 MHz NMR spectrometers or at the University of Western Ontario using a Bruker AVIII HD 400 MHz, or Varian INOVA 600 MHz spectrometer (standard characterization). ^{1}H NMR experiments were carried out using a *zg* pulse program (90° pulse) with a recycle delays (*D*1) of 2-5 s. ^{13}C NMR was carried out with ^{1}H decoupling unless specified otherwise. For ^{13}C NMR (including HSQC/HMBC experiments), probes were automatically tuned and matched to the optimal operating frequencies before acquisition. ^{1}H and ^{13}C NMR spectra are referenced to the residual solvent peak for DMSO-d_6 (^{1}H: 1.94 ppm, ^{13}C: 118.26 ppm) or $CDCl_3$ (^{1}H: 7.26 ppm, ^{13}C: 77.16 ppm), as appropriate. ^{1}H and ^{13}C peak assignments were determined by HSQC and HMBC analyses, with aid from NOESY/ROESY experiments where additional information was required. DOSY spectra were acquired with the Bruker *ledbpgp2s* pulse sequence and processed using Mestrenova's Bayesian DOSY transform algorithm. Details of acquisition and processing parameters are included in the caption of each spectrum.

Deuterated solvents were obtained from Sigma Aldrich and Cambridge Isotope Laboratories and used without any further purification. Samples were prepared by centrifugation prior to analysis, or filtration through a glass fiber plug (~0.7 μm pore size) if suspended solids were present. NMR signals are reported in terms of chemical shift (δ) in parts-per-million (ppm), multiplicity, coupling constants (in Hz) and relative integral, in

that order. The following abbreviations for multiplicity are used: s = singlet, d = doublet, t = triplet, q = quartet, quint = quintet, m = multiplet (denotes complex pattern), dd = doublet of doublets, dt = doublet of triplets, td = triplet of doublets, and br = broad signal. Spectra were digitally processed (phase and baseline corrections, integration, apodization) using Mestrenova 14.0.1-23559 (Licensed to Dr. Derrick Roberts). Exponential window functions were applied to all 1D spectra at 0.3–2 Hz to digitally enhance signal-to-noise where required. 1D spectra were baseline corrected with the ablative (^{1}H) and Whittaker smoother (^{13}C) correction functions.

Low-resolution mass spectrometry

Low resolution electrospray ionization (ESI) mass spectra were collected by the authors using a Bruker amazon SL mass spectrometer system with methanol as the carrier solvent (flow rate of 0.3 mL/min). ESI mass spectra were recorded in enhanced resolution mode (mass range *m*/*z* 50–2200). This instrument was configured and maintained by Dr Nicholas Proschogo, Mass Spectrometry Staff Scientist at The University of Sydney.

High-resolution mass spectrometry

High resolution ESI mass spectra were collected by the authors at The University of Sydney using a Bruker Solarix 2xR 7T Fourier Transform Ion Cyclotron Resonance (FTICR) mass spectrometer, maintained by Dr Nicholas Proschogo. The spectrometer was calibrated to tolerances of <5.0 ppm across 150-2000 m/z range prior to measurement, and samples were measured as solutions in MeOH. Alternatively, the samples were characterized at The University of Western Ontario using a Bruker micrOTOF 11 mass spectrometer, maintained by Dr. Haidy Metwally. The spectrometer was calibrated to tolerances of <5.0 ppm across 100-2000 m/z range each time prior to measurement; and samples were measured as solutions in MeOH.

FTIR

FT-IR spectra were obtained using a PerkinElmer FT-IR Spectrum Two instrument with attenuated total reflectance sampling (Western University, Canada).

Analytical size-exclusion chromatography (SEC)

Analytical size exclusion chromatography was performed at the University of Sydney using a Shimadzu Prominence UFLC (ultra-fast liquid chromatography) system fitted with a Shim-pack GPC-800DP guard column followed by two in-series Phenogel columns (5 μm, 104 Å and 105 Å). The system eluent was HPLC grade dimethyl acetamide (DMAc) containing LiBr (0.03 wt%) and BHT (each at 0.05 wt%), eluting at a flow rate of 1 mL min^{-1}. The column assembly was incubated at 50 °C, and retention times were calibrated using PMMA narrow standards from PSS.

Access to raw data

Raw and processed spectroscopic data are available upon request to the corresponding authors.

S3. Alkyne-functional PEtGs P1 and P2

S3.1. Polymerization of acetal-bridged of P1a-b

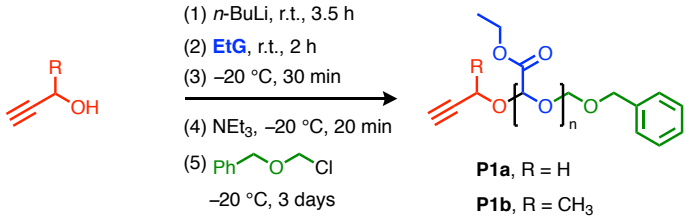

Synthesis of P1a and representative procedure for the preparation of acetal-bridged PEtG: To a flame-dried Schlenk flask under nitrogen at atmospheric pressure, 20 mL dry toluene, propargyl alcohol (0.074 mL, 1.3 mmol, 1.0 equiv.) and 2.5 M *n*-butyllithium hexane solution (0.50 mL, 1.3 mmol, 1.0 equiv.) were added at 0 ºC and allowed to stir at room temperature for 3.5 h. Purified ethyl glyoxylate (5.0 mL, 64 mmol, 50 equiv.) was added to this flask and stirred at room temperature for 2 h. The solution was subsequently cooled to -20 ºC and stirred for 30 min. Freshly distilled NEt_3 (1.4 mL, 10 mmol, 6.0 equiv.) was added to the polymerization flask and the reaction mixture stirred for 20 min. To this flask, 60 wt% benzyl chloromethyl ether (6.0 mL, 25.7 mmol, 20 equiv.) was added to end-cap the polymer. The reaction mixture was stirred at -20 ºC for 30 min and kept in a -20 ºC freezer for 3 d, then allowed to gradually warm to room temperature over 2 h. The mixture was concentrated *in vacuo*. The resulting concentrate was precipitated into methanol/water (5:1, 600 mL). Then, the flask sealed and transferred into a −20 °C freezer where it was kept for 16 h before the solvent was decanted and the resulting residues were vacuum-dried to afford 3.60 g of a colorless tacky solid. Yield: 72%.

S3.1.1. Characterization data for P1a

Using the general procedure described above, polymer **P1a** was obtained as a colorless tacky solid (3.60 g, 72% yield). **^{1}H NMR** (400 MHz, $CDCl_3$) δ_H 7.4 – 7.2 (m, 5H), 5.8 – 5.4 (m, 48H), 4.8 (s, 2H), 4.6 (s, 2H), 4.3 – 4.1 (m, 101H), 2.6 – 2.4 (m, 1H), 1.5 – 1.1 (m, 163H). **SEC** (DMAc/LiBr, 50 °C, PMMA calibration) $M_{n,SEC}$ = 4.0 kg mol^{-1}, $Đ$ = 1.32.

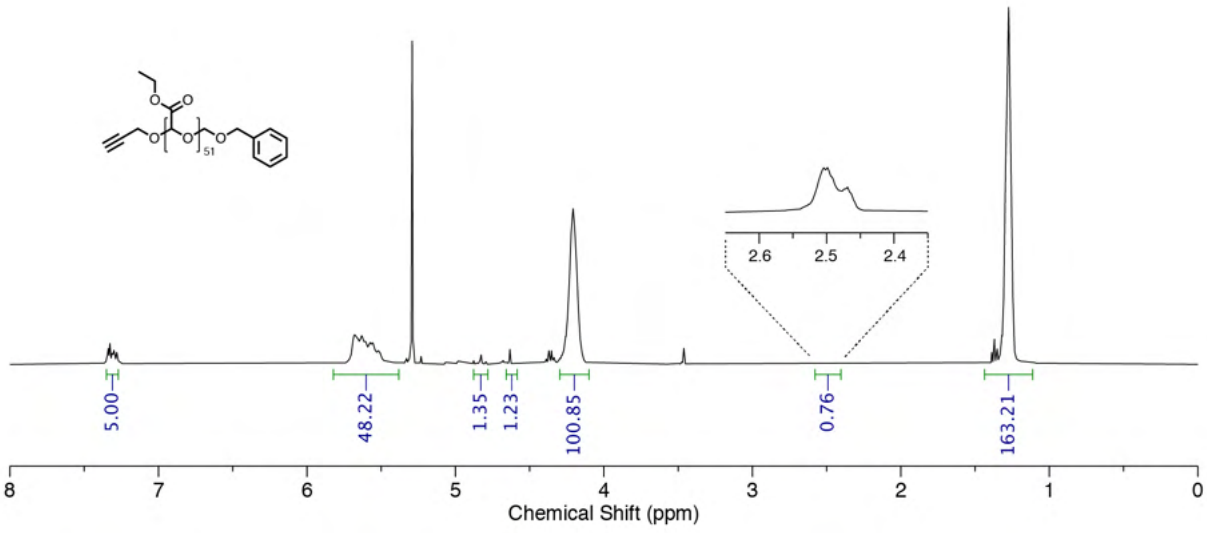

Figure S1. ^{1}H NMR spectrum (400 MHz, 300 K, $CDCl_3$) of compound **P1a**. End-group analysis using the benzyl 5H environment as reference, gives an average DP of 51 (calculated by averaging the acetal CH and ethyl CH_2 and CH_3 environments).

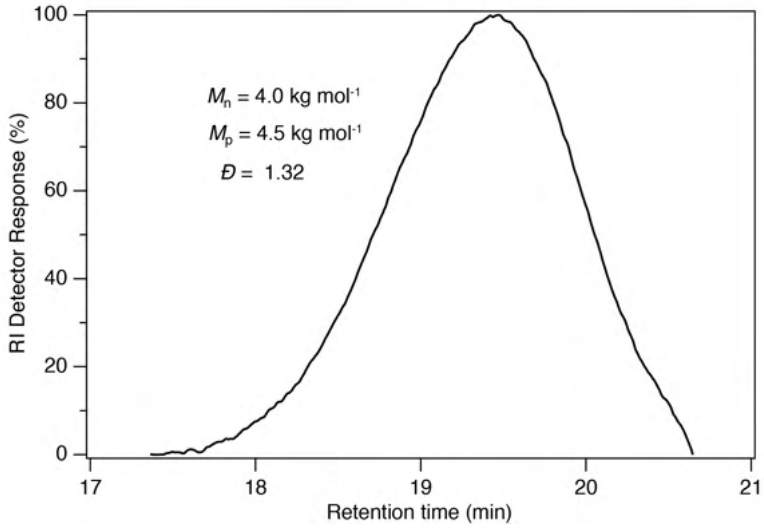

Figure S2. SEC trace (DMAc/LiBr, 50 °C, PMMA calibration) of polymer **P1a**.

S3.1.2. **Characterization data for P1b**

Using the general procedure described above, polymer **P1b** was obtained as a colorless tacky solid (2.95 g, 59% yield). **^{1}H NMR** (300 MHz, $CDCl_3$) δ_H 7.3 – 7.1 (m, 5H), 5.8 – 5.3 (m, 101H), 5.0 – 4.8 (m, 2H), 4.7 – 4.5 (m, 2H), 4.4 – 4.0 (m, 216H), 2.6 – 2.4 (m, 1H), 1.2 (t, J = 7.3 Hz, 339H). **SEC** (DMAc/LiBr, 50 °C, PMMA calibration) $M_{n,SEC}$ = 10.3 kg mol^{-1}, $Đ$ = 1.17.

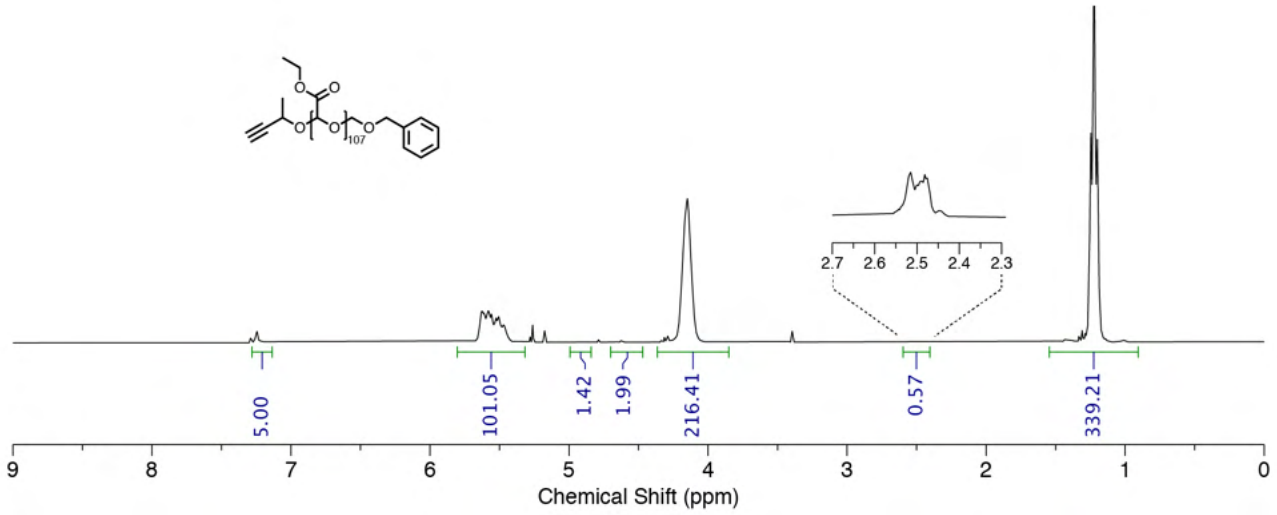

Figure S3. ^{1}H NMR spectrum (300 MHz, 300 K, $CDCl_3$) of polymer **P1b.** End-group analysis using the benzyl 5H environment as reference, gives an average DP of 107 (calculated by averaging the acetal CH and ethyl CH_2 and CH_3 environments).

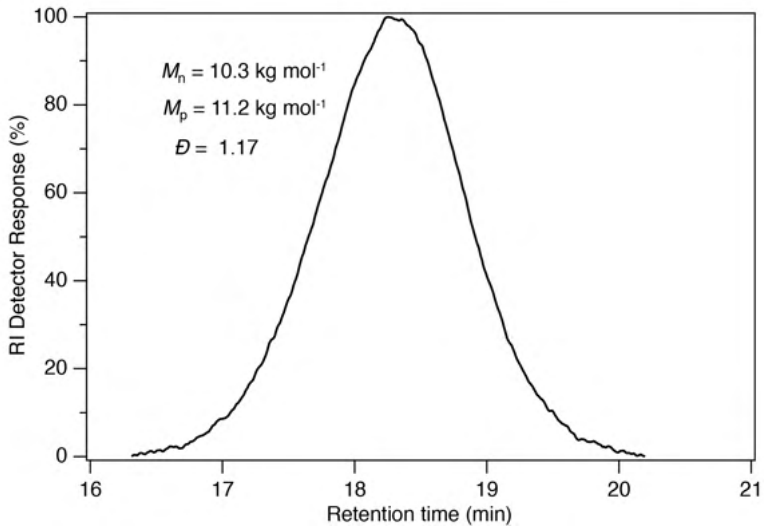

Figure S4. SEC trace (DMAc/LiBr, 50 °C, PMMA calibration) of polymer **P1b**.

S3.2. Polymerization of carbonate-bridged P2a-b

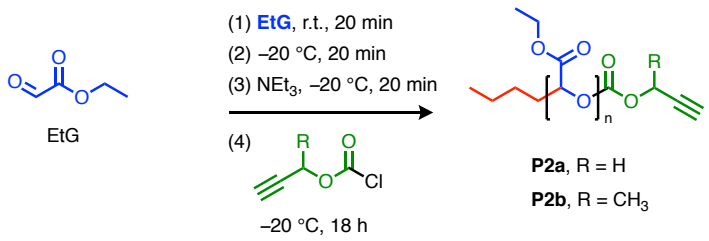

S3.2.1. Synthesis data for P2a

Preparation of propargyl chloroformate endcap. In a flame-dried Schlenk flask under nitrogen at atmospheric pressure, propargyl alcohol (0.70 mL, 12 mmol, 6.0 equiv.) and 15% (wt) phosgene in toluene solution (24 mL, 36 mmol, 18.0 equiv.) were combined and stirred at room temperature for 18 h. Excess phosgene was removed under vacuum, and the mixture was concentrated to about 3 mL.

Synthesis of P2a. Purified ethyl glyoxylate (7.0 mL, 75 mmol, 50 equiv.) was placed into a flame-dried Schlenk flask under nitrogen at atmospheric pressure. To this flask, 20 mL of dry toluene and 2.5 M *n*-butyllithium hexane solution (0.55 mL, 1.4 mmol, 1.0 equiv.) were added at room temperature and allowed to mix for 20 min. The solution was subsequently cooled to -20 ºC and stirred for 20 min. Freshly distilled NEt_3 (1.1 mL, 8.2 mmol, 5.9 equiv.) was added to the polymerization flask and the reaction mixture was stirred for 20 min. The propargyl chloroformate end-cap solution was cooled to -20 ºC and added to the reaction flask. The reaction mixture was stirred at -20 ºC for 24 h and then allowed to gradually warm to room temperature over 2 h. The mixture was concentrated under vacuum. The resulting concentrate was precipitated into methanol/water (5:1; 720 mL). The flask was sealed and transferred into a −20 °C freezer where it was kept for 16 h before the solvent was decanted and the resulting residues were vacuum-dried to afford 3.89 g of a colorless tacky solid. Yield: 56%. **^{1}H NMR** (400 MHz, $CDCl_3$) δ_H 5.8 – 5.4 (m, 38H), 4.8 (br. s, 2H), 4.5 – 4.1 (m, 82H), 2.6 (br. s, 1H), 1.6 – 1.0 (m, 132H), 0.9 (br. s, 3H). **SEC** (DMAc/LiBr, 50 °C, PMMA calibration) $M_{n,SEC}$ = 5.3 kg mol^{-1}, $Đ$ = 1.31.

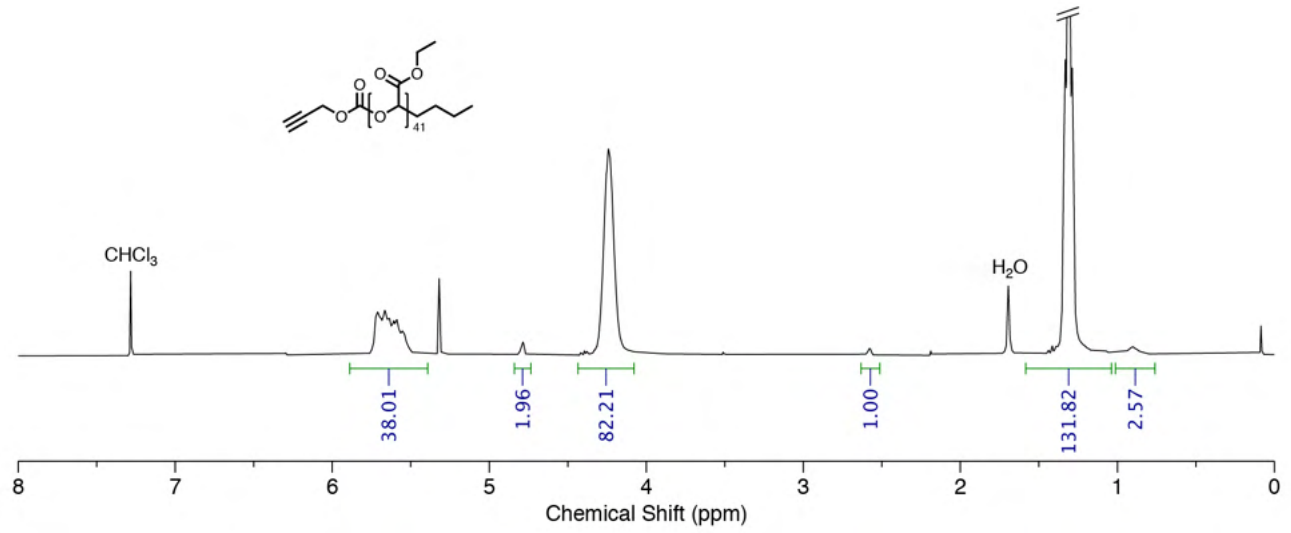

Figure S5. ^{1}H NMR spectrum (300 MHz, 300 K, $CDCl_3$) of polymer **P2a**. End-group analysis using the alkyne 1H environment as reference, gives an average DP of 41 (calculated by averaging the acetal CH and ethyl CH_2 and CH_3 environments).

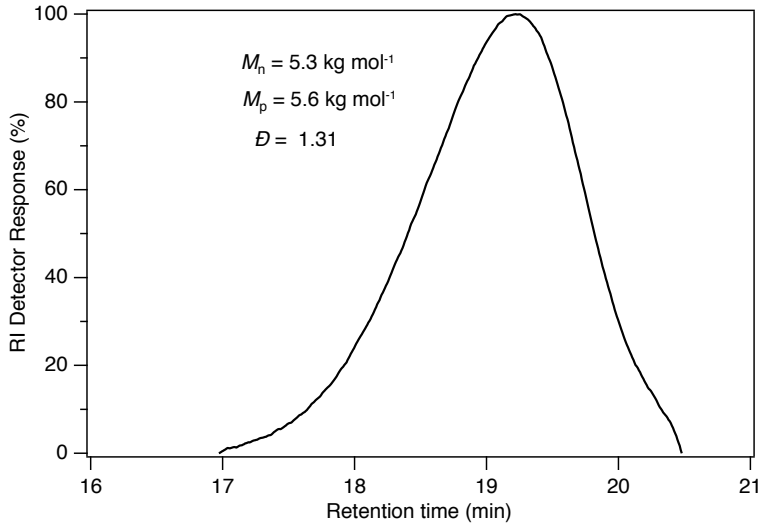

Figure S6. SEC trace (DMAc/LiBr, 50 °C, PMMA calibration) of polymer **P2a**.

S3.2.2. **Synthesis data for P2b**

Preparation of but-3-yn-2-yl chloroformate. In a flame-dried Schlenk flask under nitrogen at atmospheric pressure, 3-butyn-2-ol (0.85 mL, 12 mmol, 7.0 equiv.) and 15% (wt) phosgene in toluene solution (24 mL, 36 mmol, 21.0 equiv.) were combined and stirred at room temperature for 48 h. Excess phosgene was removed under vacuum, and the mixture was concentrated to about 3 mL.

Synthesis of P2b. Purified ethyl glyoxylate (8.0 mL, 86 mmol, 50 equiv.) was placed into a flame dried Schlenk flask under nitrogen at atmospheric pressure. To this flask, 20 mL of dry toluene and 2.5 M *n*-butyllithium hexane solution (0.68 mL, 1.7 mmol, 1.0 equiv.) were added at room temperature and allowed to mix for 20 min. The solution was subsequently cooled to -20 ºC and stirred for 20 min. Freshly distilled NEt_3 (1.4 mL, 10 mmol, 6.0 equiv.) was added to the polymerization flask and the reaction mixture was stirred for 20 min. The

but-3-yn-2-yl chloroformate end-cap solution was cooled to -20 ºC and added to the reaction flask. The reaction mixture was stirred at -20 ºC for 30 min and kept in a -20 ºC freezer for 2 d, then allowed to gradually warm to room temperature over 2 h. The mixture was concentrated under vacuum. The resulting concentrate was precipitated into 720 mL solvent mixture (methanol/water = 5/1). Then the flask was sealed and transferred into a −20 °C freezer where they were kept for 16 h before the solvent was decanted and the resulting residues were vacuum-dried to afford the product as a colorless tacky solid (4.55 g, 57% yield). **^{1}H NMR** (400 MHz, $CDCl_3$) δ_H 5.9 – 5.4 (m, 33H), 4.4 – 4.0 (m, 74H), 2.5 (br. s, 1H), 1.6 – 1.5 (m, 3H), 1.4 – 1.1 (m, 114H), 0.9 (br. s, 3H). **SEC** (DMAc/LiBr, 50 °C, PMMA calibration) $M_{n,SEC}$ = 4.7 kg mol^{-1}, $Đ$ = 1.27.

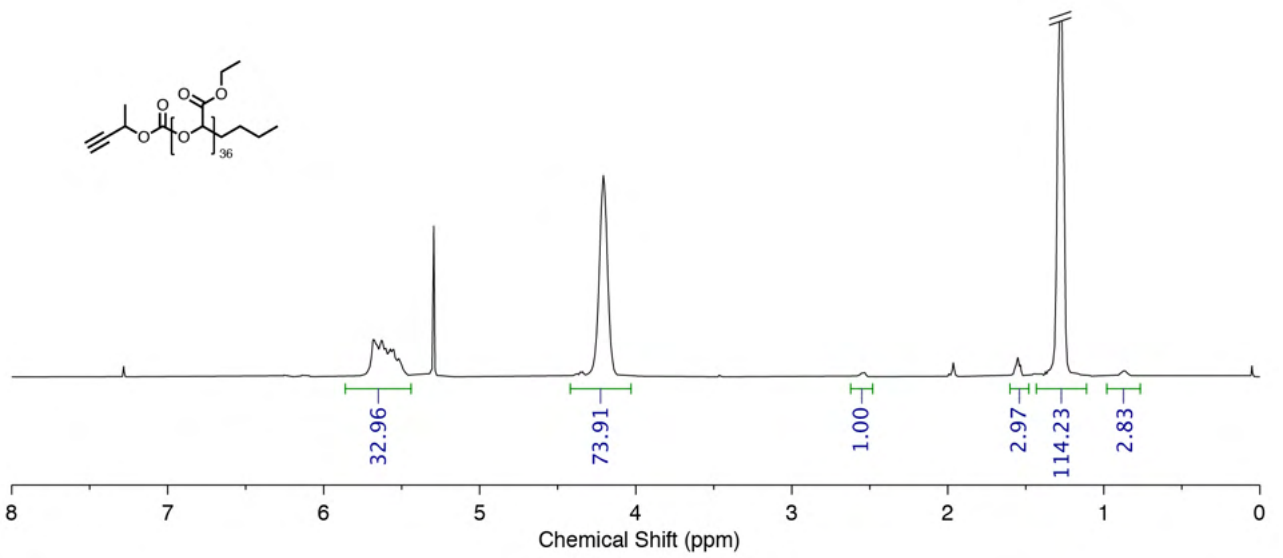

Figure S7. ^{1}H NMR spectrum (400 MHz, 300 K, $CDCl_3$) of compound **P2b.** End-group analysis using the alkyne 1H environment as reference, gives an average DP of 36 (calculated by averaging the acetal CH and ethyl CH_2 and CH_3 environments).

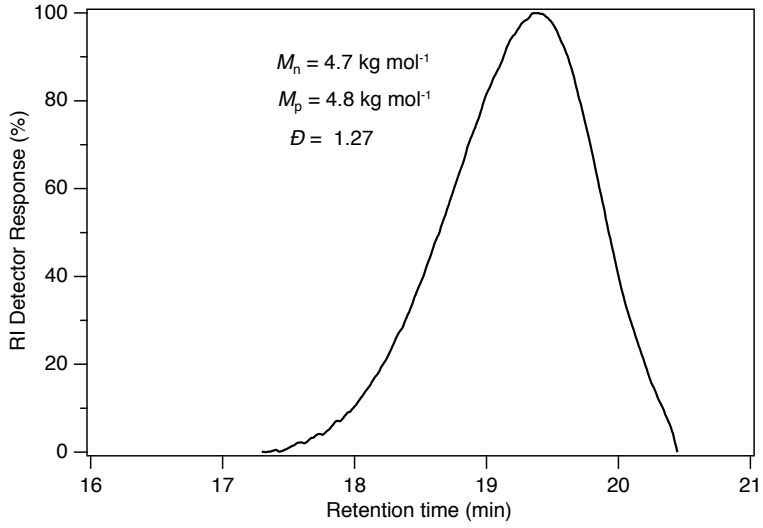

Figure S8. SEC trace (DMAc/LiBr, 50 °C, PMMA calibration) of polymer **P2b**.

S4. Allyl-capping of alkyne-terminated PEtGs

S4.1. Synthesis of acetal-bridged polymers P3a-b

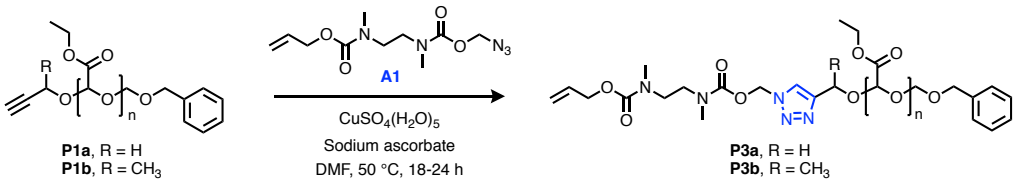

***Representative procedure*:** Azide **A1** (40 mg, 0.15 mmol, 2.0 equiv.) was added to a solution of **P1a** (318 mg, 0.03 mmol at M_n ~ 5.2 kg mol^{-1}) in DMF (2 mL). Copper sulfate pentahydrate (12 mg, 0.048 mmol) and sodium ascorbate (27 mg, 0.14 mmol) were added, and the mixture stirred at 50 °C for 16 h. The reaction mixture was diluted with EtOAc (20 mL), washed with aqueous EDTA (2% *w*/*v*, 3 × 20 mL), water (5 × 20 mL) and brine (2 × 20 mL). The organic layer was collected, and the solvent removed under reduced pressure. The resulting gummy solid was dissolved in CH_2Cl_2 (~0.2 mL) and Et_2O (~5 mL) was added, resulting in precipitation of a yellow-brown gummy material that was pelletized by centrifugation (1 min, 5k rpm). The supernatant was discarded, and the pellet subjected to another dissolution/precipitation cycle. The resulting pellet was dried under high vacuum at 50 °C, affording click-capped polymer **P3a**.

S4.1.1. Characterization data for polymer P3a

Polymer **P3a** was obtained as a yellow-brown gummy solid (66 mg, 13 µmol at $M_{n,NMR}$ ~ 5.1 kg mol^{-1} for DP46, 60%). **^{1}H NMR** (400 MHz, $CDCl_3$) δ_H 8.07 (s, 1H), 7.37 – 7.30 (m, 5H), 6.23 (s, 2H), 6.06 – 5.84 (m, 1H), 5.80 – 5.48 (m, 49H), 5.31 (s, 2H), 5.29 – 5.13 (m, 2H), 5.06 – 4.79 (m, 2H), 4.78 – 4.67 (m, 2H), 4.67 – 4.52 (m, 2H), 4.35 – 4.08 (m, 100H), 3.58 – 3.28 (m, 4H), 3.03 – 2.76 (m, 6H), 1.54 – 1.06 (m, 160H). **SEC** (DMAc/LiBr, 50 °C, PMMA calibration) $M_{n,SEC}$ = 3.9 kg mol^{-1}, $Đ$ = 1.37.

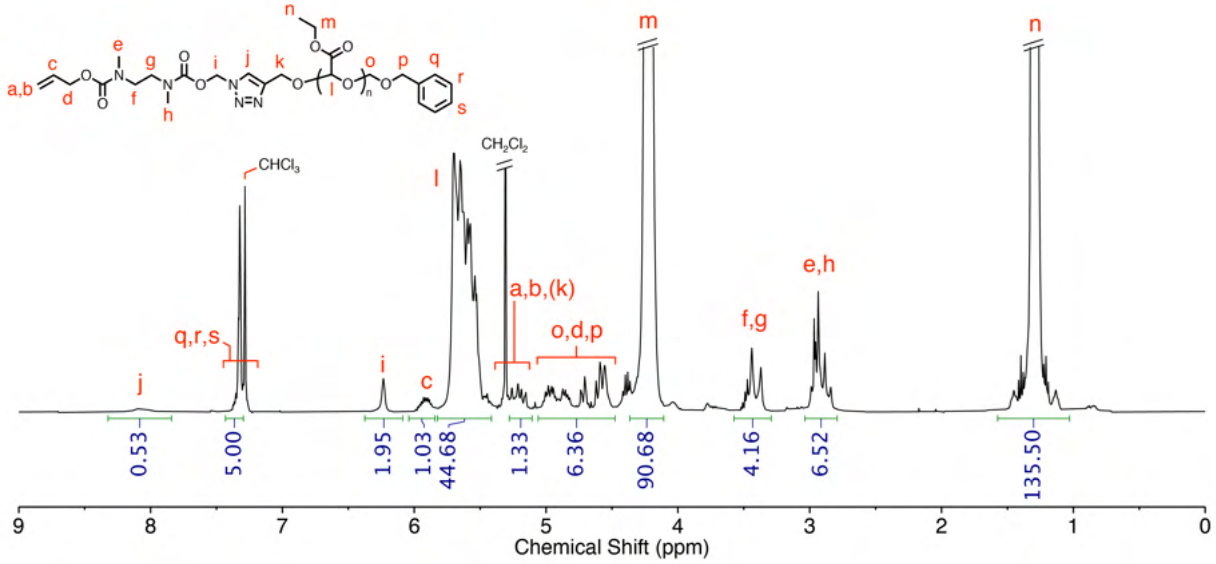

Figure S9. ^{1}H NMR spectrum (400 MHz, 300 K, $CDCl_3$) of polymer **P3a**. Peaks consistent with the attached SIT end-group are evident. Environments H_o and H_p appear to be overlapping with unassigned impurities. Complex splitting of peaks is attributed to rotamerism of the carbamate groups and the proximity of certain environments (e.g., H_k, H_o, H_p) to sterocentres along the polymer backbone.

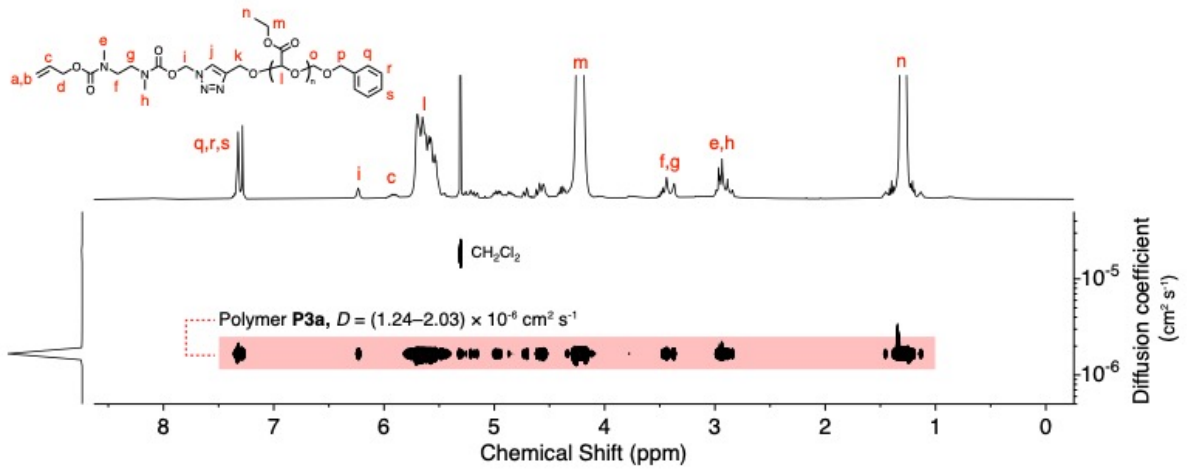

Figure S10. ^{1}H DOSY NMR spectrum (400 MHz, 300 K, $CDCl_3$) of polymer **P3a.** Co-diffusion of PEtG backbone signals and signals corresponding to the SIT end-group is consistent with successful 'click' capping of the alkyne-functional PEtG precursor (**P1a**).

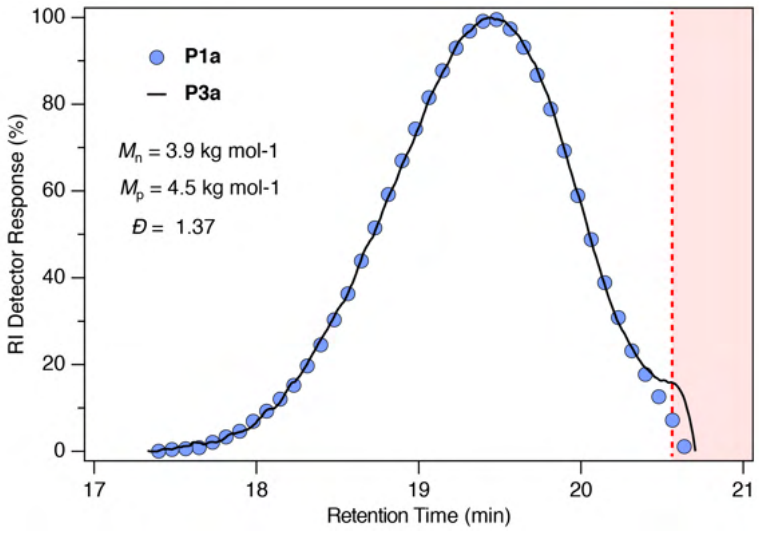

Figure S11. SEC traces (DMAc/LiBr, 50 °C, PMMA calibration) of polymer **P1a** (blue circles) and **P3a** (black line). Molar mass and dispersity values correspond to **P3a**. No measurable change in molar mass distribution and dispersity occurred following post-synthetic capping. Red shaded region indicates low molar mass exclusion limit of the SEC system.

S4.1.2. **Characterization data for polymer P3b**

Following post-modification and purification according to the general procedure, polymer **P3b** was obtained as a yellow gummy solid (69 mg, 5.6 µmol at $M_{n,NMR}$ ~12.3 kg mol^{-1} for DP116, 58% yield).

^{1}H NMR (400 MHz, $CDCl_3$) δ_H 8.7 – 7.8 (br. s, 1H), 7.4 – 7.3 (m, 5H), 6.3 (s, 1H), 6.0 – 5.8 (m, 1H), 5.8 – 5.4 (m, 112H), 5.3 – 5.1 (m, 2H), 5.0 – 4.9 (m, 2H), 4.9 – 4.8 (m, 1H), 4.8 – 4.7 (m, 2H), 4.6 – 4.5 (m, 4H), 4.5 – 3.9 (m, 237H), 3.4 (s, 4H), 2.9 (s, 6H), 1.6 (s, 3H), 1.3 (t, J = 7.1 Hz, 357H). **SEC** (DMAc/LiBr, 50 °C, PMMA calibration) $M_{n,SEC}$ = 10.4 kg mol^{-1}, $Đ$ = 1.12.

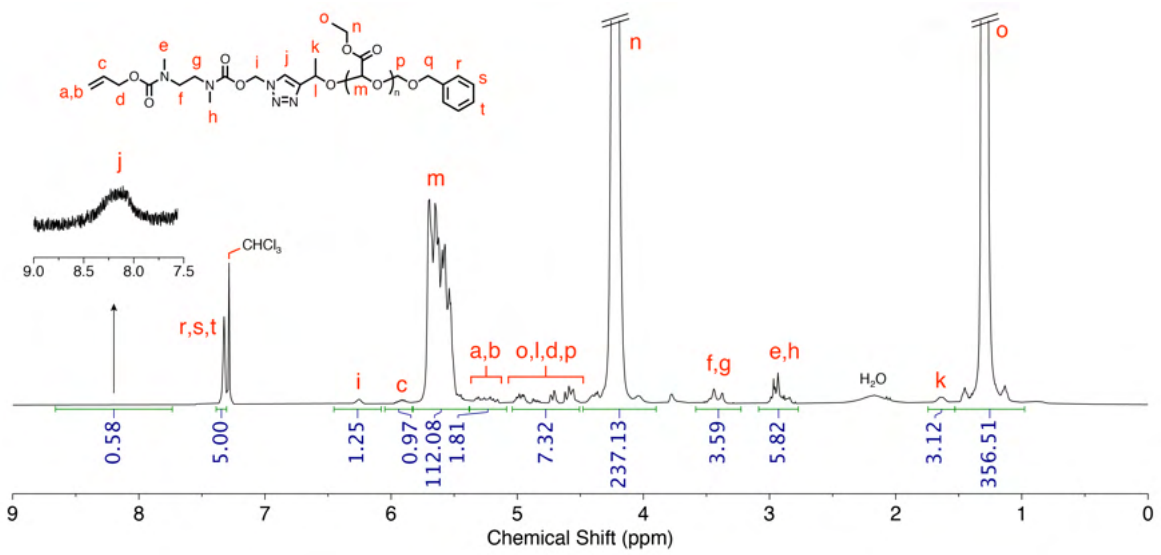

Figure S12. ^{1}H NMR spectrum (400 MHz, 300 K, $CDCl_3$) of polymer **P3b.** Peaks consistent with the 'clicked' end-group are assigned using model compound **1b** as an analogous reference. Spectra are shown at different levels of zoom to highlight peaks of the polymer backbone, 'clicked' end-group and the broad aromatic triazole signal.

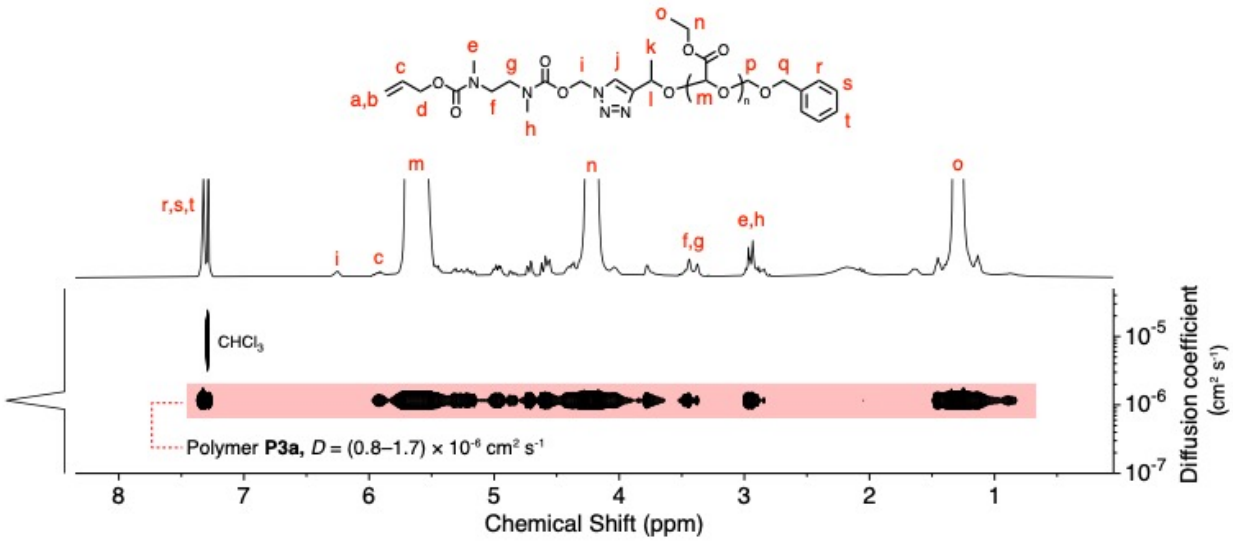

Figure S13. ^{1}H DOSY NMR spectrum (400 MHz, 300 K, $CDCl_3$) of polymer **P3b.** Co-diffusion of PEtG backbone signals and signals corresponding to the Alloc capping group is consistent with successful end-capping of the alkyne-functional PEtG precursor (**P1a**). Acquisition parameters: *d20* (Δ) = 300 ms, *p30* (δ) = 2000 µs, *td*(F1) = 16. Processing: Bayesian DOSY transform, resolution factor = 20, repetitions = 1, processed with 32 points in diffusion dimension.

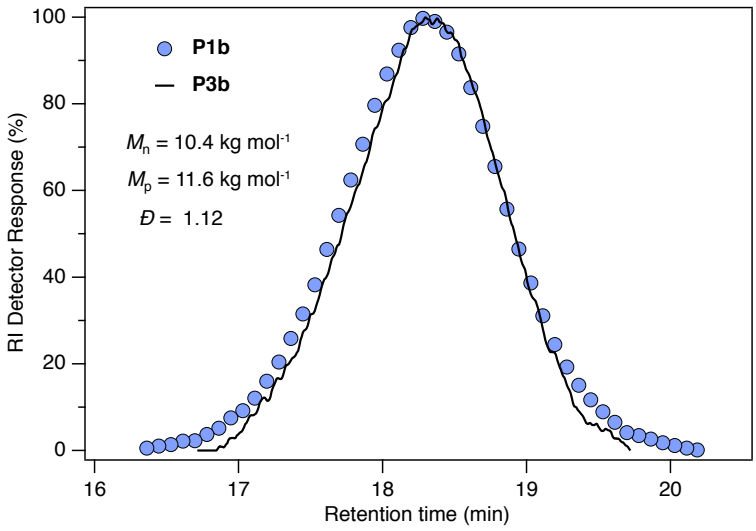

Figure S14. SEC traces (DMAc/LiBr, 50 °C, PMMA calibration) of polymer **P1b** (blue circles) and **P3b** (black line). Molar mass and dispersity values correspond to **P3b**.

S4.2. Synthesis of carbonate-bridged polymers P4a-b

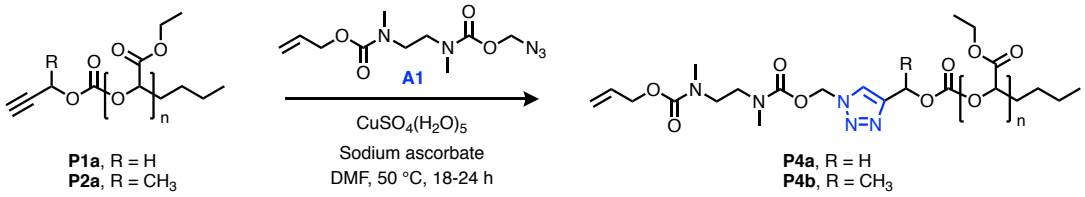

P1a, R = H
P2a, R = CH_3

P4a, R = H
P4b, R = CH_3

Polymers **P4a-b** was prepared from **P2a-b** respectively using the same CuAAC protocol as **P3a-b** (see p. 9).

S4.2.1. Characterization data for polymer P4a

Following post-modification and purification according to the general procedure, polymer **P4a** was obtained as a yellow gummy solid (87 mg, 21 µmol at $M_{n,NMR}$ ~4.2 kg mol^{-1} for DP37, 66% yield). **^{1}H NMR** (400 MHz, $CDCl_3$) δ_H 8.01 (s, 1H), 6.33 – 6.15 (m, 2H), 5.97 – 5.79 (m, 1H), 5.78 – 5.39 (m, 33H), 5.39 – 5.08 (m, 4H), 4.63 – 4.43 (m, 2H), 4.33 – 4.07 (m, 74H), 3.80 – 3.53 (m, 1H), 3.53 – 3.24 (m, 4H), 3.06 – 2.69 (m, 6H), 1.53 – 1.04 (m, 118H). **SEC** (DMAc/LiBr, 50 °C, PMMA calibration) $M_{n,SEC}$ = 5.7 kg mol^{-1}, $Đ$ = 1.27.

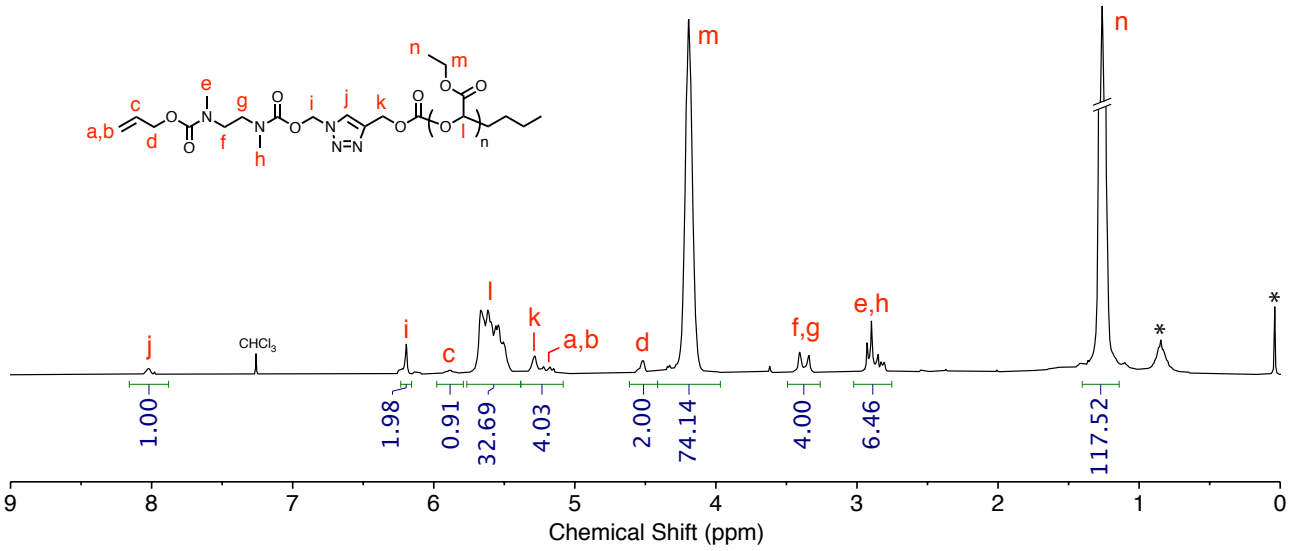

Figure S15. ^{1}H NMR spectrum (400 MHz, 300 K, $CDCl_3$) of compound **P4a** following precipitation into Et_2O. End-group analysis indicates an average DP of ~37 after end-group modification and purification (calculated by averaging the acetal CH and ethyl CH_2 and CH_3 environments). Asterisks denote residual silicone and hexane grease from glassware.

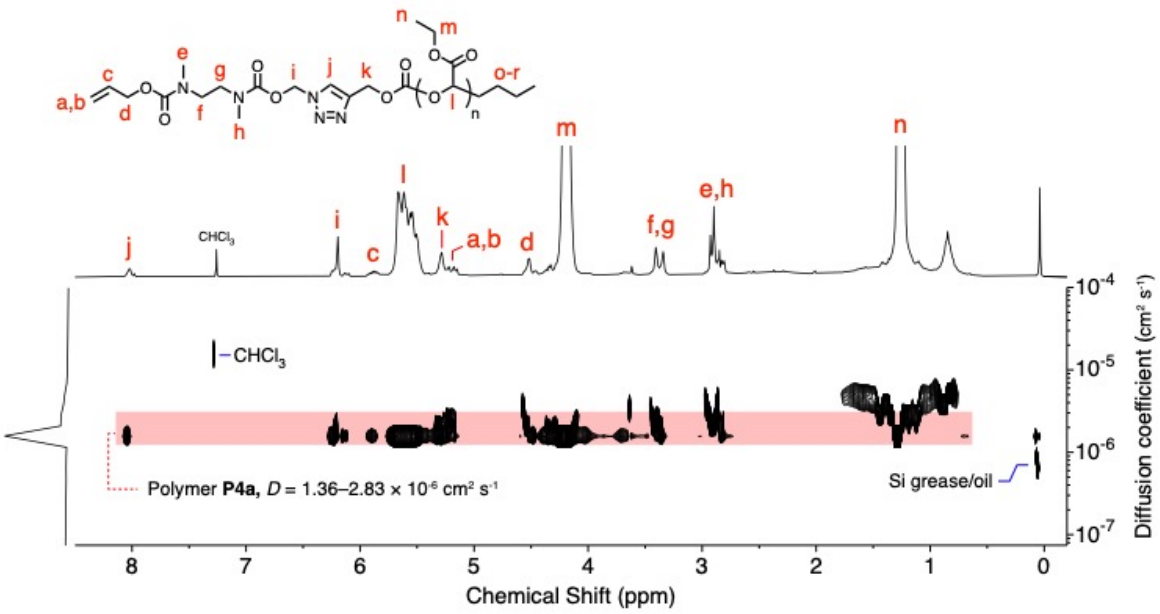

Figure S16. ^{1}H DOSY spectrum (400 MHz, 300 K, $CDCl_3$) of compound **P4a** showing co-diffusion of 'clicked' end-groups and the polymer main chain. Cross-attenuation due to relaxation is also apparent for some environments. Acquisition parameters: *d20* (Δ) = 300 ms, *p30* (δ) = 2000 µs, *td*(F1) = 16. Processing: Bayesian DOSY transform, resolution factor = 20, repetitions = 1, processed with 32 points in diffusion dimension.

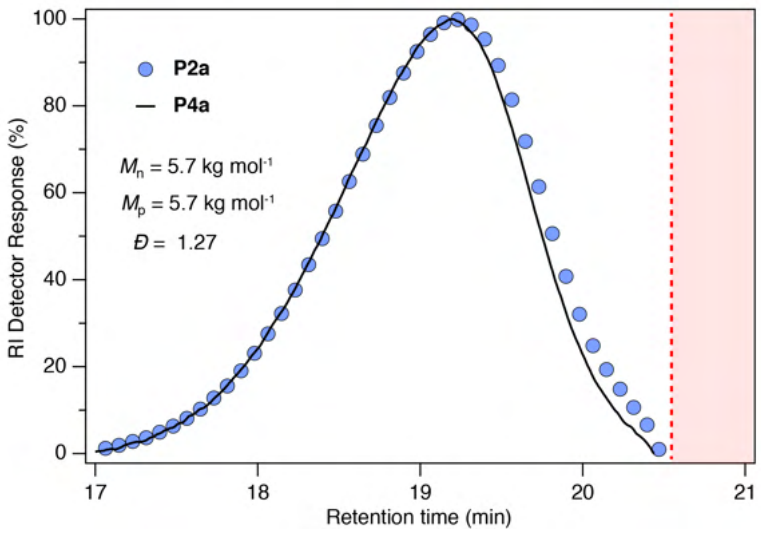

Figure S17. SEC traces (DMAc/LiBr, 50 °C, PMMA calibration) of polymer **P2a** (blue circles) and **P4a** (black line). Molar mass and dispersity values correspond to **P4a**. No significant change in polymer molecular weight distribution was noted following post-modification. Red shaded region indicates low molar mass exclusion limit of the SEC system.

S4.2.2. **Characterization data for polymer P4b**

Following post-modification and purification according to the general procedure, polymer **P4b** was obtained as a yellow-brown gummy solid (32 mg, 11 μmol at $M_{n,NMR}$ ~3.0 kg mol^{-1} for DP25, 24% yield).

^{1}H NMR (400 MHz, $CDCl_3$) δ_H 8.3 – 7.6 (m, 1H), 6.4 – 6.1 (m, 3H), 6.0 – 5.8 (m, 2H), 5.8 – 5.4 (m, 20H), 5.4 – 5.1 (m, 2H), 4.6 – 4.4 (m, 2H), 4.3 – 4.1 (m, 47H), 3.5 – 3.2 (m, 4H), 3.0 – 2.7 (m, 6H), 1.5 – 1.1 (m, 99H).

SEC (DMAc/LiBr, 50 °C, PMMA calibration) $M_{n,SEC}$ = 4.0 kg mol^{-1}, Đ = 1.36.

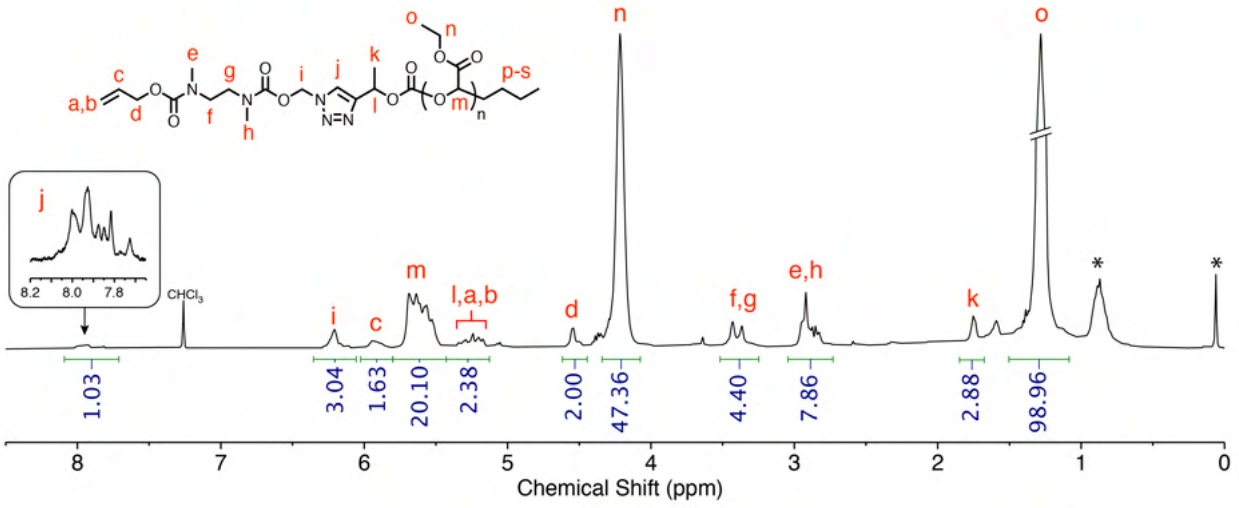

Figure S18. ^{1}H NMR spectrum (400 MHz, 300 K, $CDCl_3$) of compound **P4b** following precipitation into Et_2O. End-group analysis indicates an average DP of ~25 after end-group modification and purification (calculated by averaging the acetal CH and ethyl CH_2 and CH_3 environments). Complex splitting particularly of environment H_j is ascribed to its proximity to the adjacent racemic stereocentre. (*Note:* spectrum is vertically cut to make end-group environments clearer.) Asterisks denote residual silicone and hexane grease from glassware.

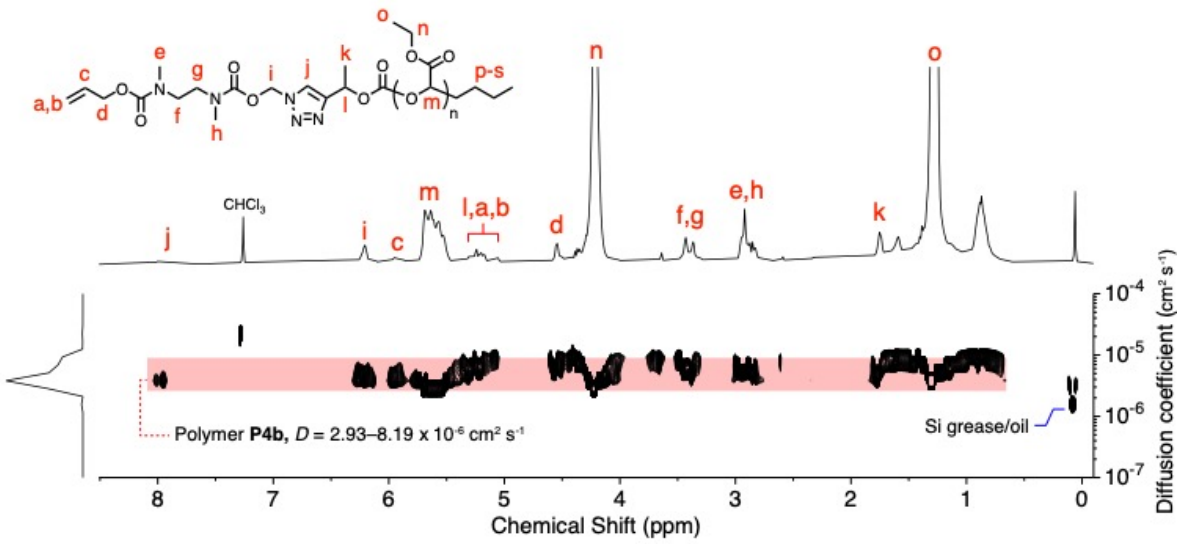

Figure S19. ^{1}H DOSY spectrum (400 MHz, 300 K, $CDCl_3$) of compound **P4b** showing co-diffusion of 'clicked' end-groups and the polymer main chain. Variance in apparent diffusion coefficient is attributed to a combination of polymer dispersity and slight differences in T_1 relaxation rates of different chemical environments within the polymer. Acquisition parameters: *d20* (Δ) = 300 ms, *p30* (δ) = 2000 µs, *td*(F1) = 16. Processing: Bayesian DOSY transform, resolution factor = 1, repetitions = 1, processed with 32 points in diffusion dimension.

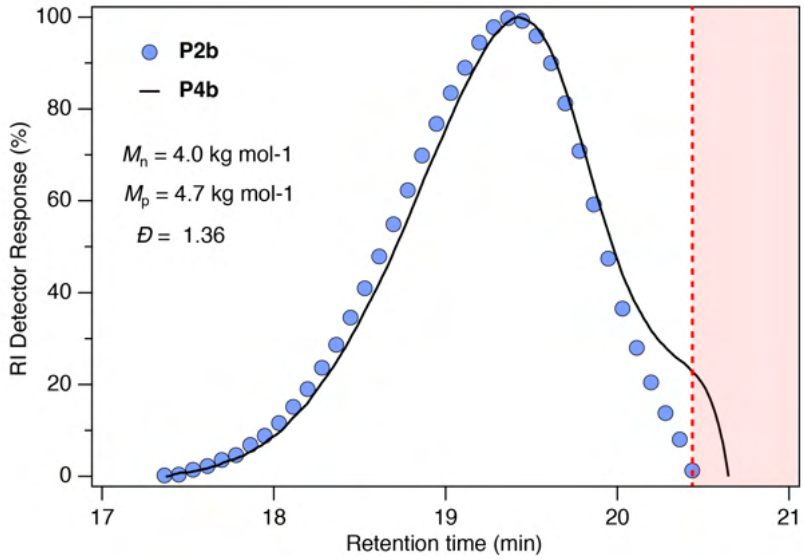

Figure S20. SEC traces (DMAc/LiBr, 50 °C, PMMA calibration) of polymer **P2b** (blue circles) and **P4b** (black line). Molar mass and dispersity values correspond to **P4b**. No significant change in polymer distribution was noted following modification. Red shaded region indicates low molar mass exclusion limit of the SEC system.

S5. Synthesis of allyl-capped acetal-bridged model compounds

S5.1. Synthesis of alkynes S1a-c

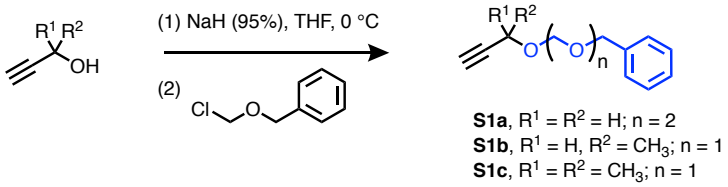

***Representative procedure*:** A suspension of sodium hydride (95% in mineral oil, 0.14 g, 5.5 mmol) in THF (5 mL) was cooled to 0 °C and propargyl alcohol (0.19 g, 3.4 mmol) was added dropwise at this temperature. The mixture was stirred for 10 min then benzyl chloromethyl ether was added (0.37 g, 2.4 mmol). The ice bath was removed and stirring was continued for ~65 h at room temperature. The resulting mixture was quenched with saturated aqueous ammonium chloride at 0 °C and extracted with ethyl acetate. The combined extracts were washed with brine, dried over sodium sulfate, and concentrated *in vacuo*. Purification of the residue by silica gel chromatography afforded compound **S1a**.

S5.1.1. Characterization data for compound S1a

Compound **S1a** was prepared according to the representative procedure and, following silica gel chromatography **(**hexane/EtOAc gradient from 20:1 to 10:1), was obtained as a colorless oil (98 mg, 0.47 mmol, 19% yield). A mixture of oligomeric products was obtained in this reaction, which we ascribe to the presence of formaldehyde in the commercial benzyl chloromethyl ether (~60% purity). Chromatographic purification afforded **S1a** as the major product alongside a bis(benzyl) side product that co-eluted with the product. This mixture was carried through to the next step for subsequent purification. Characterization data were consistent with published values.[4] **^{1}H NMR** (300 MHz, $CDCl_3$) δ_H 7.4 – 7.3 (m, 5H), 5.0 (s, 2H), 4.9 (s, 2H), 4.7 (s, 2H), 4.3 (d, J = 2.5 Hz, 2H), 2.5 (d, J = 2.4 Hz, 1H). **LRMS** (+*ve* ESI, MeOH) *m/z* 229.04 ([M+Na]$^+$, 100%).

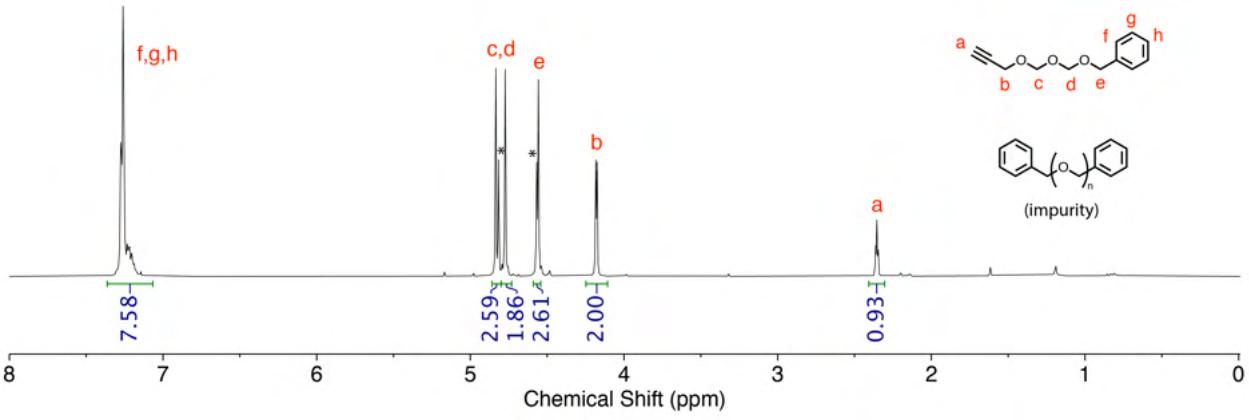

Figure S21. ^{1}H NMR spectrum (300 MHz, 300 K, $CDCl_3$) of compound **S1a** (partially purified). Asterisks denote peaks ascribed to a ~30 mol% bis(benzyl) impurity (n = 3-5) identified by mass spectrometry. The impurity co-eluted with the product by chromatography and could not be separated. Consequently, the impurity was carried through to the next step and purified at that stage.

S5.1.2. **Characterization data for compound S1b**

Compound **S1b** was prepared according to the representative procedure and, following silica gel chromatography **(**hexane/EtOAc gradient from 20:1 to 10:1), was obtained as a colorless oil (153 mg, 0.80 mmol, 37% yield). **^{1}H NMR** (400 MHz, $CDCl_3$) δ_H 7.53 – 7.27 (m, 5H), 4.97 (dd, J = 97.6, 7.0 Hz, 2H), 4.77 – 4.63 (m, 2H), 4.58 (qd, J = 6.7, 2.1 Hz, 1H), 2.49 (d, J = 2.1 Hz, 1H), 1.53 (d, J = 6.7 Hz, 3H). **^{13}C NMR** (100 MHz, $CDCl_3$) δ_C 137.9, 128.4, 127.9, 127.7, 92.3, 83.5, 73.0, 69.8, 61.5, 22.0. **LRMS** (+*ve* ESI, MeOH) *m/z* 213.1 ($[M+Na]^+$, 100%). **HRMS** (+*ve* ESI FTICR, MeOH) *m/z* calculated for $C_{12}H_{14}NaO_2$ $[M+Na]^+$: 213.0886, found 213.0887 ($|\Delta_{m/z}|$ = 0.3 ppm).

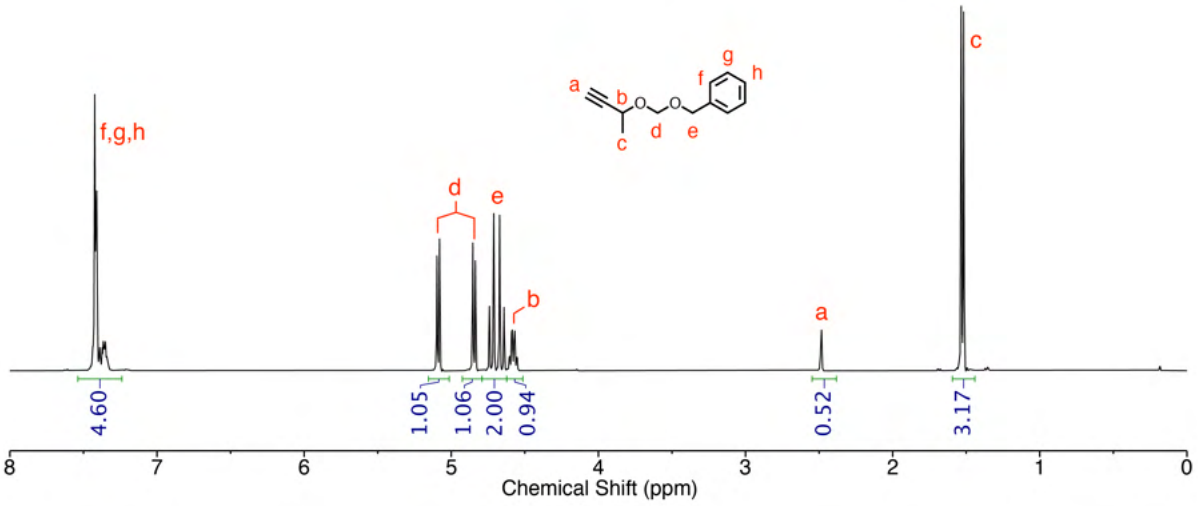

Figure S22. ^{1}H NMR spectrum (400 MHz, 300 K, $CDCl_3$) of compound **S1b.** Wide splitting of H_d is attributed to diastereotopic inequivalence resulting from the nearby propargylic stereocenter (obtained as the racemate).

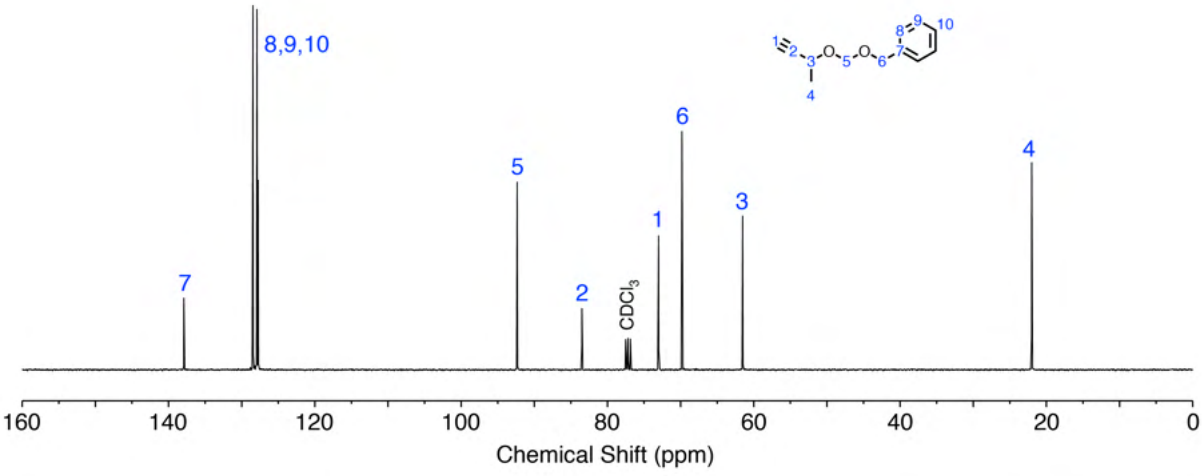

Figure S23. ^{13}C NMR spectrum (100 MHz, 300 K, $CDCl_3$) of compound **S1b.**

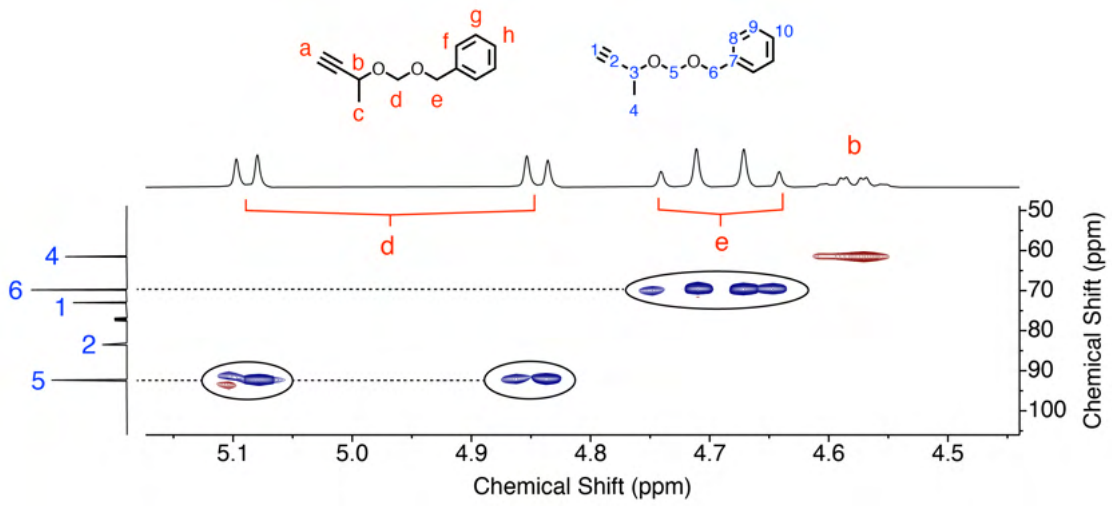

Figure S24. Partial 1H–13C HSQC spectrum (400/100 MHz, 300 K, $CDCl_3$) confirming assignments of H_d, H_e and H_b.

S5.1.3. **Characterization data for compound S1c**

Compound **S1c** was prepared according to the representative procedure and, following silica gel chromatography **(**hexane/EtOAc 40:1), was obtained as a colorless oil (60 mg, 0.30 mmol, 10% yield). **^{1}H NMR** (400 MHz, $CDCl_3$) δ_H 7.53 – 7.25 (m, 5H), 5.09 (s, 2H), 4.70 (s, 2H), 2.52 (s, 1H), 1.61 (s, 6H). **^{13}C NMR** (100 MHz, $CDCl_3$) δ_C 138.1, 128.4, 127.9, 127.6, 91.2, 85.8, 72.7, 70.9, 69.7, 30.1. **LRMS** (*+ve* ESI, MeOH) *m/z* 227.09 ([M+Na]$^+$, 100%). **HRMS** (*+ve* ESI FTICR, MeOH) *m/z* calculated for $C_{13}H_{16}NaO_2$ [M+Na]$^+$: 227.1043, found 227.1044 ($|\Delta_{m/z}|$ = 0.4 ppm).

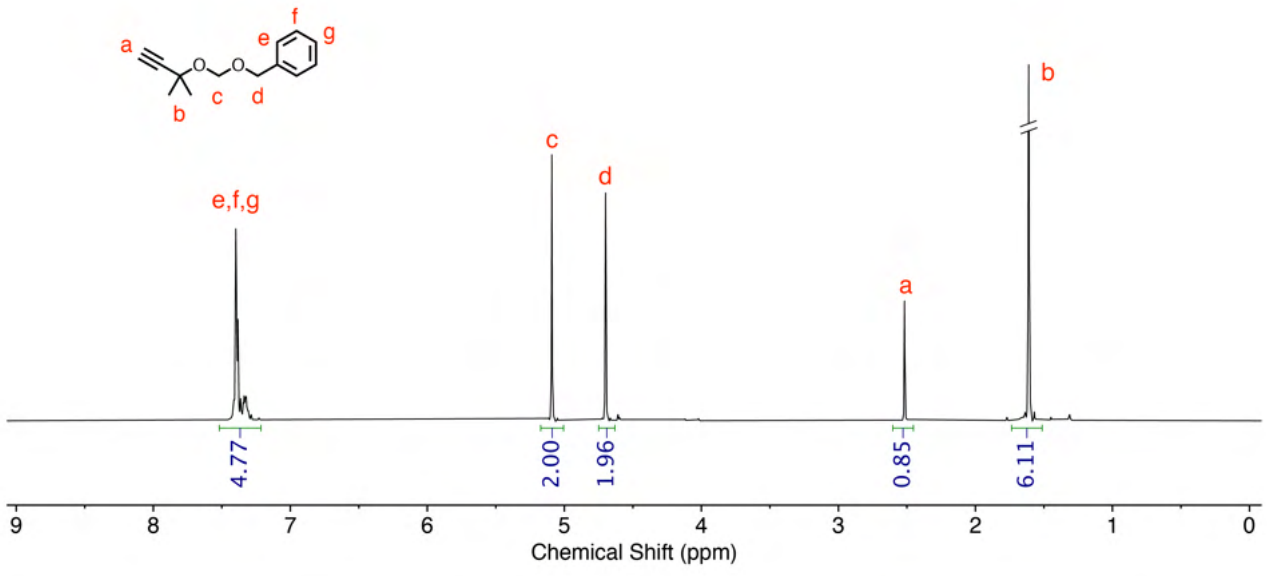

Figure S25. ^{1}H NMR spectrum (400 MHz, 300 K, $CDCl_3$) of compound **S1c.**

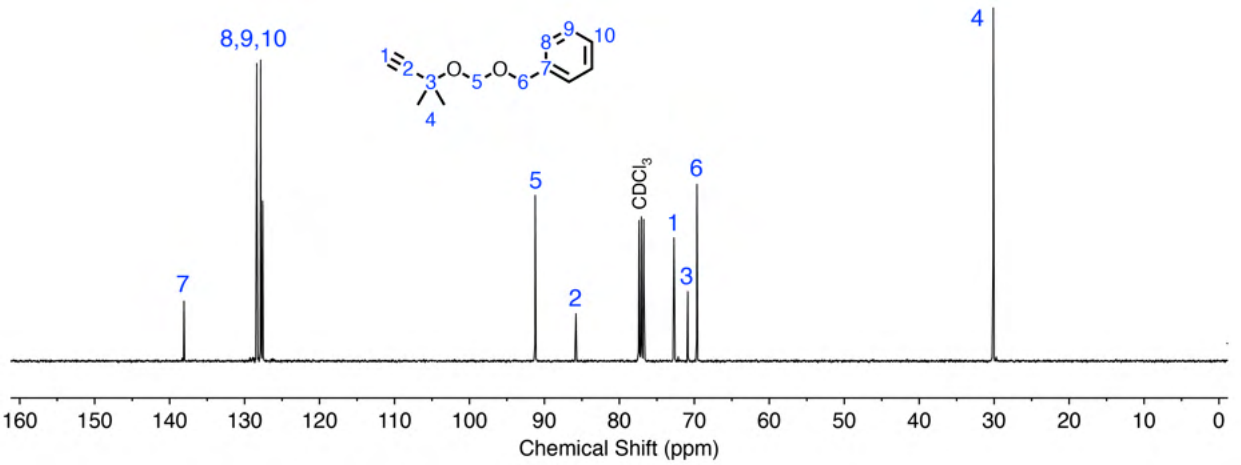

Figure S26. ^{13}C NMR spectrum (100 MHz, 300 K, $CDCl_3$) of compound **S1c.**

S5.2. Synthesis of model compounds 1a-c

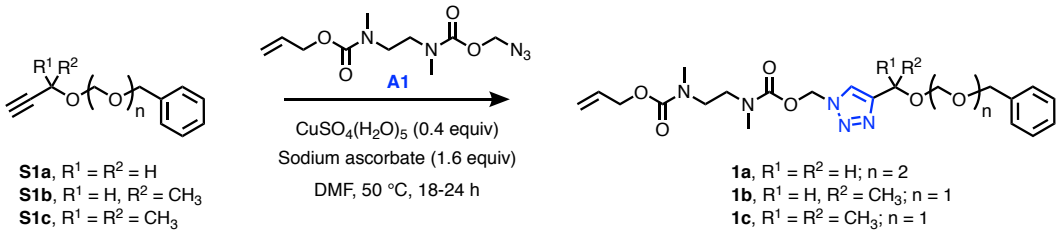

S1a, $R^1 = R^2 = H$
S1b, $R^1 = H$, $R^2 = CH_3$
S1c, $R^1 = R^2 = CH_3$

1a, $R^1 = R^2 = H$; n = 2
1b, $R^1 = H$, $R^2 = CH_3$; n = 1
1c, $R^1 = R^2 = CH_3$; n = 1

***Representative procedure*:** Method adapted from literature procedure.[5] Compound **S1a** (102 mg, 0.49 mmol), azide **A1** (107 mg, 0.39 mmol), copper(II) sulfate pentahydrate (55 mg, 0.22 mmol), and sodium ascorbate (165 mg, 0.83 mmol) were dissolved in DMF (1 mL). The reaction mixture was sparged with N_2 for 15 min then the reaction was stirred at 50 ºC overnight (16-20 h). The reaction mixture was diluted with EtOAc (20 mL), washed with aqueous EDTA (2% *w*/*v*, 3 × 20 mL), water (5 × 20 mL) and brine (2 × 20 mL). The organic layer was dried over magnesium sulfate then concentrated *in vacuo*. The crude product was purified by silica gel chromatography to furnish compound **1a**.

S5.2.1. Characterization data for compound 1a

Compound **1a** was purified via chromatography (hexane/EtOAc 2:8) to afford the purified product as a yellow oil (100 mg, 0.21 mmol, 54% yield). **^{1}H NMR** (400 MHz, DMSO-d_6) δ_H 8.43 – 8.00 (m, 1H), 7.43 – 7.20 (m, 5H), 6.25 (d, J = 3.9 Hz, 2H), 5.89 (dq, J = 16.4, 4.5 Hz, 1H), 5.40 – 5.13 (m, 2H), 4.85 (s, 4H), 4.68 (s, 2H), 4.61 (s, 2H), 4.55 – 4.35 (m, 2H), 3.48 – 3.20 (m, 4H), 2.93 – 2.68 (m, 6H). **^{13}C NMR** (100 MHz, DMSO-d_6) δ_C 156.7 – 155.2 (m), 155.0 – 153.9 (m), 144.5, 138.4, 134.8 – 133.3 (m), 128.7, 128.1, 128.0, 125.6, 119.1 – 115.5 (m), 91.7, 91.6 – 91.1 (m), 71.1, 69.7, 66.0 – 64.6 (m), 60.8, 48.4 – 44.8 (m), 35.7 – 33.5 (m). **LRMS** (+*ve* ESI, MeOH) *m*/*z* 500.23 ([M+Na]$^+$, 100%). **HRMS** (+*ve* ESI FTICR, MeOH) *m*/*z* calculated for $C_{22}H_{31}N_5NaO_7$ [M+Na]$^+$: 500.2116, found 500.2117 ($|\Delta_{m/z}|$ =0.4 ppm).

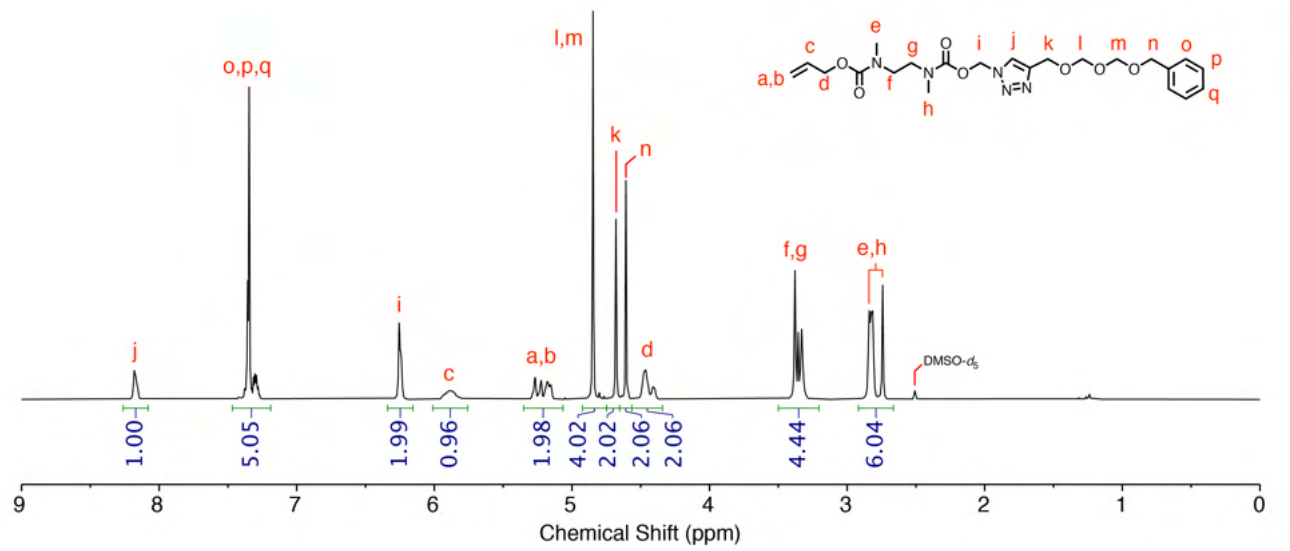

Figure S27. [1]H NMR spectrum (400 MHz, 300 K, DMSO-d_6) of compound **1a**. Complex splitting of H_d-H_h is attributed to slowly interconverting rotameric forms of the carbamate groups.

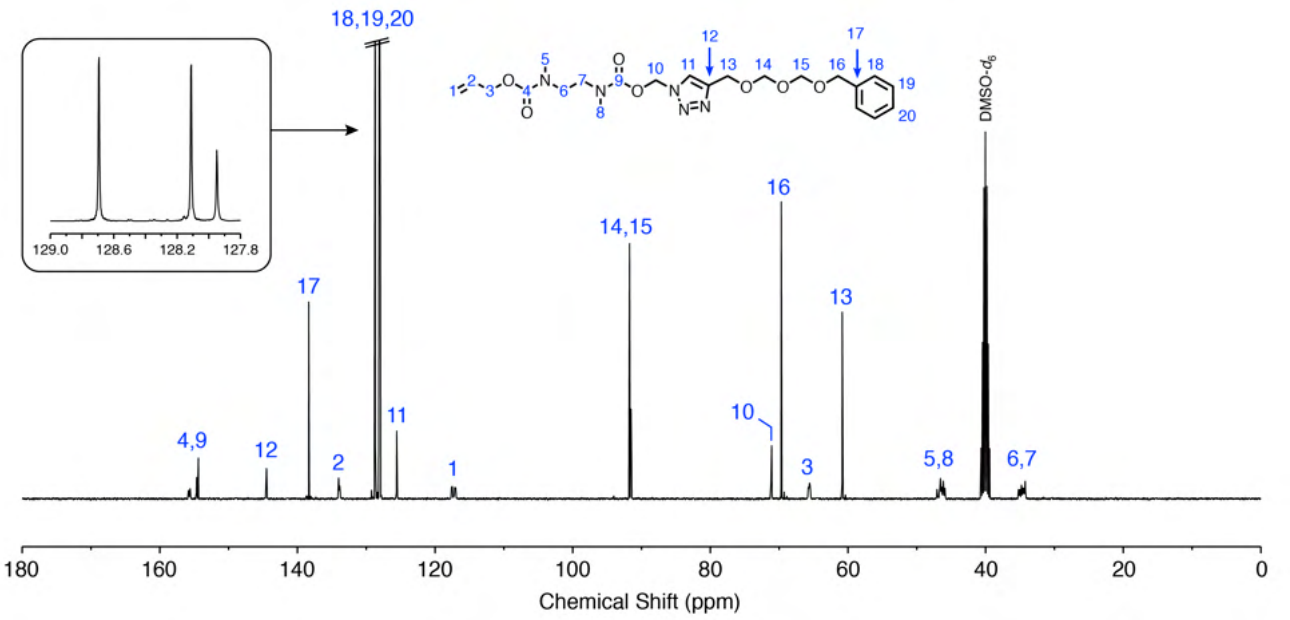

Figure S28. [13]C NMR spectrum (100 MHz, 300 K, DMSO-d_6) of compound **1a.** Similar to the [1]H spectrum, complex splitting of C_5-H_8 is attributed to the presence of carbamate rotamers.

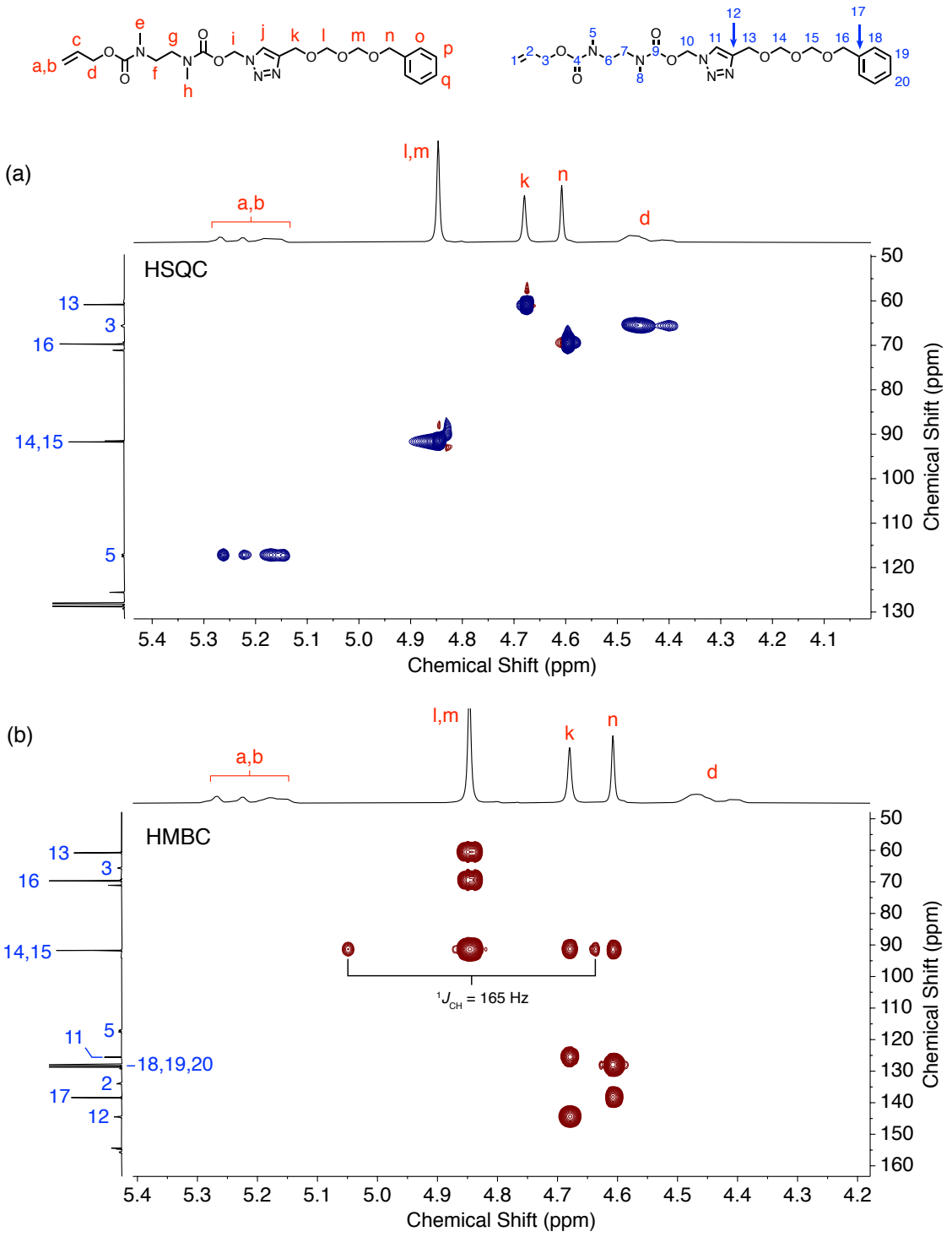

Figure S29. ^{1}H-^{13}C (a) HSQC and (b) HMBC correlation spectra (400/100 MHz, 300 K, DMSO-d_6) of compound **1a**. HSQC is phase-sensitive with all contours showing the same phase sign, consistent with all pictured signals representing methylene (CH_2) environments. In the HMBC, a $^1J_{CH}$ artifact is labelled with its characteristic coupling constant.

S5.2.2. **Characterization data for compound 1b**

Compound **1b** was purified via chromatography (hexane/EtOAc 3:7) to afford the purified product as a yellow oil (155 mg, 0.34 mmol, 56% yield). **^{1}H NMR** (400 MHz, DMSO-d_6) δ_H 8.28 – 8.00 (m, 1H), 7.48 – 7.18 (m, 5H), 6.24 (s, 2H), 6.02 – 5.77 (m, 1H), 5.38 – 5.08 (m, 2H), 4.98 (q, J = 6.6 Hz, 1H), 4.77 (dd, J = 7.0 Hz, 2H), 4.58 (q, J = 11.9 Hz, 2H), 4.51 – 4.33 (m, 2H), 3.54 – 3.20 (m, 4H), 2.99 – 2.63 (m, 6H), 1.51 (d, J = 6.6 Hz, 3H). **^{13}C NMR** (100 MHz, DMSO-d_6) δ_C 156.7 – 155.3 (m), 155.3 – 153.3 (m), 149.7, 138.5, 134.7 – 132.7 (m), 128.7, 128.1, 127.9, 124.4 – 123.3 (m), 118.6 – 116.1 (m), 94.1 – 91.3 (m), 71.7 – 70.4 (m), 69.3, 66.8, 66.1 – 65.0 (m), 48.3 – 44.9 (m), 35.9 – 33.3 (m), 21.2. **LRMS** (+*ve* ESI, MeOH) *m/z* 484.23 ([M+Na]$^+$, 100%). **HRMS** (+*ve* ESI FTICR, MeOH) *m/z* calculated for $C_{22}H_{31}N_5NaO_6$ [M+Na]$^+$: 484.2167, found 484.2168 ($|\Delta_{m/z}|$ =0.4 ppm).

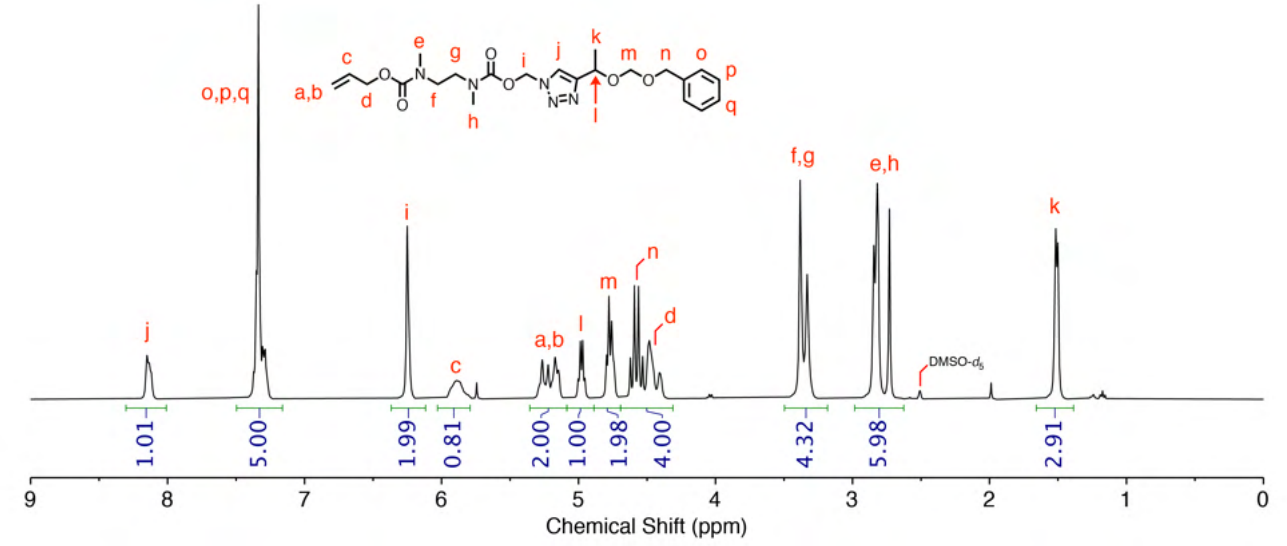

Figure S30. ^{1}H NMR spectrum (400 MHz, 300 K, DMSO-d_6) of compound **1b.** Complex splitting of signals (e.g., H_d, H_e, H_f, H_j, etc.) is attributed to carbamate rotamers.

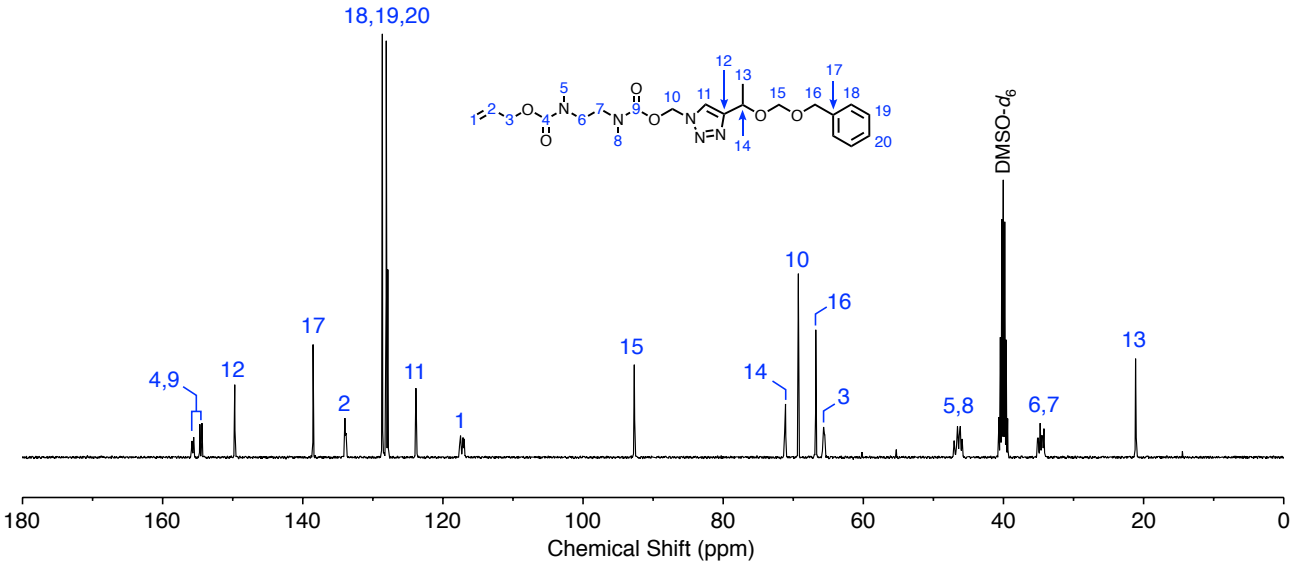

Figure S31. ^{13}C NMR spectrum (100 MHz, 300 K, DMSO-d_6) of compound **1b**. Complex splitting of signals (e.g., C_5, C_8, etc.) is attributed to carbamate rotamers.

S5.2.3. **Characterization data for compound 1c**

Compound **1c** was purified via chromatography (hexane/EtOAc 3:7) to afford the purified product as a yellow oil (23 mg, 0.048 mol, 32% yield). **^{1}H NMR** (400 MHz, DMSO-d_6) δ_H 8.28 – 7.98 (m, 1H), 7.46 – 7.14 (m, 5H), 6.20 (d, J = 5.4 Hz, 2H), 5.87 (d, J = 14.4 Hz, 1H), 5.19 (ddd, J = 29.2, 14.7, 6.6 Hz, 2H), 4.69 (s, 2H), 4.59 – 4.29 (m, 4H), 3.50 – 3.14 (m, 4H), 2.98 – 2.61 (m, 6H), 1.61 (s, 6H). **^{13}C NMR** (100 MHz, DMSO-d_6) δ_C 156.4 – 155.0 (m), 154.8 – 153.8 (m), 152.4, 138.7, 134.0, 128.6, 128.0, 127.8, 123.6, 118.1 – 116.7 (m), 89.9, 73.1, 71.2, 69.0, 65.6, 48.8 – 44.3 (m), 36.1 – 33.7 (m), 28.1. **LRMS** (+*ve* ESI, MeOH) *m/z* 498.26 ([M+Na]$^+$, 100%). **HRMS** (+*ve* ESI FTICR, MeOH) *m/z* calculated for $C_{23}H_{33}N_5NaO_6$ [M+Na]$^+$: 498.2323, found 498.2324 ($|\Delta_{m/z}|$ =0.1 ppm).

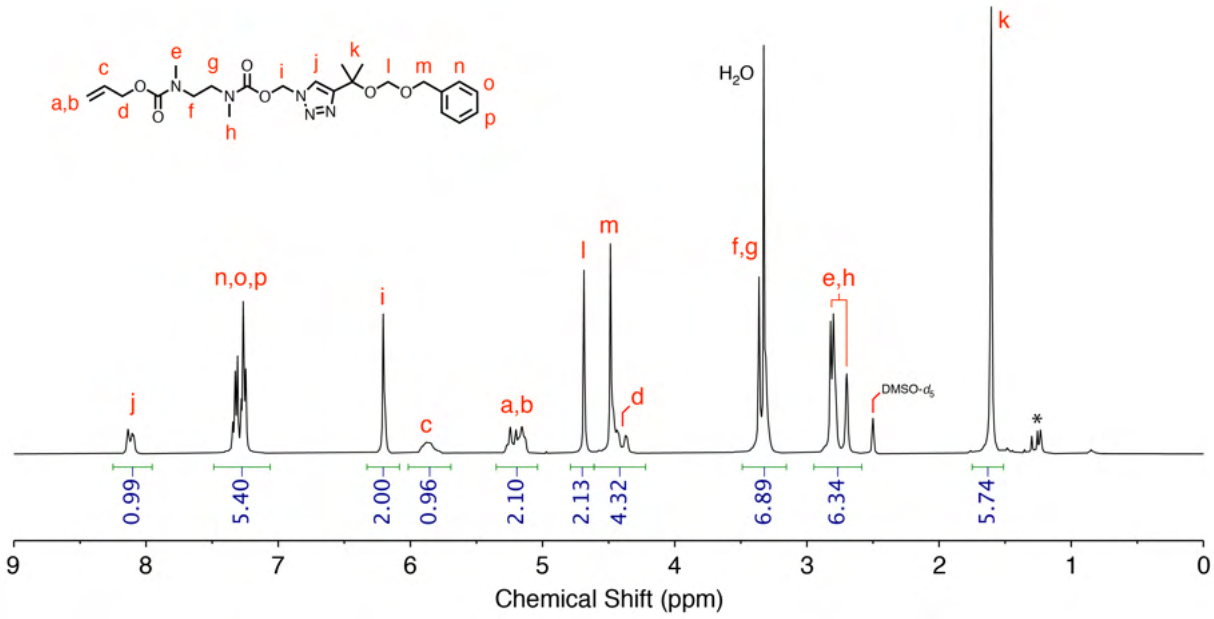

Figure S32. ^{1}H NMR spectrum (400 MHz, 300 K, DMSO-d_6) of compound **1c.** Complex splitting of signals (e.g., H_e, H_f, H_j, etc.) is attributed to carbamate rotamers. Asterisk denotes residual grease.

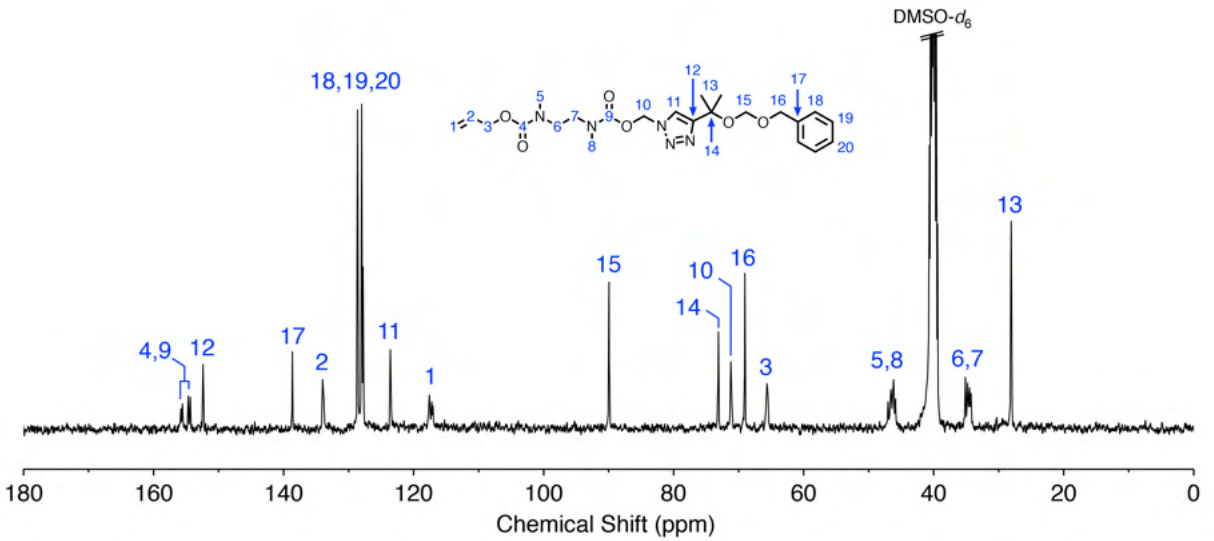

Figure S33. ^{13}C NMR spectrum (100 MHz, 300 K, DMSO-d_6) of compound **1c**. Complex splitting of signals (e.g., C_5, C_8, etc.) is attributed to carbamate rotamers.

S6. Synthesis of allyl-capped carbonate-bridged model compounds

S6.1. Synthesis of compound S3a

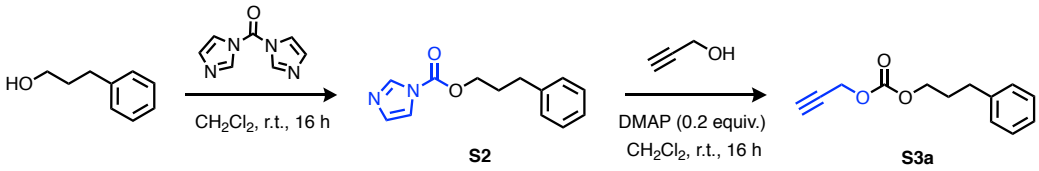

Method adapted from literature procedures.[6] An oven-dried round-bottom flask was charged with *N,N'*-carbonyldiimidazole (CDI) (754 mg, 4.65 mmol) and anhydrous CH_2Cl_2 (20 mL) and placed under a nitrogen atmosphere. 3-Phenyl-1-propanol (400 mg, 2.94 mmol) was added dropwise over 5 min to the reaction mixture, resulting in dissolution of the suspended CDI. The mixture was stirred at room temperature overnight (~18 h), then washed with water (2 × 20 mL). The organic layer was dried over $MgSO_4$, filtered and the solvent removed *in vacuo* to afford intermediate **S2** as a pale yellow, wet-looking solid (413 mg, 1.79 mmol, 61%) that was sufficiently pure for further reaction. Crude **S2** was treated with propargyl alcohol (250 mg, 4.46 mmol) in dry CH_2Cl_2 (20 mL). A catalytic amount of 4-(dimethylamino)pyridine (50 mg, 0.43 mmol) was added and the mixture stirred at room temperature overnight (~16 h). The mixture was then washed with water (3 × 20 mL), dried over $MgSO_4$, filtered and the solvent removed *in vacuo* to afford the crude product. Following silica gel chromatography (hexane:EtOAc 7:3), compound **3a** was obtained as a pale-yellow oil (333 mg, 1.53 mmol, 52% yield over 2 steps). **^{1}H NMR** (400 MHz, $CDCl_3$) δ_H 7.50 – 7.01 (m, 5H), 4.77 (d, J = 2.5 Hz, 2H), 4.24 (t, J = 6.5 Hz, 2H), 2.77 (t, J = 7.7 Hz, 2H), 2.60 (t, J = 2.4 Hz, 1H), 2.15 – 1.98 (m, 2H). **^{13}C NMR** (100 MHz, $CDCl_3$) δ_C 154.5, 140.8, 128.4, 128.4, 126.0, 77.1, 75.7, 67.7, 55.1, 31.7, 30.1. **LRMS** (*+ve* ESI, MeOH) *m/z* 241.01 ([M+Na]$^+$, 100%). **HRMS** (*+ve* ESI FTICR, MeOH) *m/z* calculated for $C_{13}H_{14}NaO_3$ [M+Na]$^+$: 241.0835, found 241.0836 ($|\Delta_{m/z}|$ =0.6 ppm).

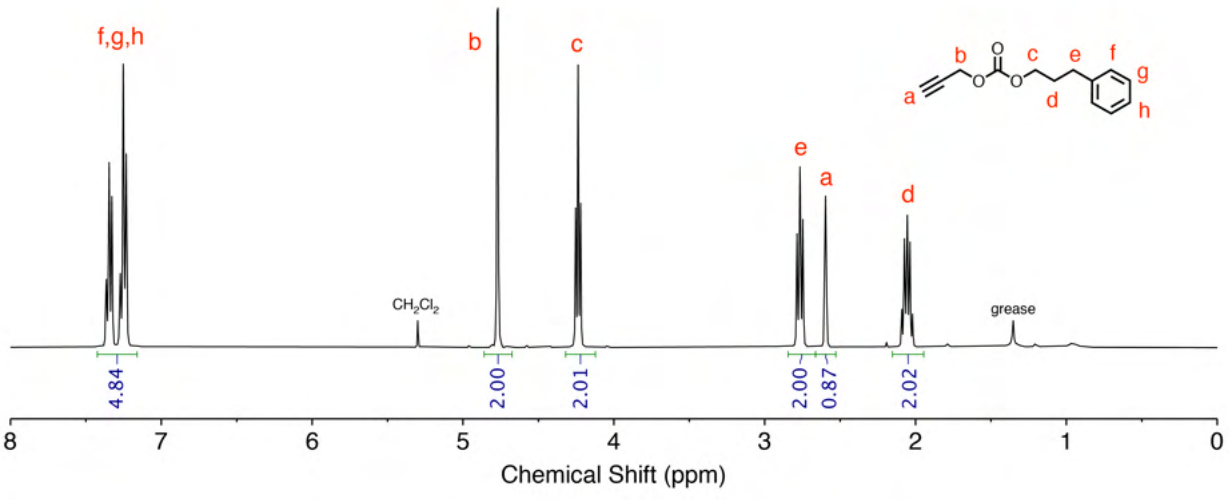

Figure S34. ^{1}H NMR spectrum (400 MHz, 300 K, $CDCl_3$) of compound **S3a.**

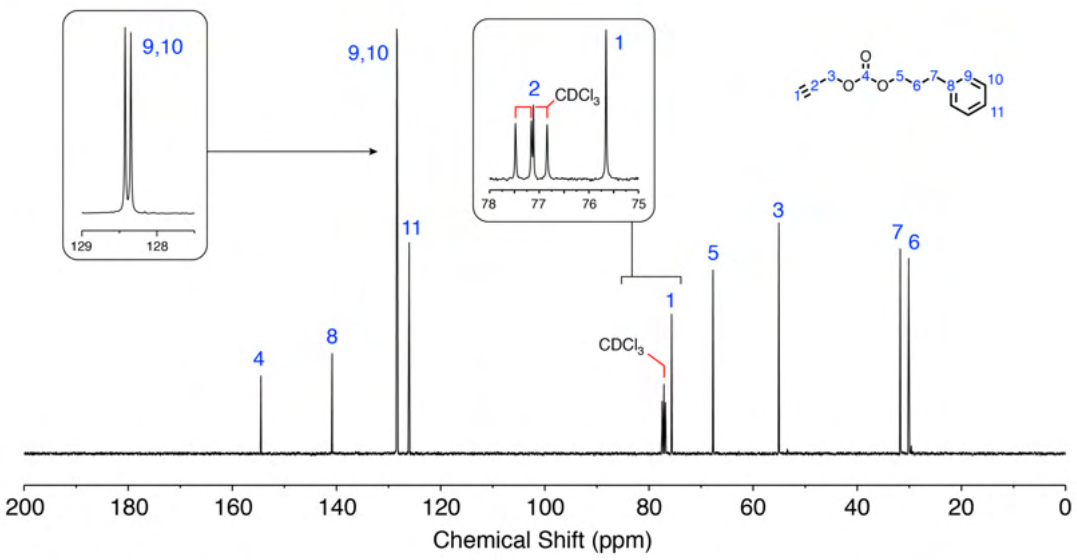

Figure S35. ^{13}C NMR spectrum (100 MHz, 300 K, $CDCl_3$) of compound **S3a.**

S6.2. Synthesis of compound S3b

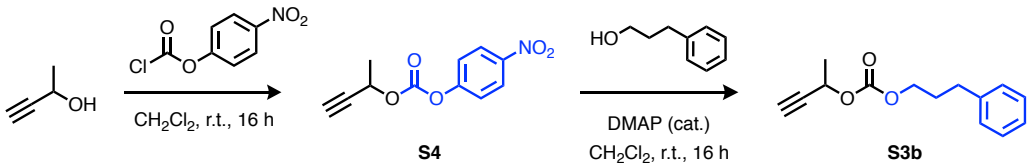

Pyridine (69 mg, 0.87 mmol) was added to a solution of 4-nitrophenyl chloroformate (162 mg, 0.806 mmol) in dry CH_2Cl_2 (10 mL), resulting in the formation of a white suspension. 3-Butyn-2-ol (52 mg, 0.74 mmol) was added dropwise over 15 min and the mixture stirred at room temperature overnight (~18 h). The solvent was removed under reduced pressure and the crude product redissolved in ethyl acetate (5 mL), and washed with aqueous HCl (1 M, 15 mL), water (2 × 10mL) and brine (1 × 10mL). The organic layer was dried over $MgSO_4$ and concentrated under reduced pressure, yielding **S4** as a beige-colored solid (170 mg, 99%) which was sufficiently pure for further reaction. **S4** (170 mg, 0.723 mmol) was treated with 3-phenyl-1-propanol (90 mg, 0.66 mmol), pyridine (49 mg, 0.62 mmol) and 4-dimethylaminopyridine (9 mg, 0.08 mmol) in CH_2Cl_2 (16 mL) and allowed to stir room temperature for 42 h. The mixture was washed with water (3 × 10 mL), dried over $MgSO_4$, and concentrated under reduced pressure. The crude mixture was purified via chromatography (7:3) to afford the product as a light-yellow oil (148 mg, 0.64 mmol, 86% yield over 2 steps).

^{1}H NMR (400 MHz, $CDCl_3$) δ_H 7.38 – 7.29 (m, 2H), 7.29 – 7.17 (m, 3H), 5.35 (qd, J = 6.7, 2.1 Hz, 1H), 4.21 (dt, J = 9.0, 6.5 Hz, 2H), 2.88 – 2.71 (m, 2H), 2.56 (d, J = 2.1 Hz, 1H), 2.12 – 1.97 (m, 2H), 1.61 (d, J = 6.7 Hz, 3H). **^{13}C NMR** (100 MHz, $CDCl_3$) δ_C 154.3, 141.0, 128.5, 128.4, 126.1, 81.5, 73.8, 67.6, 63.9, 31.9, 30.2, 21.3. **LRMS** (+*ve* ESI, MeOH) *m/z* 255.12 ([M+Na]$^+$, 100%). **HRMS** (+*ve* ESI FTICR, MeOH) *m/z* calculated for $C_{14}H_{16}NaO_3$ [M+Na]$^+$: 255.0992, found 255.0993 ($|\Delta_{m/z}|$ =0.4 ppm).

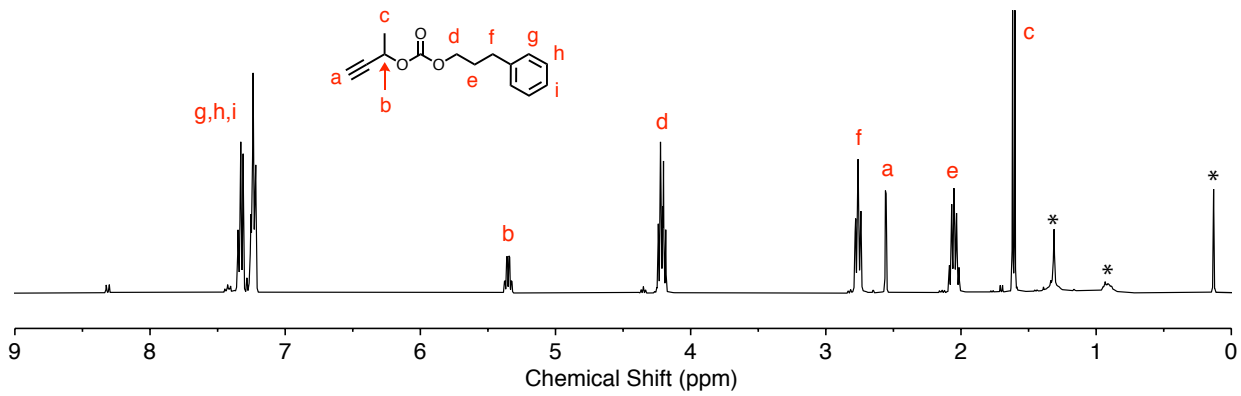

Figure S36. ^{1}H NMR spectrum (400 MHz, 300 K, $CDCl_3$) of compound **S3b.**

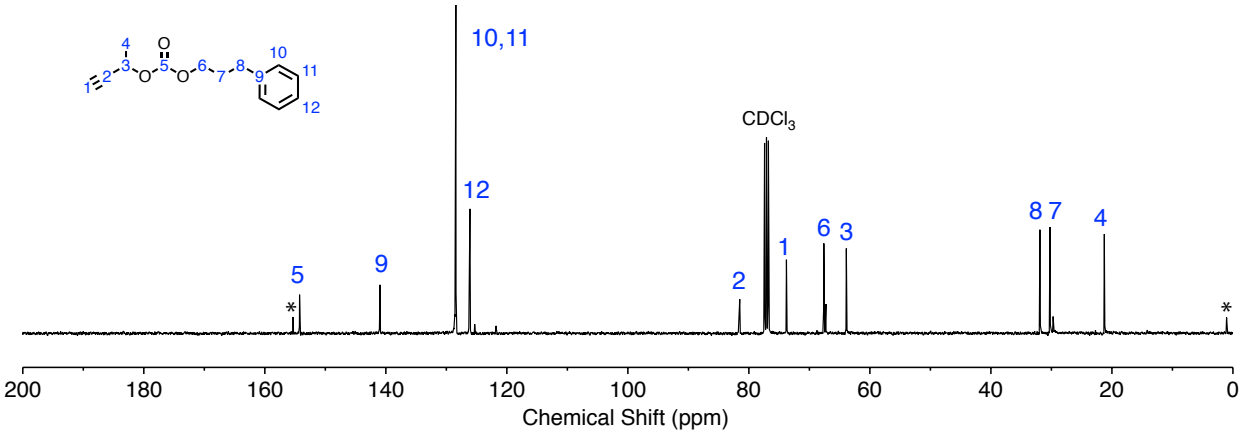

Figure S37. ^{13}C NMR spectrum (100 MHz, 300 K, $CDCl_3$) of compound **S3b.**

S6.3. Synthesis of model compounds 2a-b

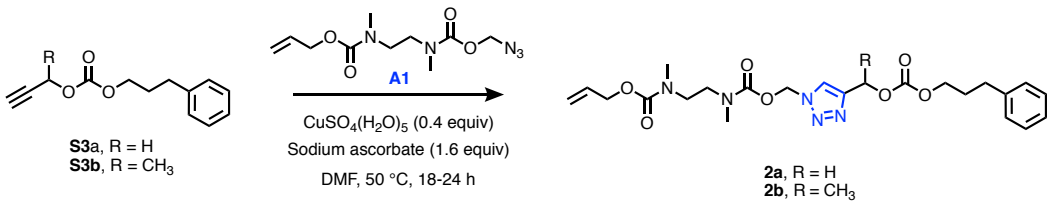

Compounds **2a-b** were synthesized using the same CuAAC protocol as compounds **1a-c** (see p. 19).

S6.3.1. Characterization data for model compound 2a

Compound **2a (**hexane/EtOAc 3:7) was obtained as a colorless oil (146 mg, 0.297 mmol, 64%).

^{1}H NMR (400 MHz, DMSO-d_6) δ_H 8.37 – 8.09 (m, 1H), 7.37 – 7.09 (m, 5H), 6.26 (d, J = 4.1 Hz, 2H), 5.36 – 5.01 (m, 4H), 4.58 – 4.26 (m, 2H), 4.10 (t, J = 6.5 Hz, 2H), 3.48 – 3.20 (m, 4H), 2.97 – 2.68 (m, 6H), 2.62 (dd, J = 8.7, 6.7 Hz, 2H), 2.01 – 1.76 (m, 2H). **^{13}C NMR** (100 MHz, DMSO-d_6) δ_C 155.3, 155.1, 154.3, 154.1, 153.9, 142.1 – 141.6 (m), 140.9, 133.7 – 133.1 (m), 128.3, 128.2, 126.1, 125.8, 117.4 – 115.9 (m), 70.6, 67.1, 65.7 – 64.4 (m), 60.1, 47.1 – 44.4 (m), 35.3 – 33.1 (m), 31.1, 29.7. **LRMS** (+*ve* ESI, MeOH) *m/z* 512.24 ([M+Na]$^+$, 100%). **HRMS** (+*ve* ESI FTICR, MeOH) *m/z* calculated for $C_{23}H_{31}N_5O_7Na$ [M+Na]$^+$: 512.2115, found 512.2116 ($|\Delta_{m/z}|$ =0.1 ppm).

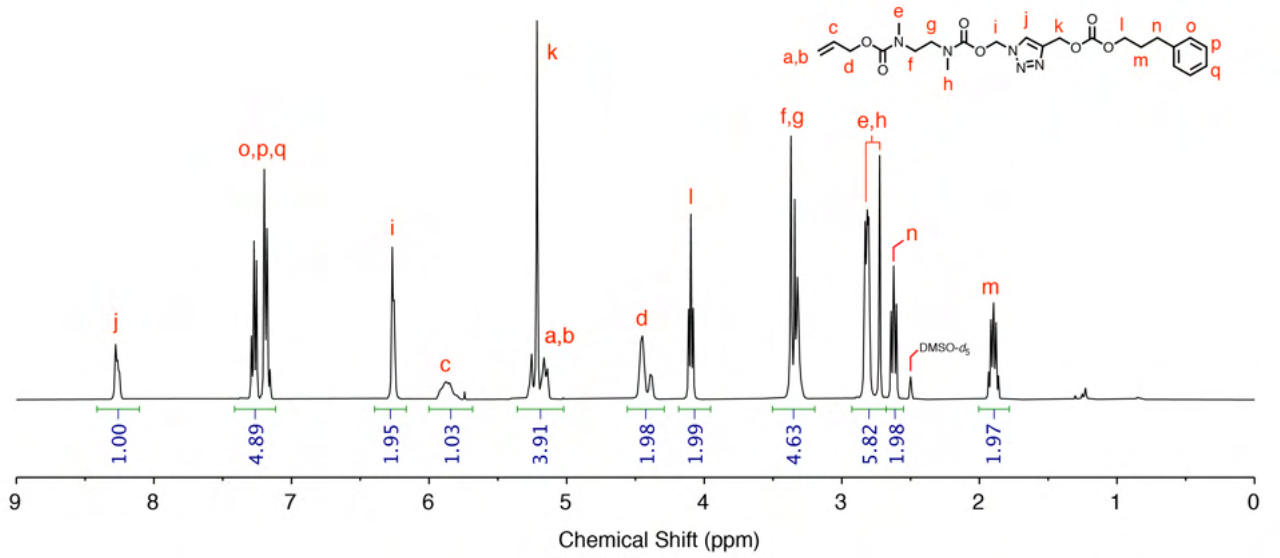

Figure S38. ^{1}H NMR spectrum (400 MHz, 300 K, DMSO-d_6) of compound **2a.**

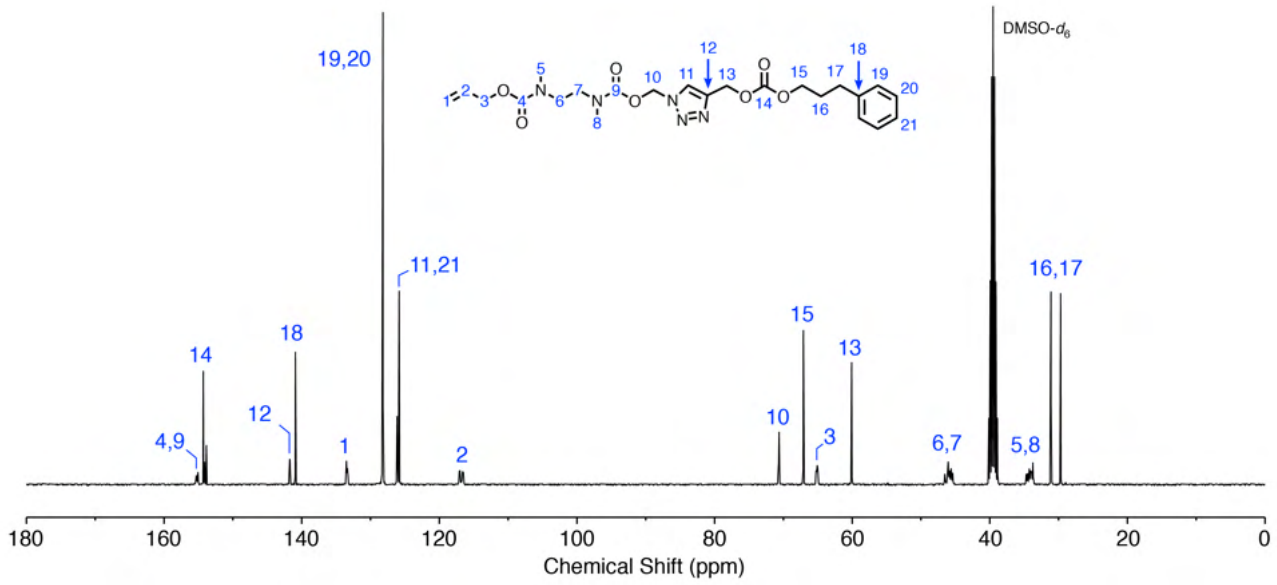

Figure S39. ^{13}C NMR spectrum (100 MHz, 300 K, DMSO-d_6) of compound **2a.**

S6.3.2. **Characterization data for model compound 2b**

Following purification by column chromatography **(**hexane/EtOAc 7:3), compound **2b** was obtained as a colorless oil (35 mg, 0.070 mmol, 55%). **^{1}H NMR** (400 MHz, $CDCl_3$) δ_H 8.31 – 8.09 (m, 1H), 7.43 – 7.07 (m, 5H), 6.24 (d, J = 5.8 Hz, 2H), 5.99 – 5.78 (m, 2H), 5.33 – 5.06 (m, 2H), 4.55 – 4.33 (m, 2H), 4.08 (td, J = 6.7, 2.5 Hz, 2H), 3.36 (d, J = 9.1 Hz, 4H), 2.91 – 2.69 (m, 6H), 2.62 (dd, J = 8.8, 6.7 Hz, 2H), 1.95 – 1.84 (m, 2H), 1.70 – 1.53 (m, 3H). **^{13}C NMR** (100 MHz, $CDCl_3$) δ_C 156.4 – 155.4 (m), 154.9 – 154.3 (m), 147.0, 141.4, 134.7 – 133.1 (m), 129.6 – 127.8 (m), 126.4, 124.8, 117.8 – 116.7 (m), 71.1, 68.7, 67.4, 65.6, 47.7 – 45.2 (m), 35.7 – 33.5 (m), 31.6, 30.2, 19.9. **LRMS** (+*ve* ESI, MeOH) *m/z* 526.23 ([M+Na]$^+$, 100%). **HRMS** (+*ve* ESI FTICR, MeOH) *m/z* calculated for $C_{24}H_{33}N_5NaO_7$ [M+Na]$^+$: 526.2272, found 526.2273 ($|\Delta_{m/z}|$ =0.2 ppm).

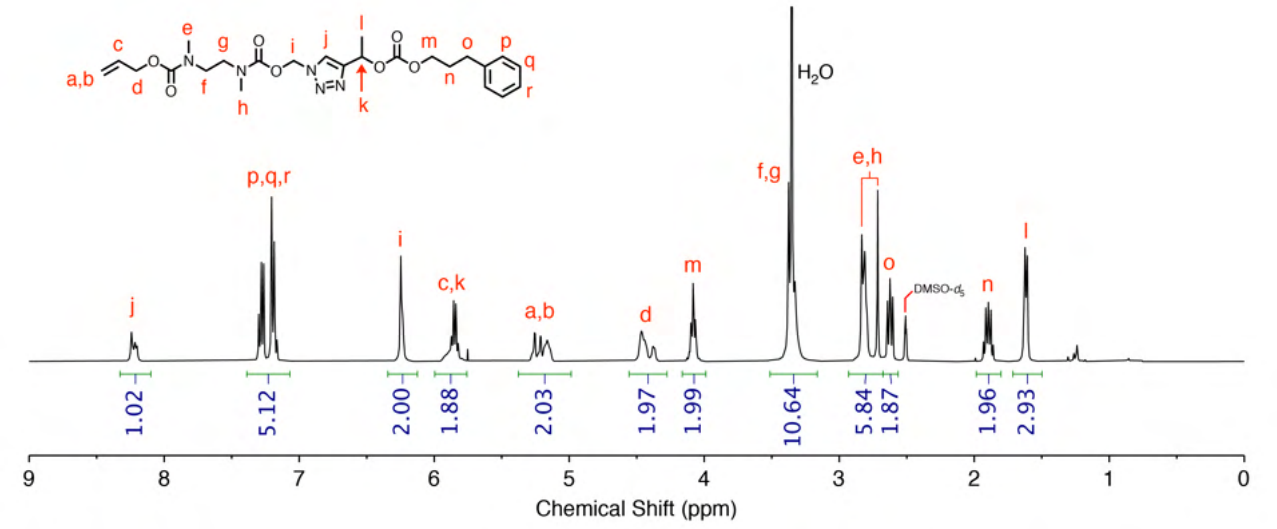

Figure S40. ^{1}H NMR spectrum (400 MHz, 300 K, DMSO-d_6) of compound **2b.**

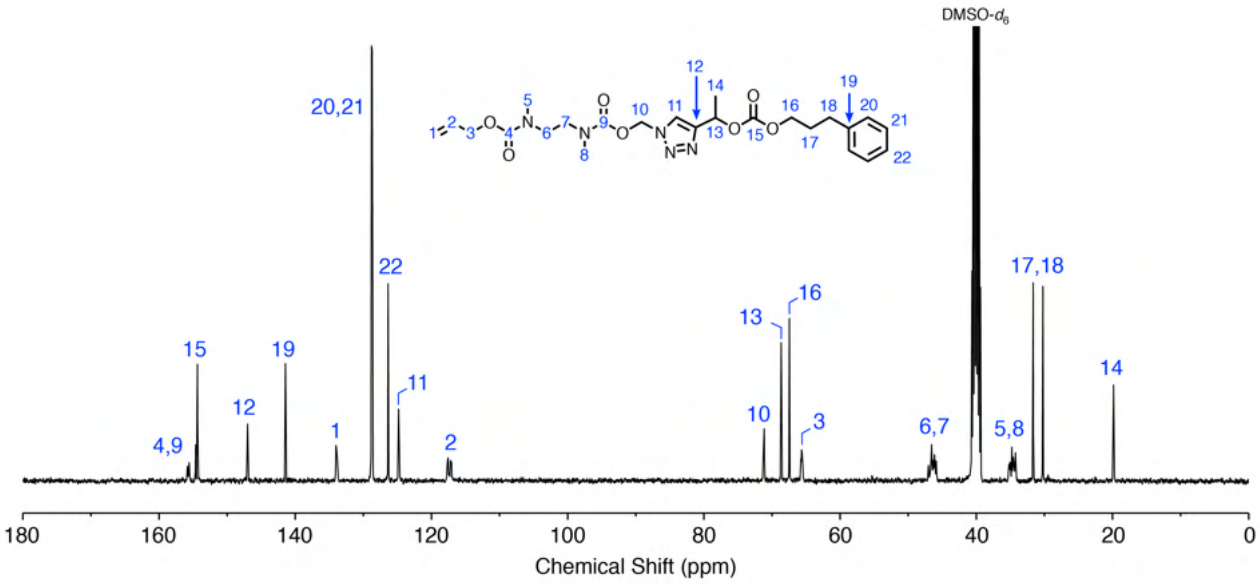

Figure S41. ^{13}C NMR spectrum (100 MHz, 300 K, DMSO-d_6) of compound **2b**.

S7. Synthesis of *o*-nitrobenzyl-capped azide linker (A2)

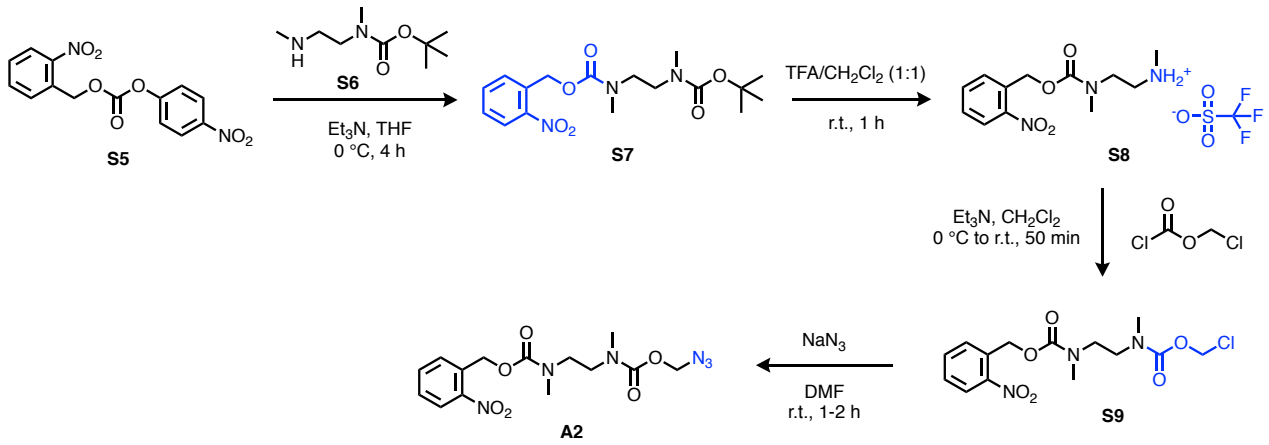

Figure S42. Scheme outlining the synthesis of *o*-nitrobenzyl linker precursor **A2**. Compounds **S5** and **S6** were prepared according to published methods.[7]

S7.1. Synthesis of compound S7

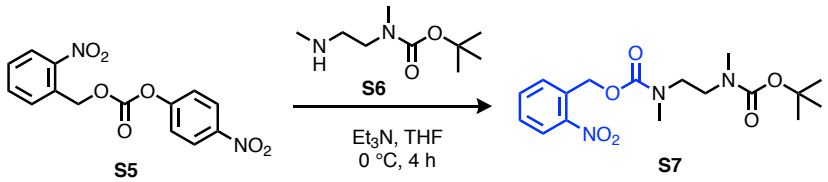

Compound **S6** (0.40 g, 2.1 mmol) and triethylamine (0.32 mL, 2.3 mmol, 1.2 equiv.) were dissolved in dry THF (5 mL) under N_2. Compound **S5** (0.61 g, 1.9 mmol, 1.0 equiv.) was added and the reaction mixture was stirred at 0 °C for 4 h. The crude product was diluted with 20 mL ethyl acetate then washed with aqueous citric acid (0.5 M, 3 × 30 mL) and then the aqueous layers were collected and extracted with EtOAc (3 × 20 mL). The organic layers were combined and dried over $MgSO_4$, filtered, and concentrated *in vacuo*. The product was purified by column chromatography (hexane/EtOAc 1:1) to yield compound **S7** (0.57 g, 1.6 mmol, 81%) as a yellow oil. **^{1}H NMR** (400 MHz, $CDCl_3$) δ_H 8.07 (d, 1H, J = 7.6 Hz), 7.64 (t, 1H, J = 7.3 Hz), 7.53–7.60 (m, 1H), 7.46 (t, 1H, J = 7.5 Hz), 5.51 (s, 2H), 3.40 (bs, 4H), 2.97 (d, 3H, J = 12.4 Hz), 2.86 (d, 3H, J = 10.1 Hz), 1.42 (s, 9H). **^{13}C NMR** (100 MHz, $CDCl_3$) δ_C 28.5, 34.9, 35.5, 46.1–47.5, 64.1, 124.8–125.5, 128.8–129.5, 133.0–133.8, 155.7–155.8. **HRMS** (+ve, EI-MS) Calculated for $C_{17}H_{25}N_3O_6$ [M^+]: 367.1743, found 367.1742. ($|\Delta_{m/z}|$ =0.3 ppm)

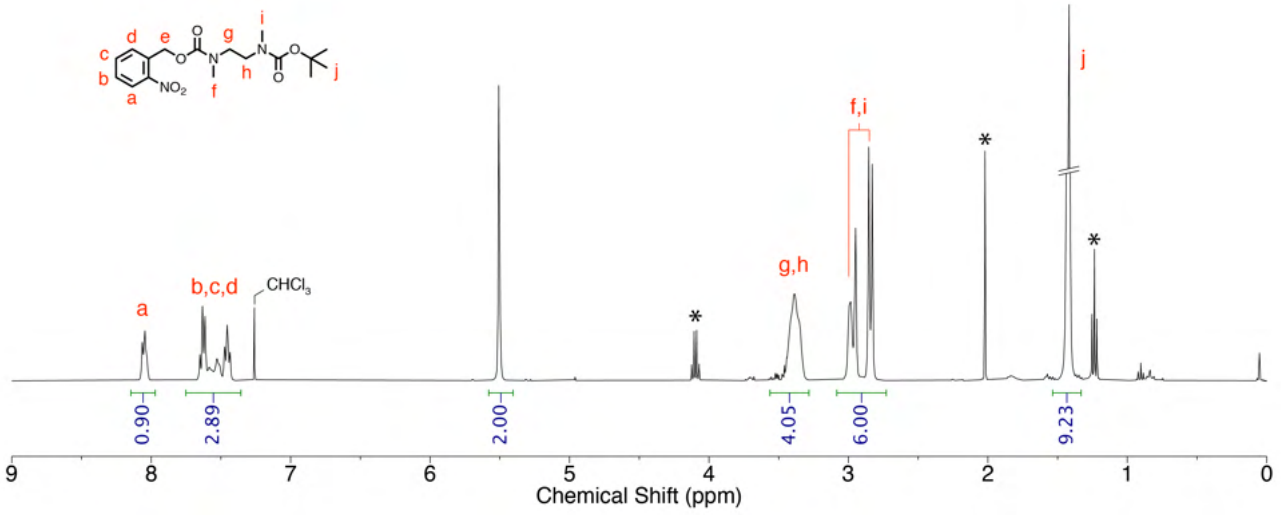

Figure S43. ^{1}H NMR spectrum (400 MHz, 300 K, $CDCl_3$) of compound **S7**. Asterisks correspond to residual ethyl acetate. Complex slitting and lineshape broadening are attributed to carbamate rotamers.

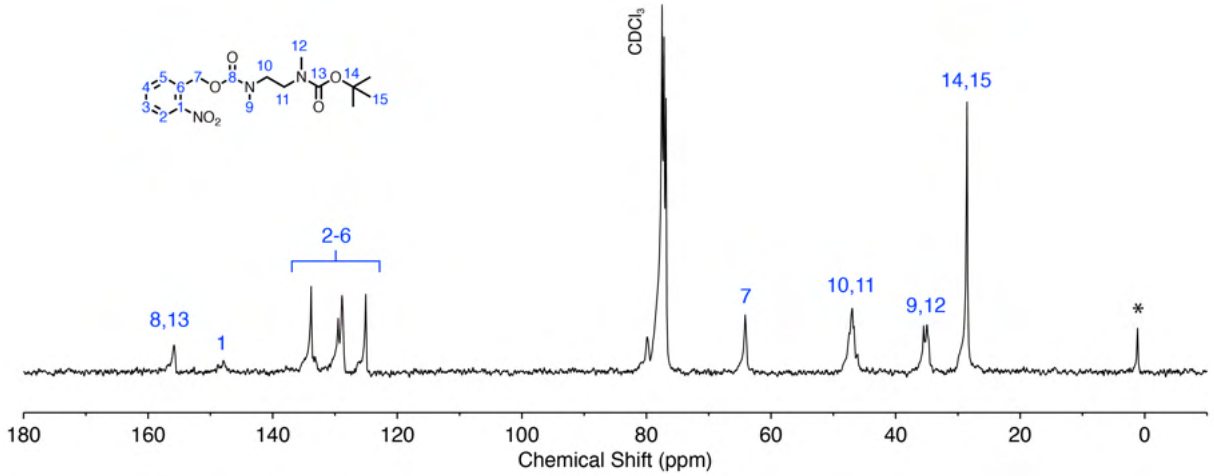

Figure S44. ^{13}C NMR spectrum (100 MHz, 300 K, $CDCl_3$) of compound **S7.** Complex slitting and lineshape broadening are attributed to carbamate rotamers.

S7.2. Synthesis of compound S8

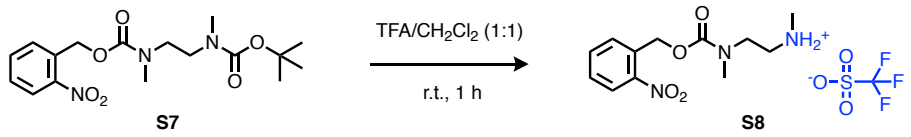

Compound **S7** (96 mg, 0.26 mmol) was dissolved in a 1:1 (*v*/*v*) mixture of trifluoroacetic acid:CH_2Cl_2 (1 mL) and stirred at room temperature for 1 h. CH_2Cl_2 and TFA were removed in vacuo to yield compound **S8** (66 mg, 0.16 mmol, 91%) as a dark yellow oil. **^{1}H NMR** (400 MHz, $CDCl_3$) δ_H 8.84 (bs, 4H), 8.08 (d, 1H, J = 8.2 Hz), 7.67 (t, 1H, J = 7.6 Hz), 7.59 (d, 1H, J = 7.8 Hz), 7.50 (t, 1H, J = 8.5 Hz), 5.50 (s, 2H), 3.66 (t, 2H, J = 5.4 Hz), 3.28 (s, 2H), 3.01 (s, 3H), 2.79 (s, 3H). **^{13}C NMR** (100 MHz, $CDCl_3$): δ_C 33.8, 35.0, 46.3, 48.5, 64.9, 125.1, 129.1, 132.1, 134.1, 147.5, 157.6, 161.6. **HRMS** (+ve, EI-MS) Calculated for $C_{12}H_{18}N_3O_4$ [M+]: 268.1292, found 268.1298 ($|\Delta_{m/z}|$ = 2 ppm).

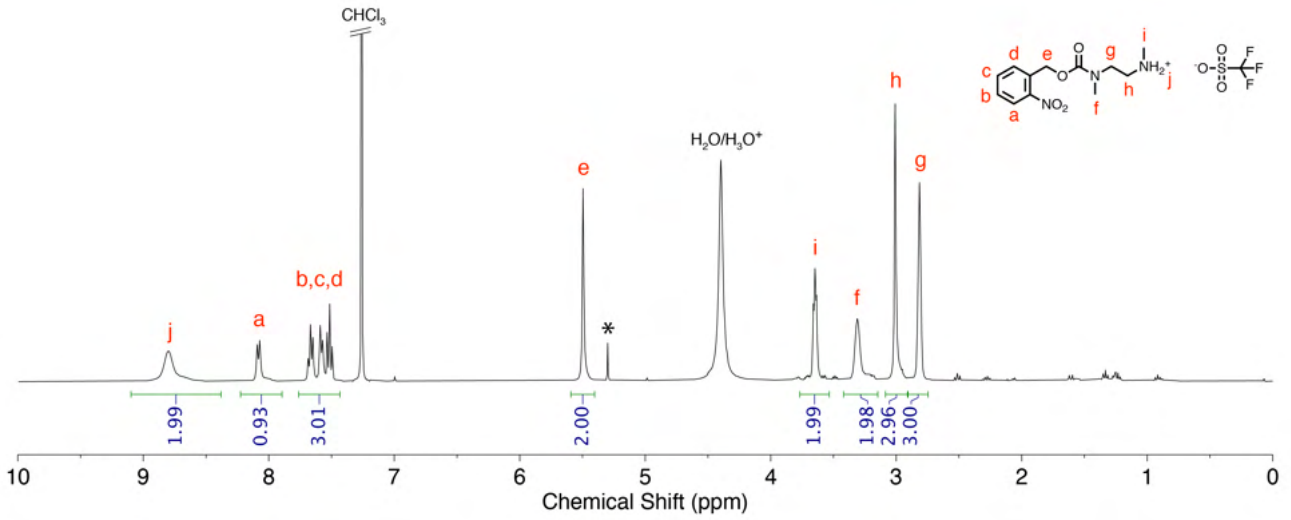

Figure S45. ^{1}H NMR spectrum (400 MHz, 300 K, $CDCl_3$) of compound **S8**. The asterisk corresponds to residual CH_2Cl_2. Complex slitting and lineshape broadening are attributed to carbamate rotamers.

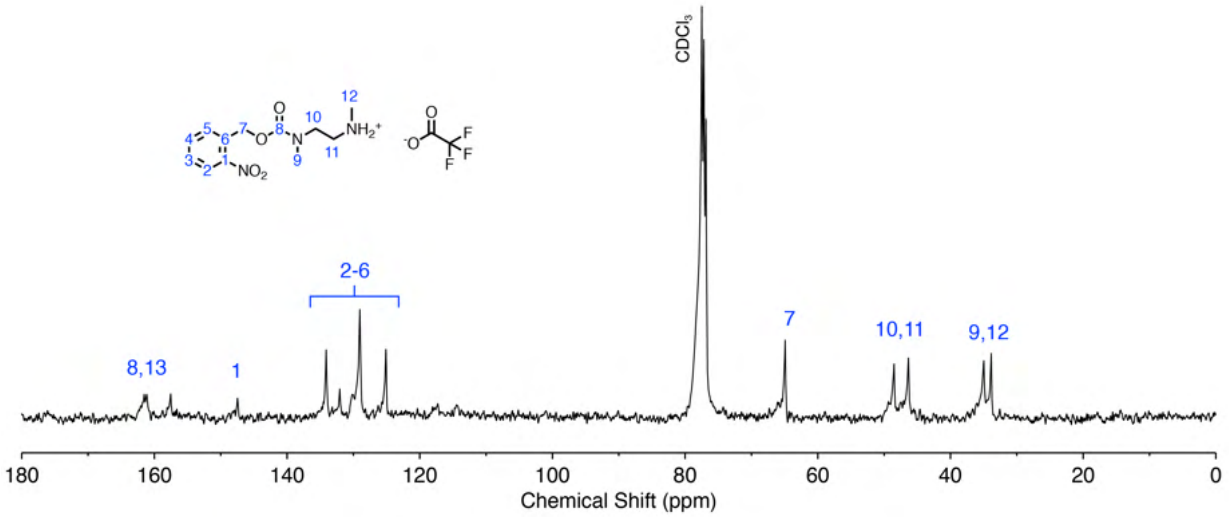

Figure S46. ^{13}C NMR spectrum (100 MHz, 300 K, $CDCl_3$) of compound **S8.** Complex slitting and lineshape broadening are attributed to carbamate rotamers.

S7.3. Synthesis of compound S9

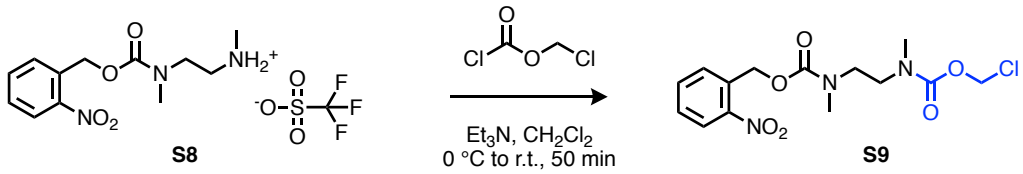

Compound S8 (0.61 g, 2.3 mmol, 1.0 equiv.) was dissolved in 5 mL of dry CH_2Cl_2 and dry Et_3N (0.38 mL, 2.7 mmol, 1.2 equiv.) was added. Chloromethyl chloroformate (0.24 mL, 2.3 mmol, 1.2 equiv.) was added at 0 °C, over 20 min then the reaction mixture was stirred at room temperature for 30 min. To the crude product, 5 mL of deionized water was added, and then the mixture was extracted with CH_2Cl_2 (3 × 5 mL). The organic layers were combined, washed with $NaHCO_3$ (3 × 10 mL) and brine (10 mL). The organic layers were then dried over $MgSO_4$, filtered, and concentrated *in vacuo* to yield compound **S9** (0.50 g, 60%) as a dark amber oil. **^{1}H NMR** (400 MHz, $CDCl_3$) δ_H 8.06 (t, 1H, J = 8.3 Hz), 7.42–7.68 (m, 3H), 5.76 (t, 2H, J = 15.1 Hz), 5.52 (s, 2H), 3.42–3.50 (m, 4H), 2.93–3.02 (m, 6H). **^{13}C NMR** (100 MHz, $CDCl_3$) δ_C 34.6–36.7, 46.7– 48.0, 64.3, 71.0, 125.1–129.8, 133.8, 153.6–155.9. FT-IR (ATR, cm^{-1}): 1578, 1614, 1702, 1786, 2940. **HRMS** (+ve, EI-MS) Calculated for $C_{14}H_{18}ClN_3O_6$ [M+]: 359.0884, found 359.0869 ($|\Delta_{m/z}|$ = 4 ppm).

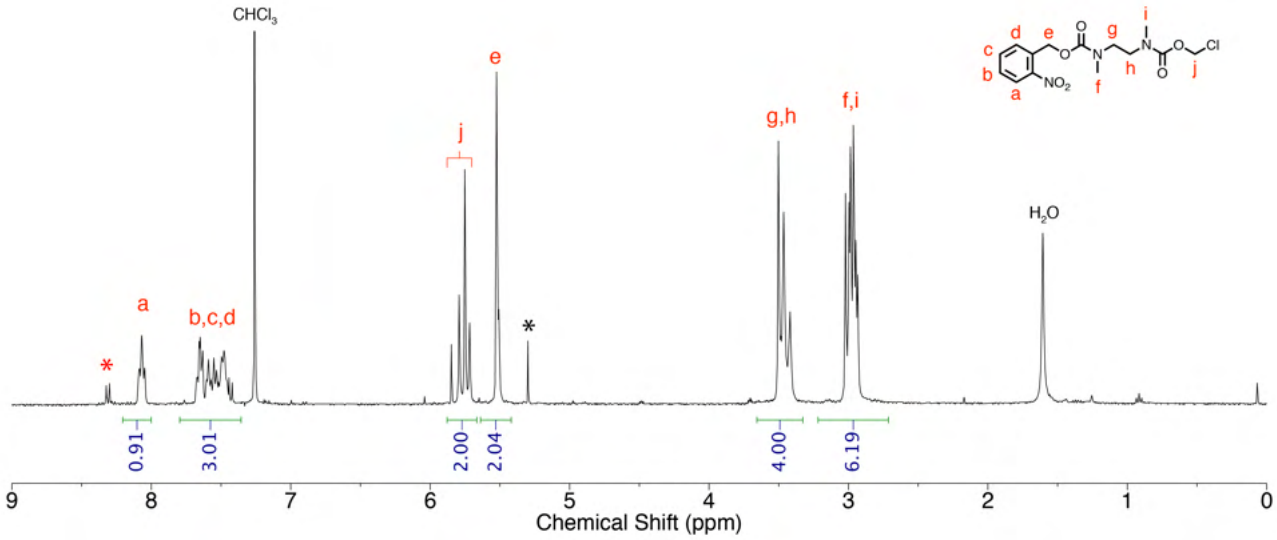

Figure S47. ^{1}H NMR spectrum (400 MHz, 300 K, $CDCl_3$) of compound **S9.** Asterisk denotes residual CH_2Cl_2. Complex slitting and lineshape broadening are attributed to carbamate rotamers.

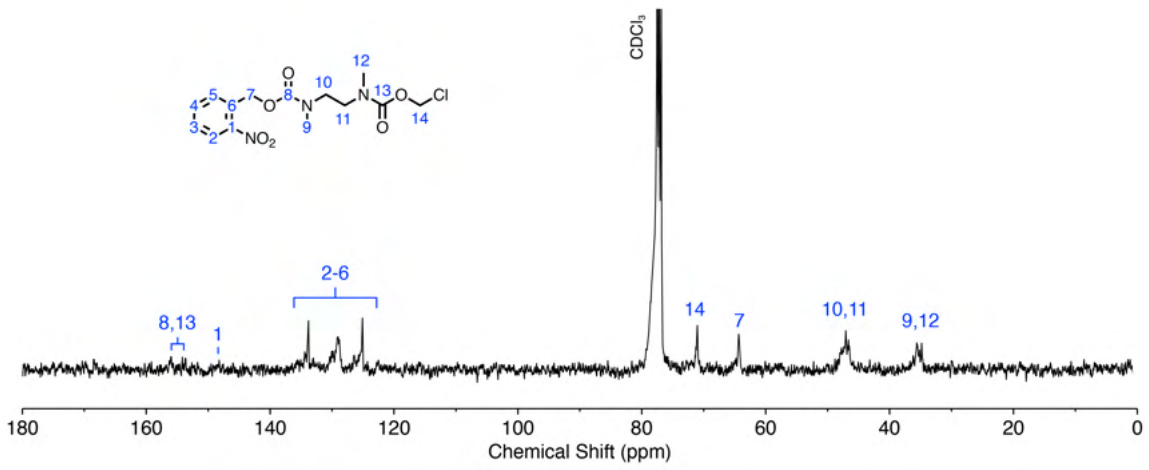

Figure S48. ^{13}C NMR spectrum (100 MHz, 300 K, $CDCl_3$) of compound **S9.** Complex slitting and lineshape broadening are attributed to carbamate rotamers.

S7.4. Synthesis of azide linker A2

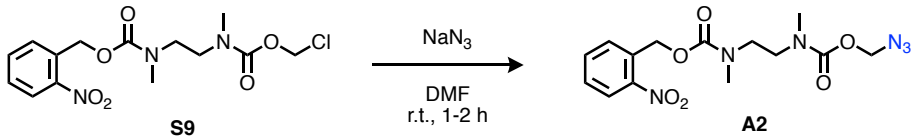

A solution of compound **S9** (0.10 g, 0.28 mmol, 1.1 equiv.) and sodium azide (19 mg, 0.29 mmol, 1.0 equiv.) in in DMF (1 mL) was stirred at room temperature for 1–2 h, monitoring the reaction progress by ^{1}H NMR spectroscopy. Upon completion, the reaction mixture was diluted with EtOAc (30 mL) and washed with deionized water (3 × 5 mL), then washed with brine (5 mL). The organic layers were collected and dried over $MgSO_4$, filtered, and concentrated in vacuo to yield compound **A2** (0.35 g, 55%) a light brown oil. **^{1}H NMR** (400 MHz, $CDCl_3$) δ_H 8.064–8.08 (m, 1H), 7.47–7.66 (m, 1H), 5.52 (s, 2H), 5.13 (t, 2H, J = 14.0 Hz), 3.42–3.49 (m, 4H), 2.93-3.01 (m, 6H). **^{13}C NMR** (100 MHz, CDCl3) δ_C 34.6–35.4, 46.3–47.4, 75.6–75.8, 124.9, 126.5–129.8, 132.3–133.7, 155.1– 155.9. FT-IR (ATR, cm-1): 1525, 1578, 1698, 2107, 2940. **HRMS** (+ve, EI-MS) Calculated for $C_{14}H_{18}N_6O_6$ [M+]: 366.1288, found 366.1277. ($|\Delta_{m/z}|$ = 3 ppm)

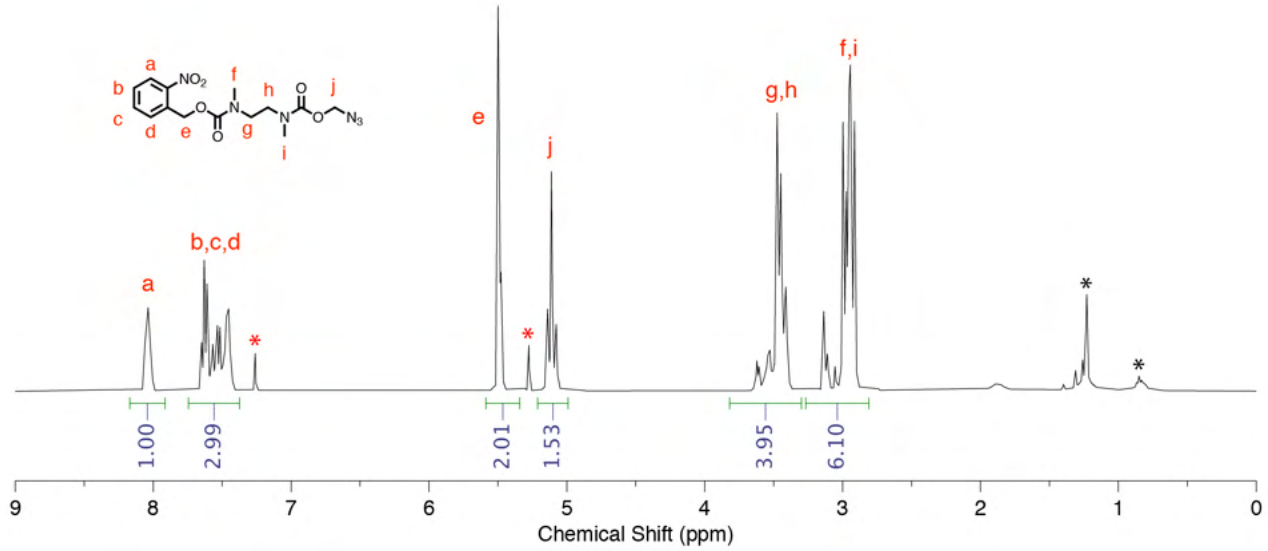

Figure S49. ^{1}H NMR spectrum (400 MHz, 300 K, $CDCl_3$) of compound **A2**. Asterisks denote residual solvent peaks ($CHCl_3$, hexanes, CH_2Cl_2). Note that the spectra are complicated by rotamers about the carbamate bonds.

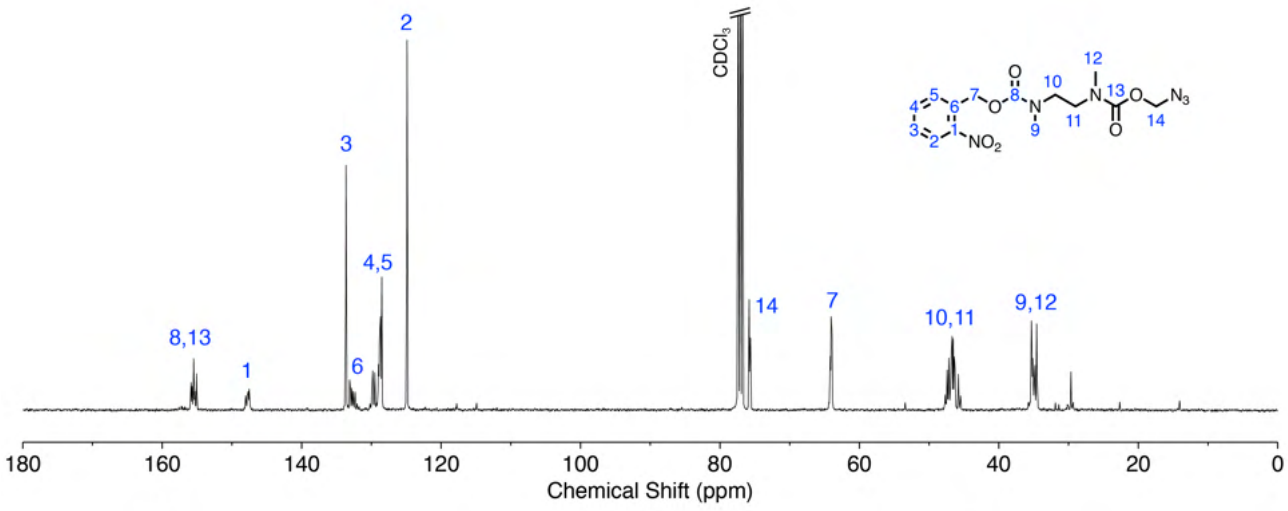

Figure S50. ^{13}C NMR spectrum (100 MHz, 300 K, $CDCl_3$) of compound **A2**. Complex slitting is attributed to carbamate rotamers.

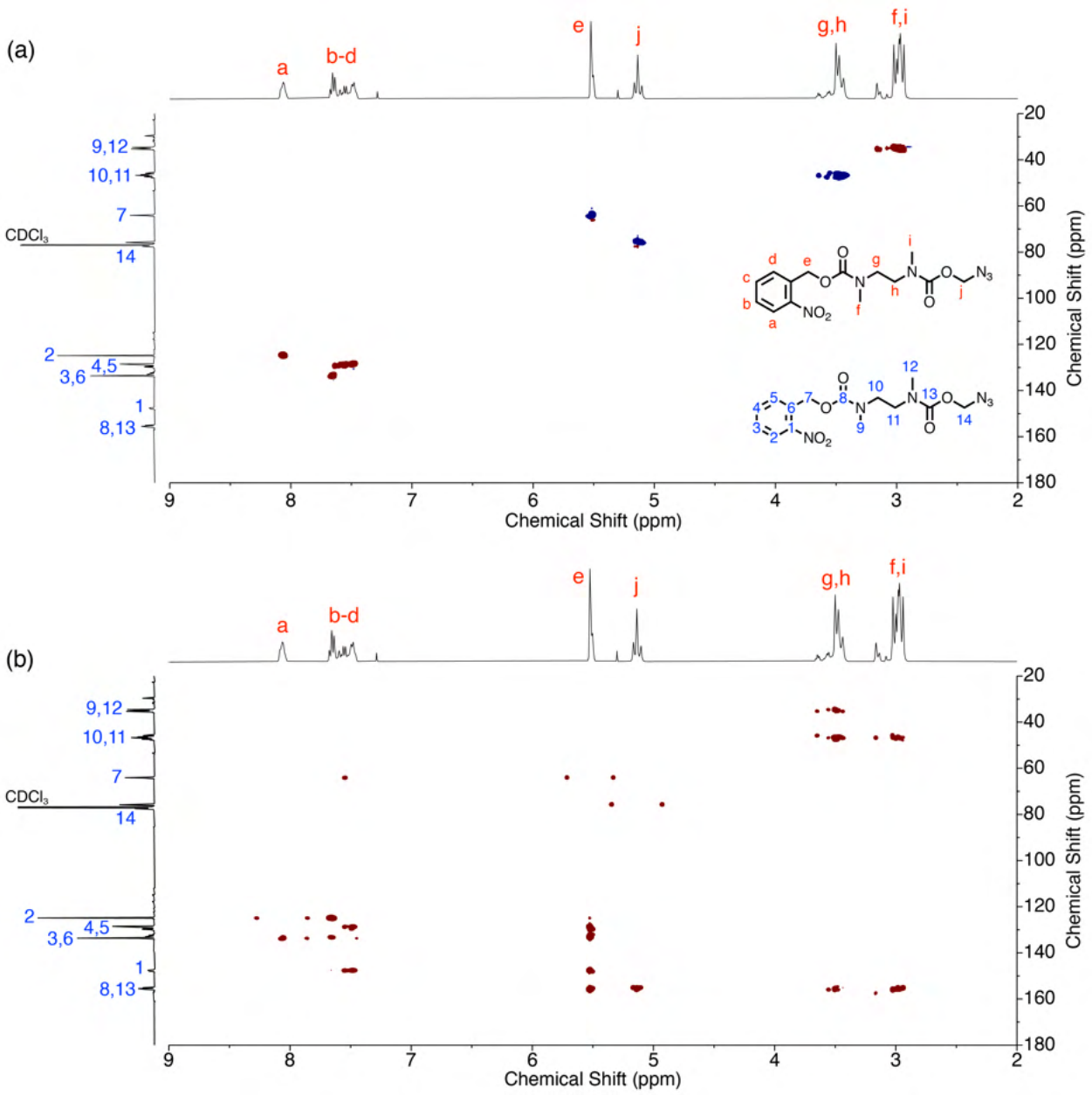

Figure S51. $^{1}H–^{13}C$ HSQC/HMBC spectra (400/100 MHz, 300 K, $CDCl_3$) of compound **A2.**

S8. *o*-Nitrobenzyl-capped carbonate-bridged PEtG (P5)

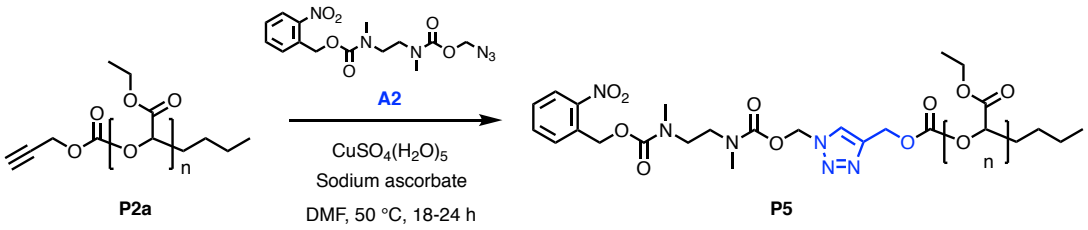

Following the general procedure for the polymer 'click' capping (see Section S4.1), polymer **P5** was obtained as a yellow-brown gummy solid (158 mg, 28.2 µmol at $M_{n,NMR}$ ~5.6 kg mol^{-1} for DP53, 59%).

^{1}H NMR (400 MHz, $CDCl_3$) δ_H 8.2 – 7.9 (m, 1H), 7.7 – 7.6 (m, 1H), 7.6 – 7.4 (m, 2H), 6.4 – 6.0 (m, 2H), 5.8 – 5.4 (m, 52H), 4.5 – 4.0 (m, 106H), 3.5 – 3.3 (m, 4H), 3.1 – 2.8 (m, 6H), 1.5 – 1.1 (m, 165H). **SEC** (DMAc/LiBr, 50 °C, PMMA calibration) $M_{n,SEC}$ = 6.9 kg mol^{-1}, $Đ$ = 1.21.

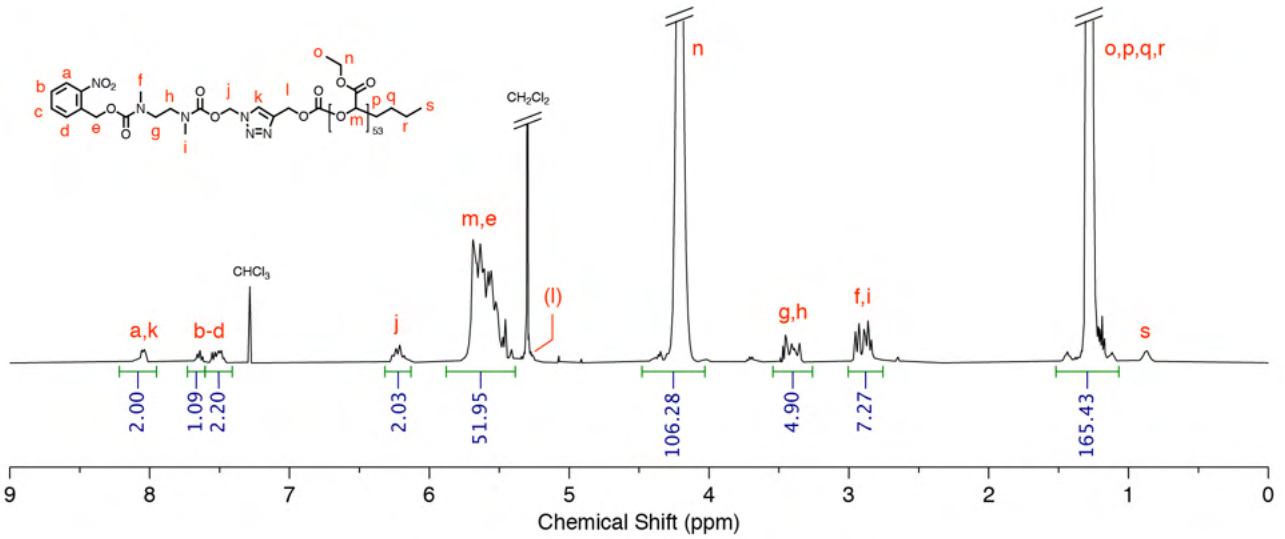

Figure S52. ^{1}H NMR spectrum (400 MHz, 300 K, $CDCl_3$) of polymer **P5**.

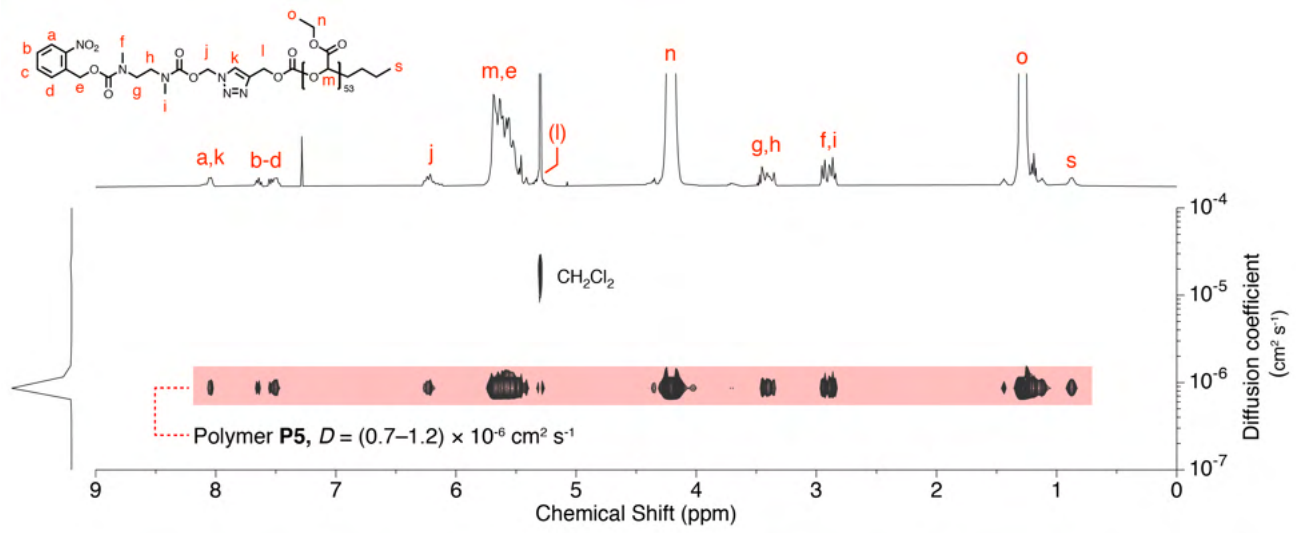

Figure S53. ^{1}H DOSY NMR spectrum (400 MHz, 300 K, $CDCl_3$) of polymer **P5**. Co-diffusion of peaks corresponding to the *o*-nitrobenzyl end-group, SIT linker and PEtG backbone supports successful post-synthetic 'click'-capping. Acquisition parameters: *d20* (Δ) = 300 ms, *p30* (δ) = 2000 µs, *td*(F1) = 16. Processing: Bayesian DOSY transform, resolution factor = 20, repetitions = 1, processed with 32 points in diffusion dimension.

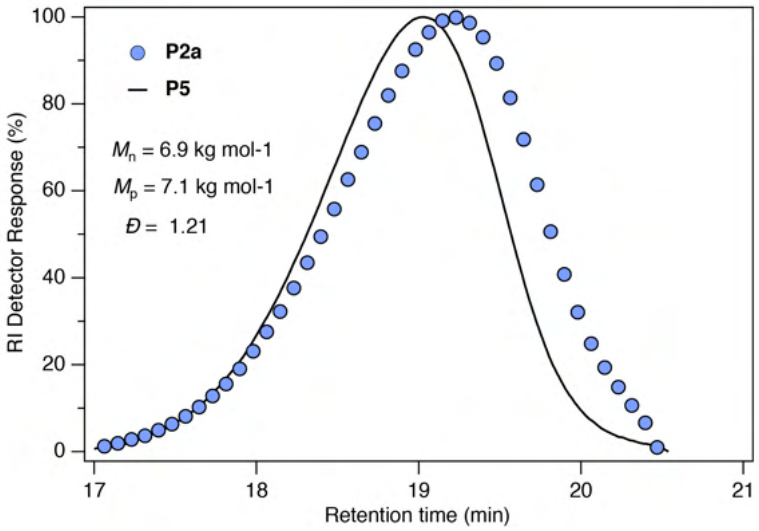

Figure S54. SEC traces (DMAc/LiBr, 50 °C, PMMA calibration) of polymer **P2b** (blue circles) and **P5** (black line). Molar mass and dispersity values correspond to **P5**. The shift to higher molar mass values following PSM is attributed to fractionation of the sample (i.e., loss of lower molar mass chains) during purification by precipitation.

S9. Self-immolation kinetics experiments

S9.1. General kinetics measurement procedure

Analysis of the self-immolation kinetics of polymers **P3a-b** and **P4a-b**, and model compounds **1a-c** and **2a-b**, were performed in DMSO-d_6/D_2O (9:1 or 8:2 *v*/*v*, as specified) to verify the mechanism of self-immolation in a mixed aqueous-organic solvent environment. The choice of solvent was limited by the solubility of the polymer — higher aqueous fractions resulted in precipitation. Experiments were performed at 65 °C (338 K)* to accelerate kinetics measurements and thus make efficient use of available spectrometer time, and to permit facile comparison to previously reported self-immolation measurements.[3, 5]

Representative experimental procedure for alloc-capped molecules

Experiments were performed at 9-12 mmol polymer (final concentration). Polymer **P3a** (28 mg, 5.5 μmol) was dissolved in DMSO-d_6 (395 μL) and D_2O (45 μL) and added to a 5 mm NMR tube. The tube was inserted into the NMR spectrometer, equilibrated at 65 °C until stable (~5 min) then the spectrometer was tuned and matched, locked and shimmed. An initial spectrum was collected for concentration calibration (typically *ds* = 2, *ns* = 8, running a *zg30* pulse program with a *D1* recycle delay of 2 s to ensure complete longitudinal relaxation of the sample between each scan to enable quantitative integration of the spectrum). The tube was ejected from the spectrometer, and morpholine (10 μL, 118 μmol, 20 equiv.) was added, followed by a suspension of $Pd(PPh_3)_4$ (~1 μmol) in DMSO-d_6 (10 μL), and the tube mixed rapidly before returning the sample to the spectrometer. The sample was generally left out of the spectrometer for <1 min, remaining within 5 °C of the target temperature. Upon returning to the spectrometer, the sample was re-shimmed and kinetics timepoints were collected immediately. Variable delays were controlled using dummy scans.

Data processing workflow

Our data analysis method is described in our previous work[3] and has been used here without significant modification. Arrayed ^1H spectra at different timepoints were stacked into a single plot in Mestrenova and all spectra were normalized to a region in the spectrum that maintains consistent integration values (typically, the region from 0.5 to 1.5 ppm for polymers and 1.5 to 2.0 ppm for model compounds are used as the integrals of the substrates and products do not shift from this region and therefore remain constant throughout the kinetics experiments). Peak integrals over time were computed using the arrayed data analysis function in Mestrenova 14.0.1 and were normalized by diving integral values by the number of protons each environment represents.

Timecourse data were fitted to monoexponential decay models where data appeared satisfactorily to obey a first or pseudo-first order rate law, as described in our previous work.[3] This allowed estimation of (pseudo)-first order rate constants for some of the degradation profiles (especially model compounds). These rate constants have been converted to more intuitive half-life values by dividing the fitted exponential time constants (τ) by ln(2).

*The actual sample temperature inside the NMR spectrometer was determined according to the calibration method described in the 1995 Bruker VTU user manual version 001 using a 100% ethylene glycol sample.

S9.2. Kinetics I: Acetal-bridged polymers and models

S9.2.1. Polymer P3a

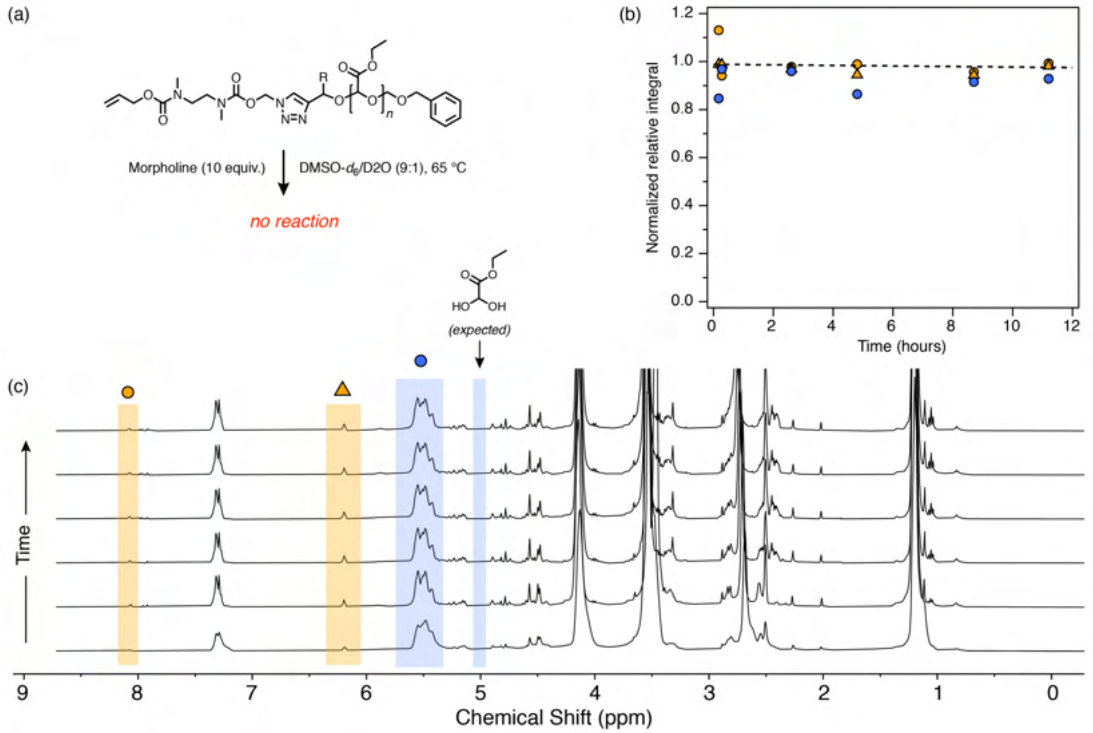

Figure S55. ^{1}H NMR control analysis of polymer **P3a** with morpholine (10 equiv.) and no catalyst (400 MHz, DMSO-d_6/D_2O = 9:1, 338 K). (a) Reaction scheme. Proton environments used for kinetics analysis are highlighted with markers. (b) Degradation plot extracted from the stacked NMR spectra. (c) Stacked NMR spectra recorded at different times following addition of morpholine to the sample.

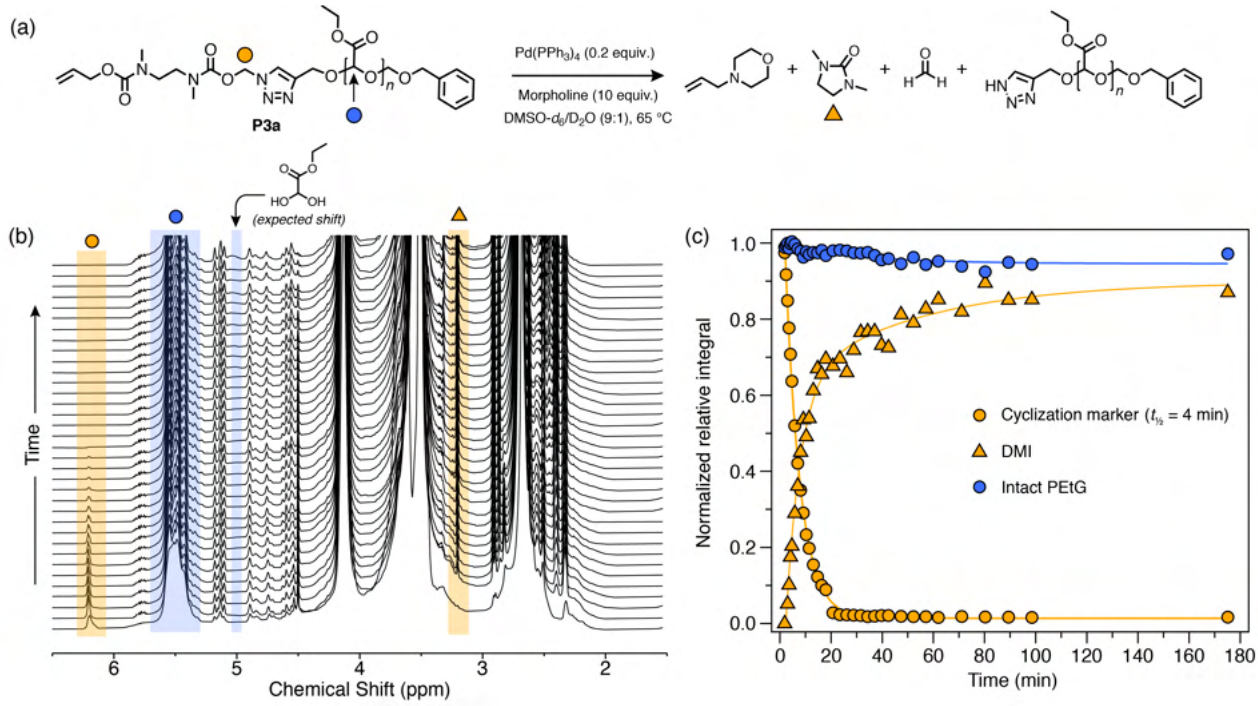

Figure S56. ^{1}H NMR self-immolation analysis of polymer **P3a** (400 MHz, DMSO-d_6/D_2O = 9:1, 338 K). (a) Reaction scheme. Proton environments used for kinetics analysis are highlighted with markers. (b) Stacked NMR spectra during kinetics monitoring. (c) Degradation plot. Markers correspond to environments highlighted in the reaction scheme. Diamine cyclization exhibited pseudo first-order (monoexponential) kinetics, allowing estimation of the cyclization half-life.

S9.2.2. **Polymer P3b**

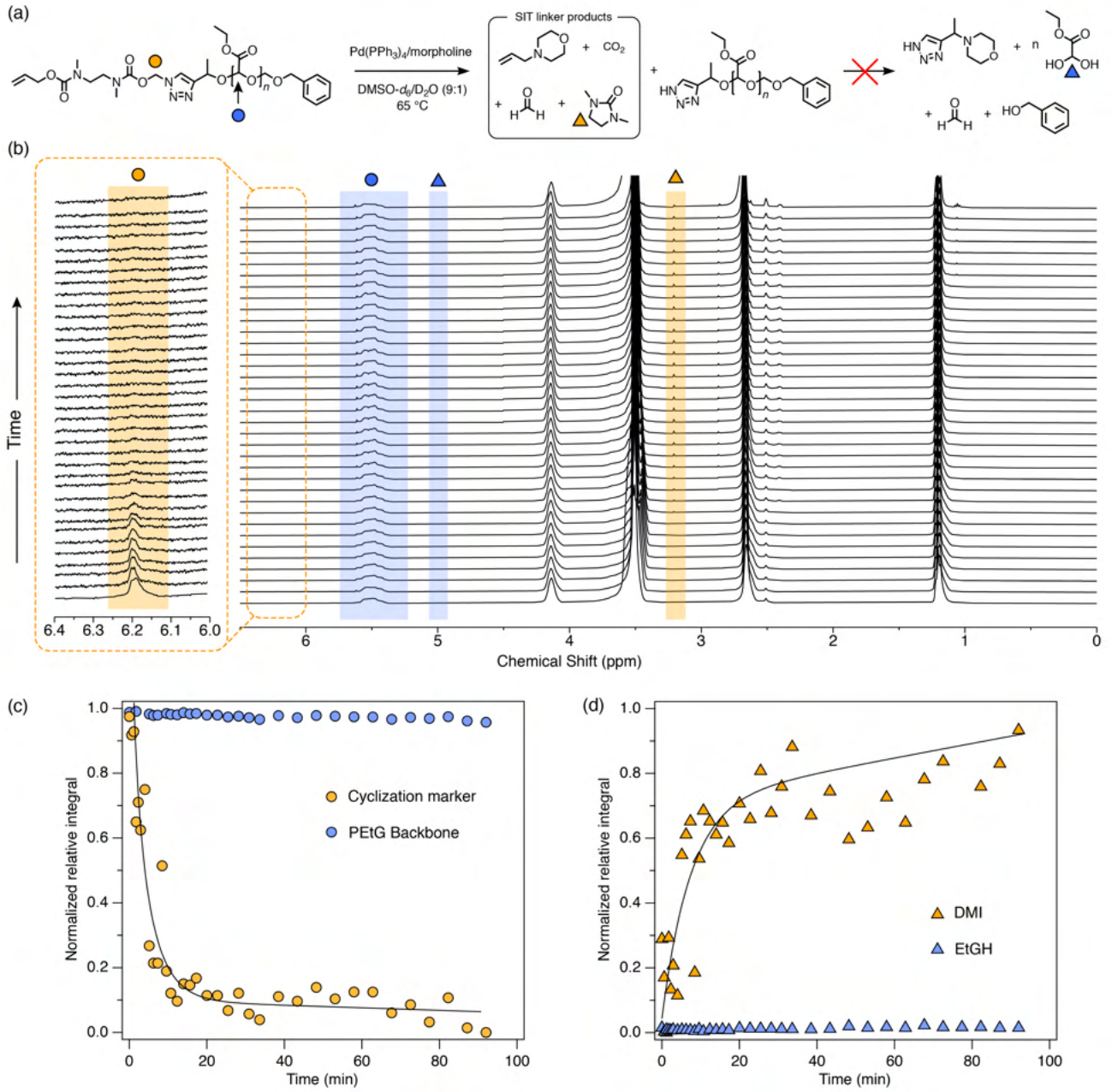

Figure S57. ^{1}H NMR self-immolation analysis of polymer **P3b** (400 MHz, DMSO-d_6/D_2O = 9:1, 338 K). (a) Reaction scheme. Proton environments used for kinetics analysis are highlighted with markers. (b) Stacked NMR spectra collected during kinetics monitoring. Inset included to highlight the low intensity peak of the environment used to monitor cyclization of the diamine spacer. (c) Degradation plot and (d) product formation plot. Markers correspond to environments highlighted in the reaction scheme. Curves are included only as visual guides and do not indicate data fitting.

S9.2.3. **Acetal-bridged model compounds 1a-c**

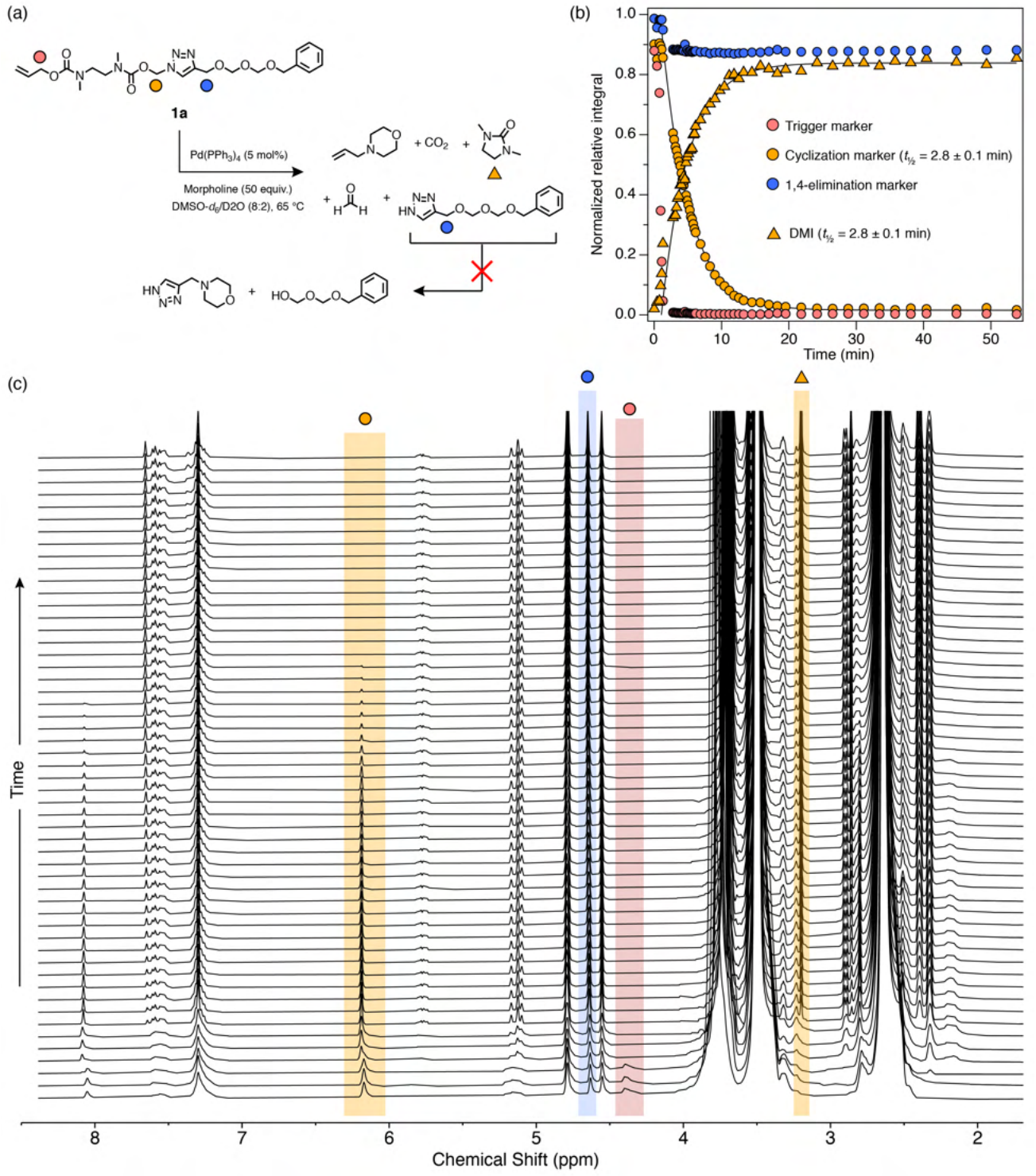

Figure S58. ^{1}H NMR self-immolation analysis of compound **1a** (25 mM in DMSO-d_6/D_2O = 8:2, 400 MHz, 338 K). (a) Reaction scheme. Proton environments used for kinetics analysis are highlighted with markers. (b) Kinetics plot. Markers correspond to environments highlighted in the reaction scheme. Curves indicate fitted monoexponential decay models. (c) Stacked NMR spectra collected during kinetics monitoring.

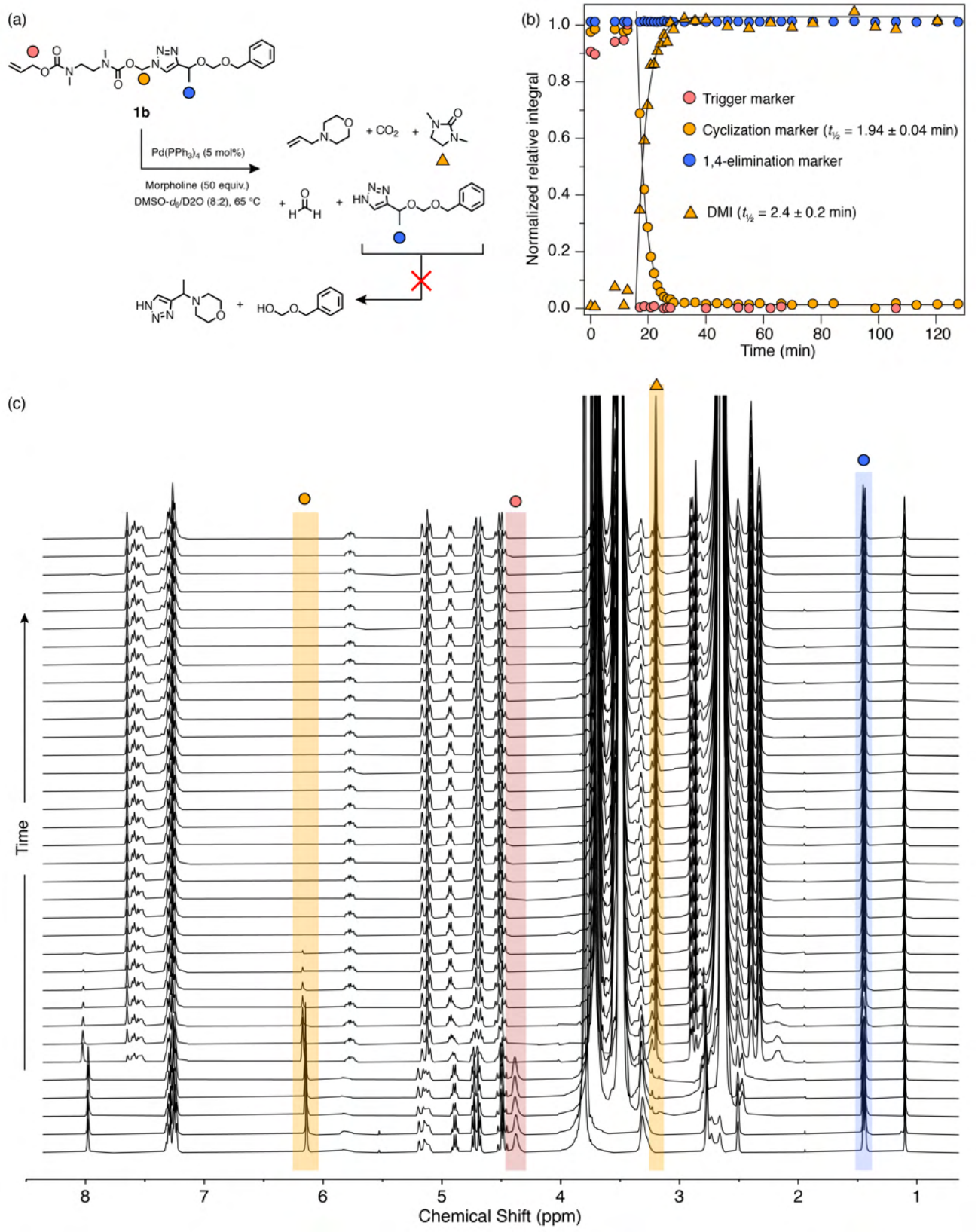

Figure S59. ^{1}H NMR self-immolation analysis of compound **1b** (25 mM in DMSO-d_6/D_2O = 8:2, 400 MHz, 338 K). (a) Reaction scheme. Proton environments used for kinetics analysis are highlighted with markers. (b) Kinetics plot. Markers correspond to environments highlighted in the reaction scheme. Curves indicate fitted monoexponential decay models. (c) Stacked NMR spectra collected during kinetics monitoring.

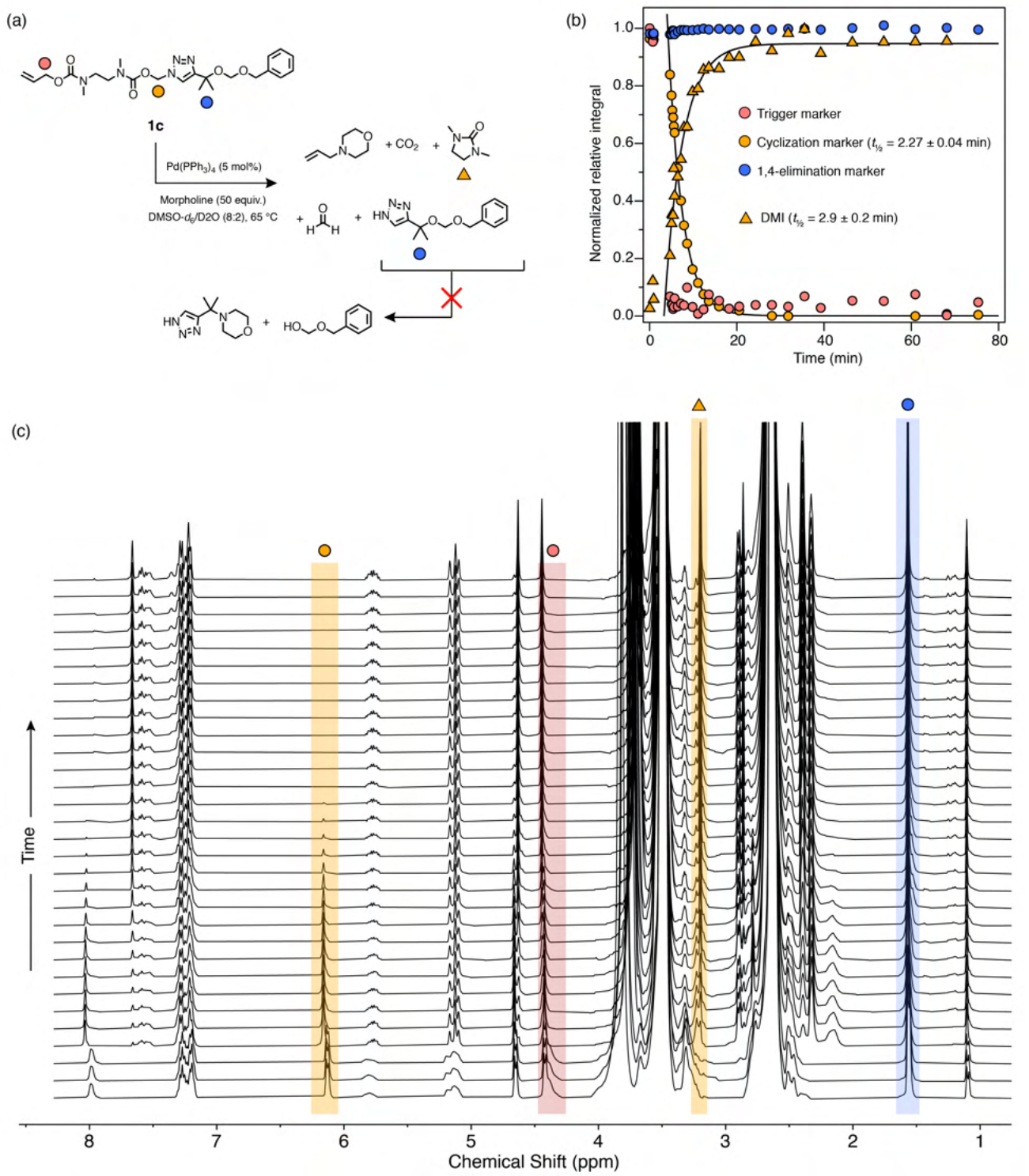

Figure S60. ^{1}H NMR self-immolation analysis of compound **1c** (25 mM in DMSO-d_6/D_2O = 8:2, 400 MHz, 338 K). (a) Reaction scheme. Proton environments used for kinetics analysis are highlighted with markers. (b) Kinetics plot. Markers correspond to environments highlighted in the reaction scheme. Curves indicate fitted monoexponential decay models. (c) Stacked NMR spectra collected during kinetics monitoring.

S9.3. Kinetics II: Carbonate-bridged polymers and models

S9.3.1. Polymer P4a

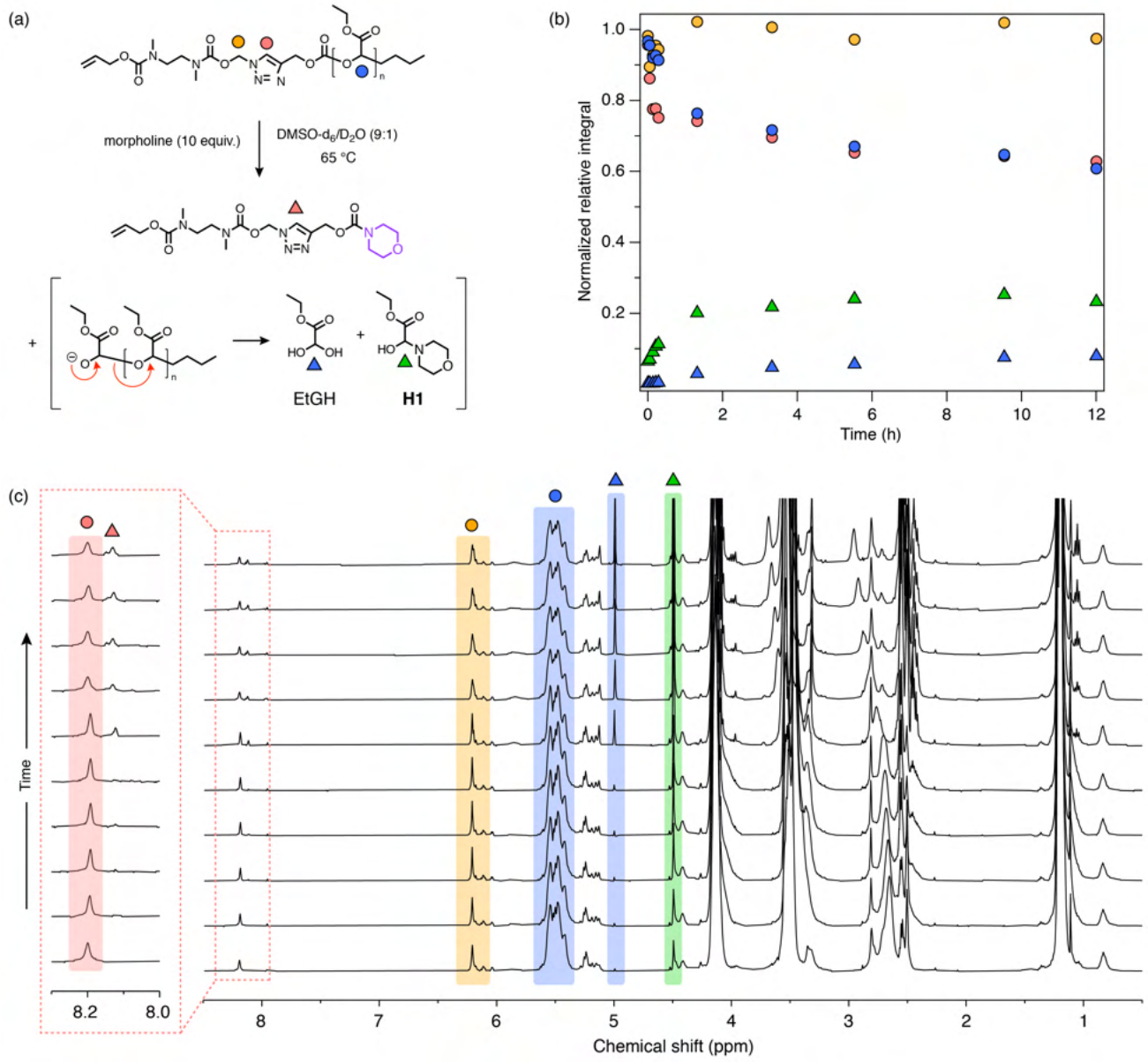

Figure S61. ^{1}H NMR control analysis of polymer **P4a** with morpholine (10 equiv.) (400 MHz, DMSO-d_6/D_2O = 9:1, 338 K). **(a)** Reaction scheme showing the proposed base hydrolysis pathway via attack at the carbonate group, leading to the formation of a SIT linker fragment, EtGH and hemiaminal **H1 (**see auxiliary discussion in Section S10 for characterization of hemiaminal **H1**). Proton environments used for kinetics analysis are highlighted with markers. **(b)** Degradation plot corresponding to the NMR stack shown in (c). Markers are colored according to the proton environments shown in (a) and the proton signal integrals highlighted in (c). **(c)** NMR spectra showing changes in key integrals over time following the addition of morpholine. Inset shows that the triazole environment of **P4a** decreases, and a new peak at slightly lower chemical shift (red triangle) appears, indicating the formation of a new triazole species. The N_α CH_2 environment (orange triangle) does not appreciably change, suggesting that fragmentation of the SIT linker occurs at the carbonate group, producing the putative fragmentation products depicted in (a).

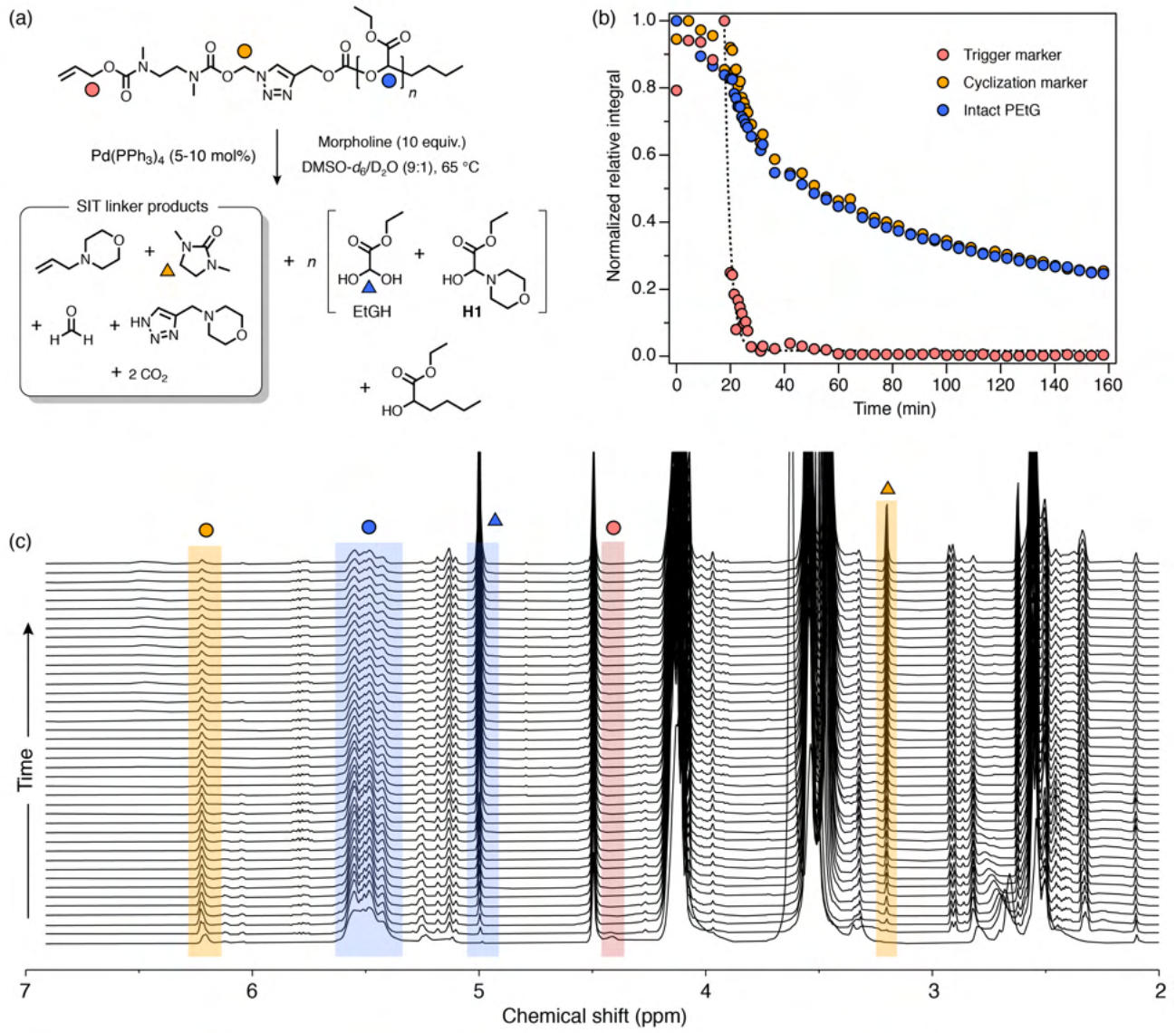

Figure S62. ^{1}H NMR self-immolation analysis (400 MHz, DMSO-d_6/D_2O = 9:1, 338 K) of polymer **P4a** over 2 h total reaction time, depicting the trigger cleavage, cyclization and PEtG depolymerization stages of the cascade. **(a)** Reaction scheme showing the proposed degradation pathway. Proton environments used for the degradation plot analysis are highlighted with markers. **(b)** Degradation plot showing the degradation of key parts of polymer **P4a** following catalyst addition at ~20 min. Prior to catalyst addition (<20 min), only morpholine was present alongside the polymer. **(c)** NMR stack highlighting key proton integrals that were tracked over time to generate the degradation plot.

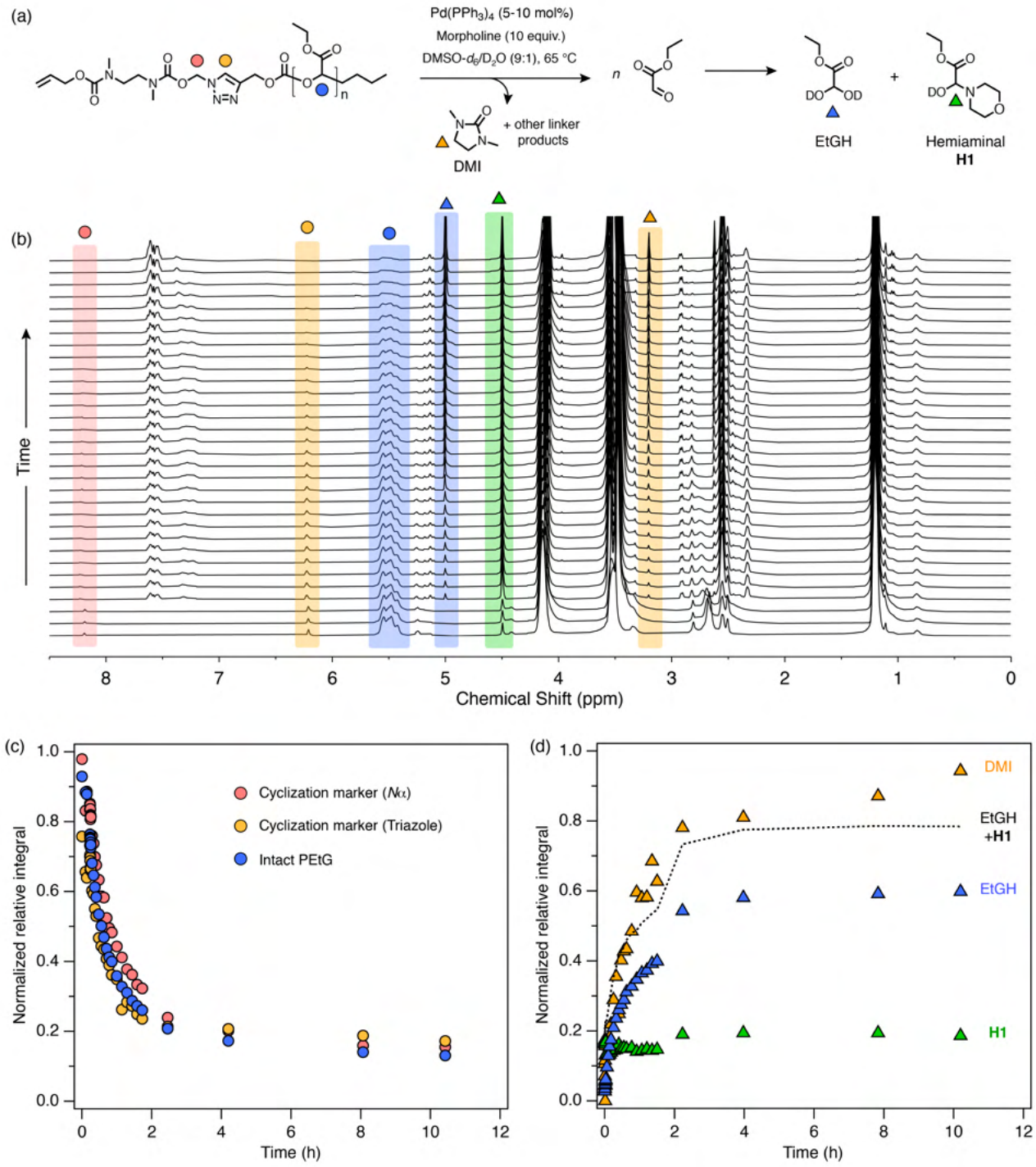

Figure S63. ^{1}H NMR self-immolation analysis (400 MHz, DMSO-d_6/D_2O = 9:1, 338 K) of polymer **P4a** over 10 h total reaction time (a replicate experiment to the data shown in Figure S62), comparing the formation of degradation products DMI, EtGH, and hemiaminal **H1** (see Section S10). **(a)** Reaction scheme showing the proposed degradation pathway. Integrals of proton environments used for the degradation plot are highlighted with markers. **(b)** NMR stack highlighting key proton signals tracked over time to generate the degradation plot. **(c)** Degradation plot depicting loss of the cyclization spacer and PEtG backbone following catalyst addition. **(d)** Plot showing the formation of key products DMI, EtGH and hemiaminal **H1**. The dotted black line, which represents the summed relative integrals of EtGH and **H1**, agrees reasonably well with the relative integral of DMI and indicates that most of the EtG liberated from depolymerization is converted to EtGH and hemiaminal **H1**.

S9.3.2. **Degradation kinetics of polymer P4b**

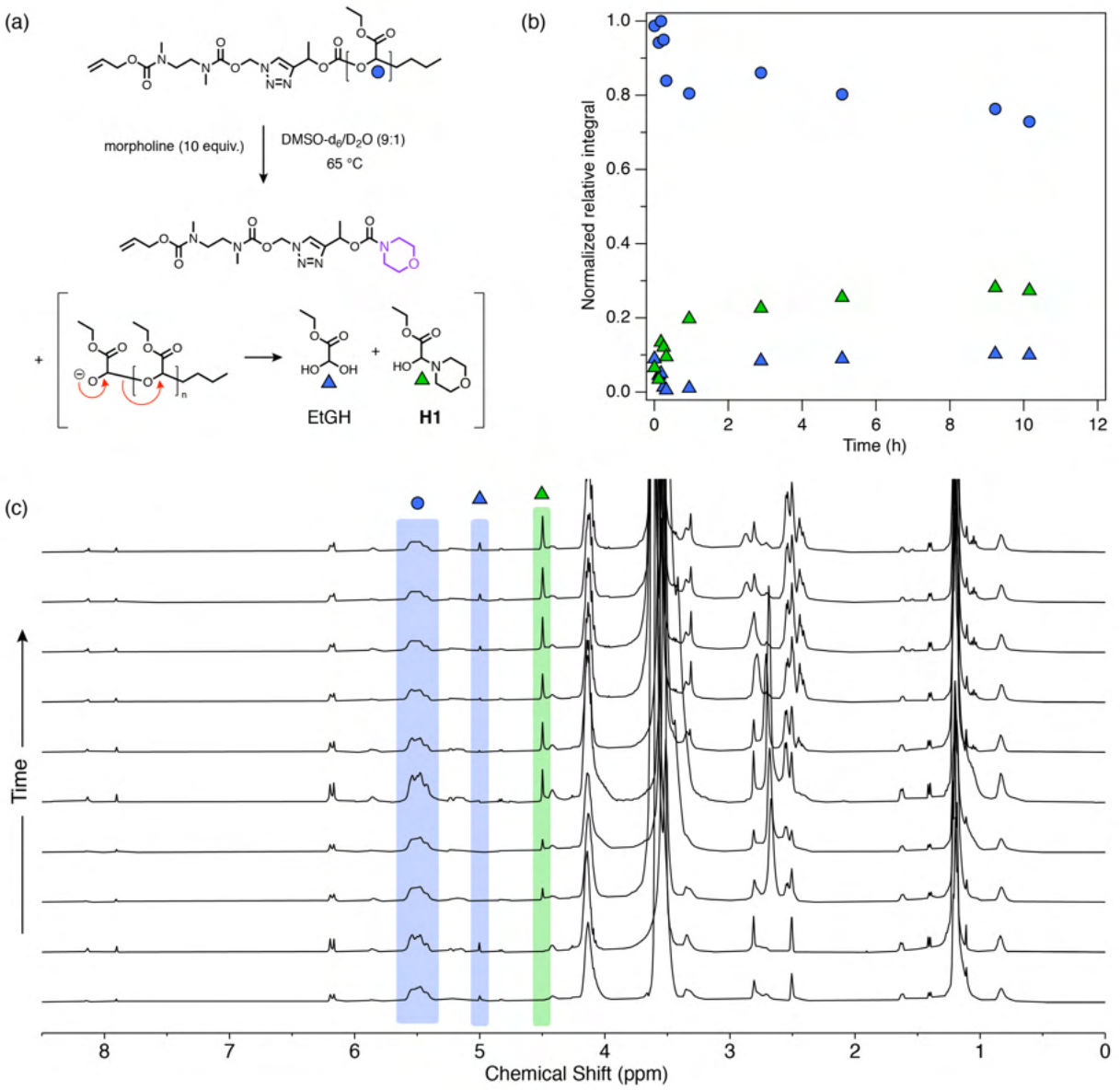

Figure S64. ^{1}H NMR control experiment of caged polymer **P4b** with morpholine (10 equiv.) (400 MHz, DMSO-d_6/D_2O = 9:1, 338 K). **(a)** Reaction scheme showing the proposed base hydrolysis pathway, analogous to that observed for **P4a**. Proton environments used for degradation analysis are highlighted with markers. **(b)** Degradation plot corresponding to the NMR stack shown in (c). Markers are colored according to the proton environments shown in (a) and the proton signal integrals highlighted in (c). **(c)** NMR spectra showing changes in key integrals over time following the addition of morpholine.

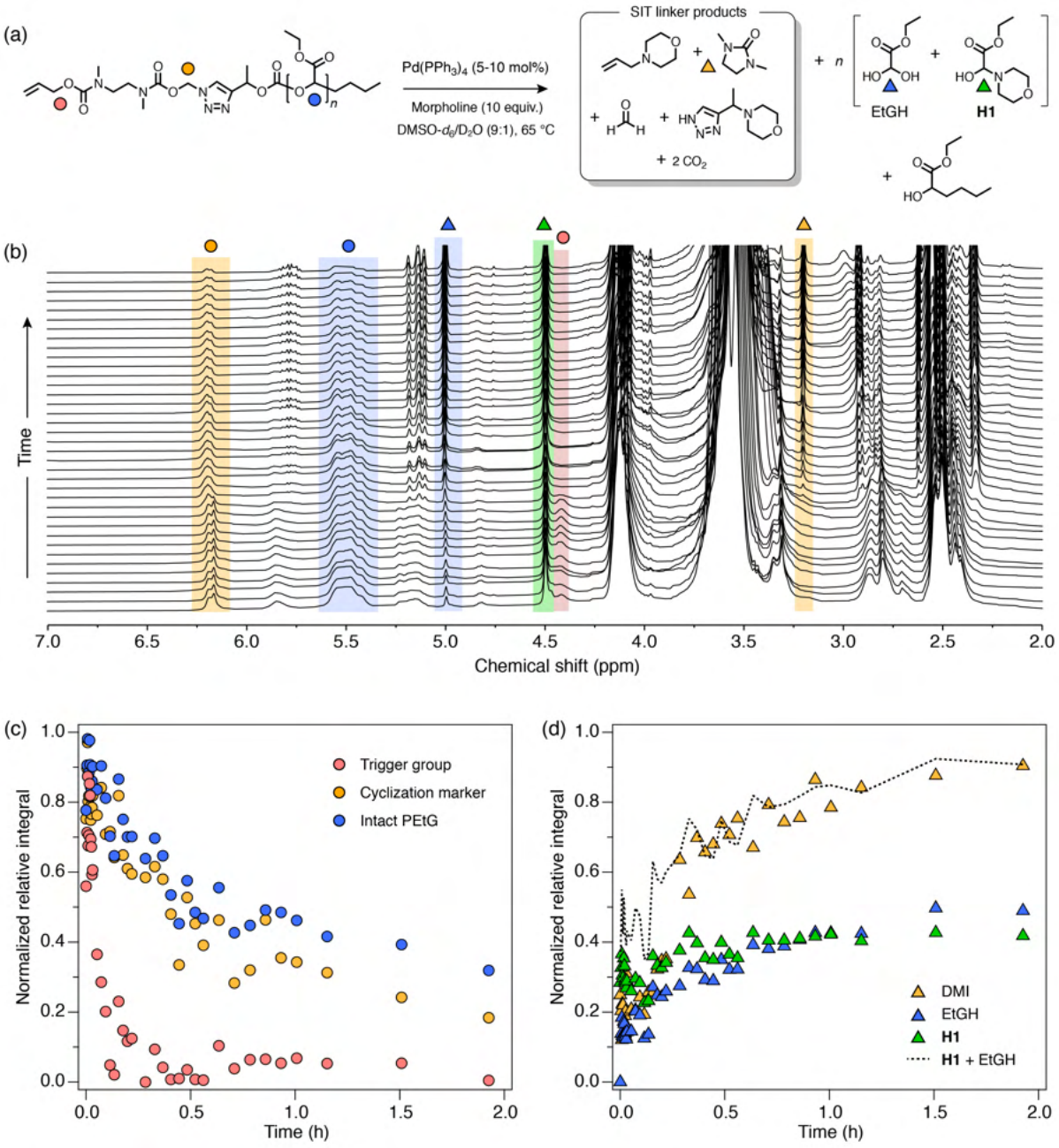

Figure S65. ^{1}H NMR self-immolation analysis (400 MHz, DMSO-d_6/D_2O = 9:1, 338 K) of polymer **P4b** over 2 h total reaction time. **(a)** Reaction scheme showing the proposed degradation pathway. Integrals of proton environments used for the degradation plot are highlighted with markers. **(b)** NMR stack highlighting key proton signals tracked over time to generate the degradation plot. **(c)** Degradation plot depicting loss of the trigger group, cyclization spacer and PEtG backbone following catalyst addition. **(d)** Plot showing the formation of key products DMI, EtGH and hemiaminal **H1**. The dotted black line, which represents the summed integrals of EtGH and **H1**, agrees with the relative integral of DMI and therefore confirms that most of the EtG liberated from depolymerization is converted to EtGH and hemiaminal **H1**.

S9.3.3. **Model compounds 2a-b**

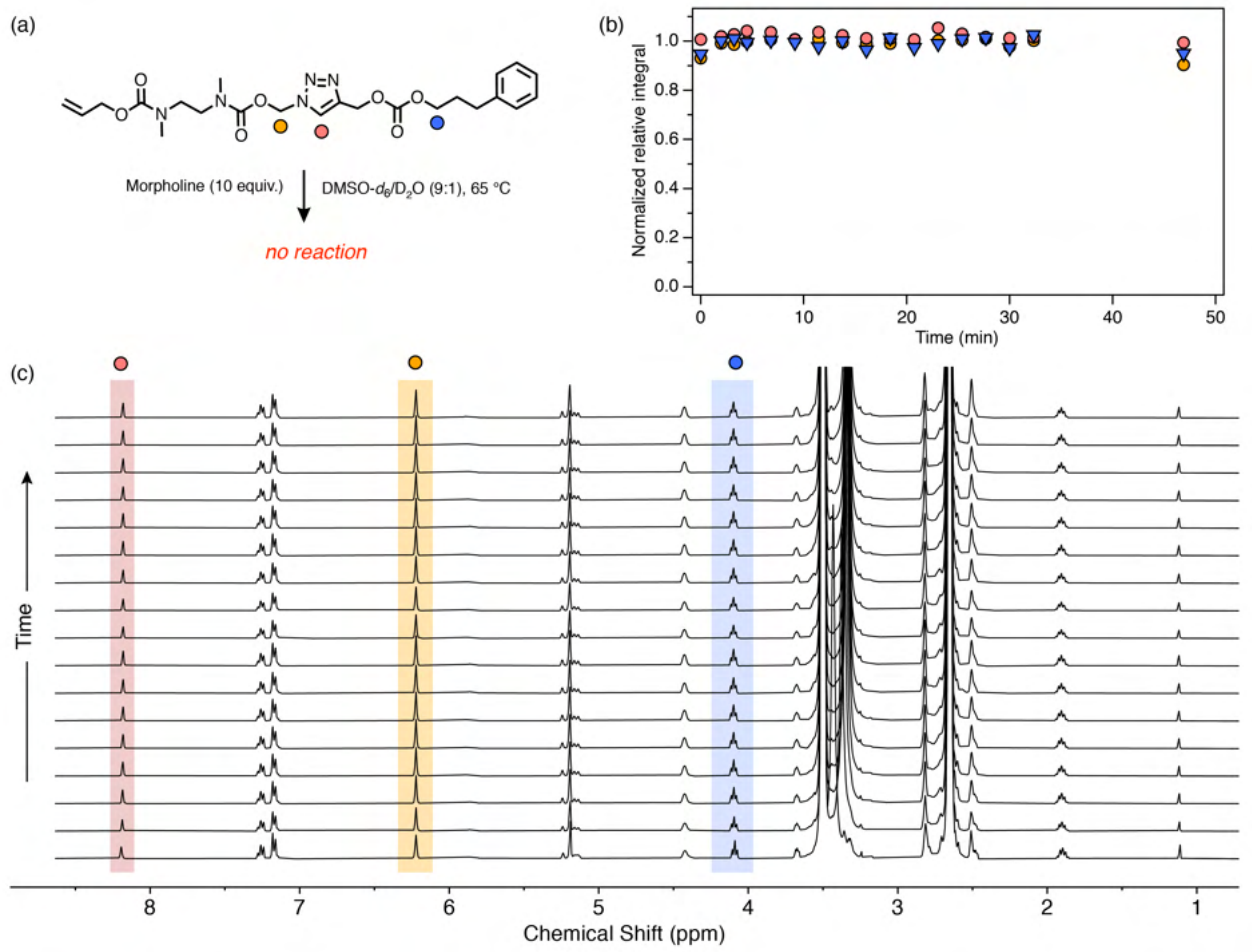

Figure S66. ^{1}H NMR control analysis of carbonate model **2a** (25 mM in DMSO-d_6/D_2O = 9:1, 400 MHz, 338 K) in the presence of morpholine (10 equiv.). This control experiment demonstrates that the carbonate group is not readily susceptible to basic hydrolysis with a 10-fold excess of a weak base. **(a)** Reaction scheme. Proton environments used for kinetics analysis are highlighted with markers. **(b)** Kinetics plot, showing no measurable degradation over 50 min. **(c)** Stacked NMR spectra corresponding to the kinetics plot in (b).

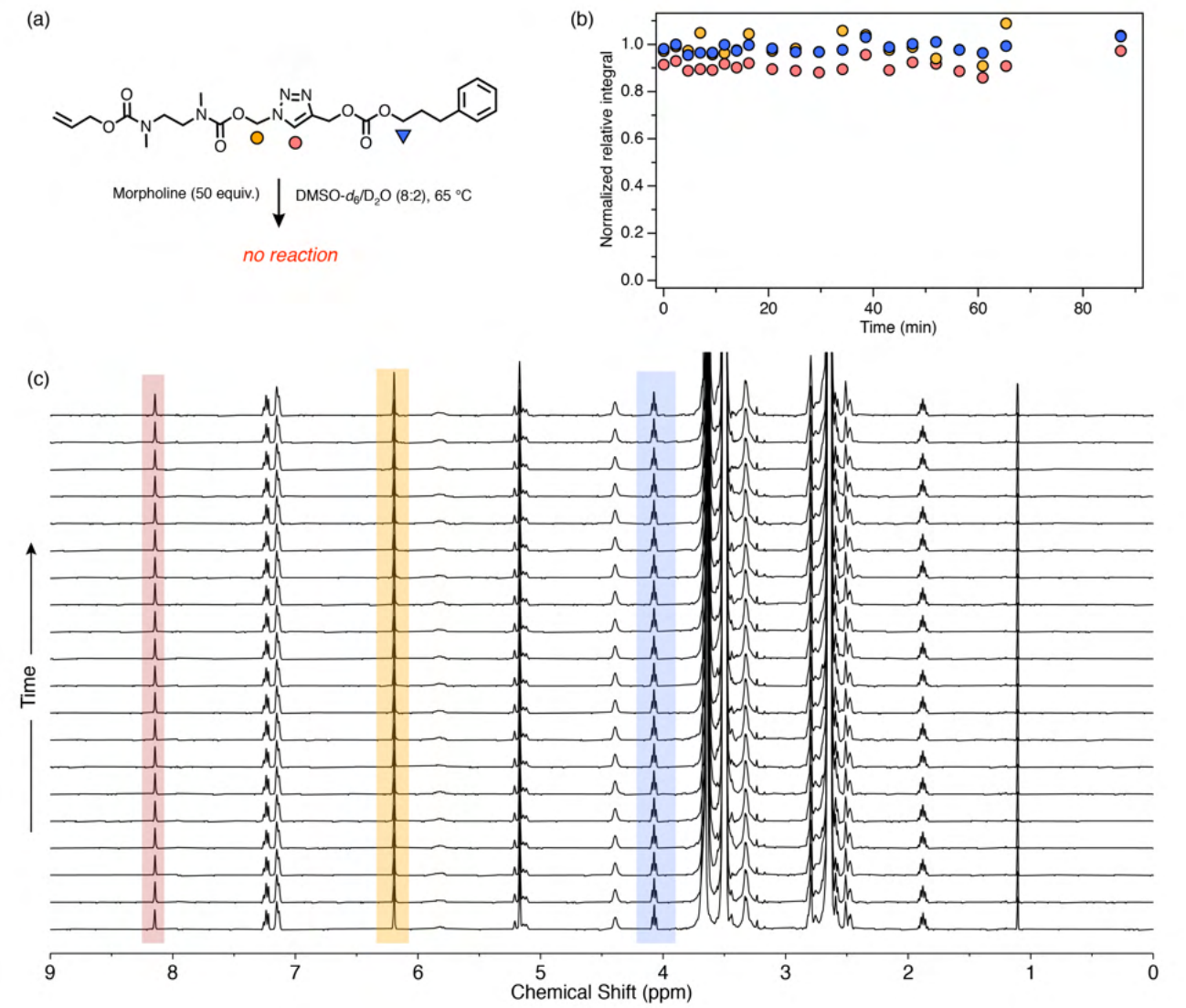

Figure S67. ^{1}H NMR control analysis of carbonate model **2a** (25 mM in DMSO-d_6/D_2O = 9:1, 400 MHz, 338 K) in the presence of morpholine (50 equiv.). This control experiment demonstrates that the carbonate group is not readily susceptible to basic hydrolysis with a 50-fold excess of a weak base. **(a)** Reaction scheme. Proton environments used for kinetics analysis are highlighted with markers. **(b)** Kinetics plot, showing no measurable degradation over 90 min. **(c)** Stacked NMR spectra corresponding to the kinetics plot in (b).

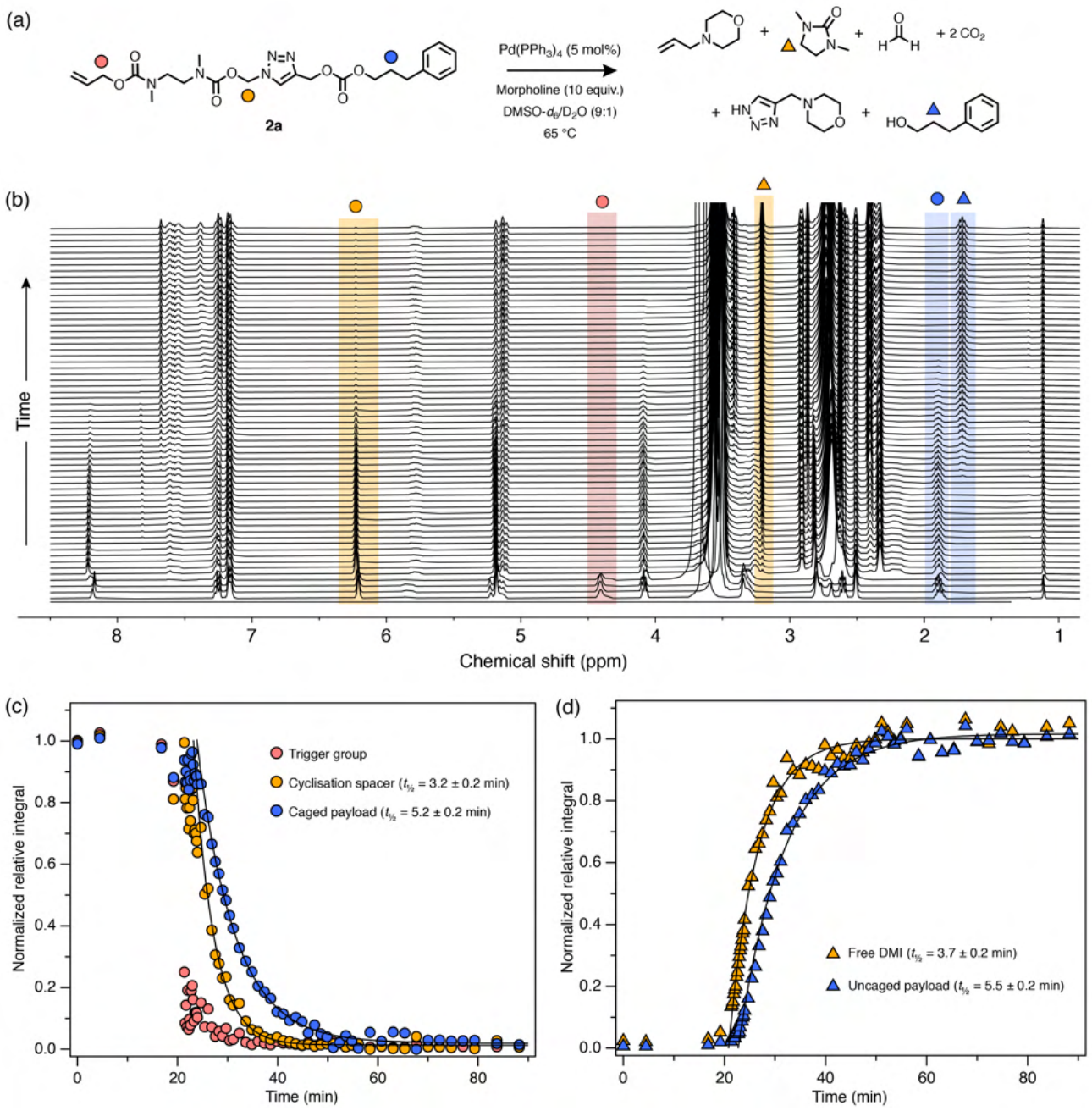

Figure S68. ^{1}H NMR self-immolation analysis of carbonate model **2a** (25 mM in DMSO-d_6/D_2O = 9:1, 400 MHz, 338 K) in the presence of morpholine (10 equiv.). Samples were equilibrated at 65 °C for 20 min, then $Pd(PPh_3)_4$ was added to initiate self-immolation. **(a)** Reaction scheme showing degradation products. Proton environments used for kinetics analysis are highlighted with markers. **(b)** Stacked NMR spectra. Markers denote proton environments whose normalized integrals were monitored to generate the kinetics plots. **(c)** Kinetics plot showing the three key degradation stages of the self-immolation cascade. Fitted curves are monoexponential decay models used to estimate the degradation half-lives. **(d)** Kinetics plot showing formation of cyclization product DMI and the alcohol payload (3-phenylpropan-1-ol). Fitted curves are monoexponential decay models used to estimate the degradation half-lives. Similar rates of cyclization and 1,4-elimination indicate that the latter process is especially rapid due to the good leaving ability of the carbonate group. However, 1,4-elimination remains the rate-determining step for payload release with this compound.

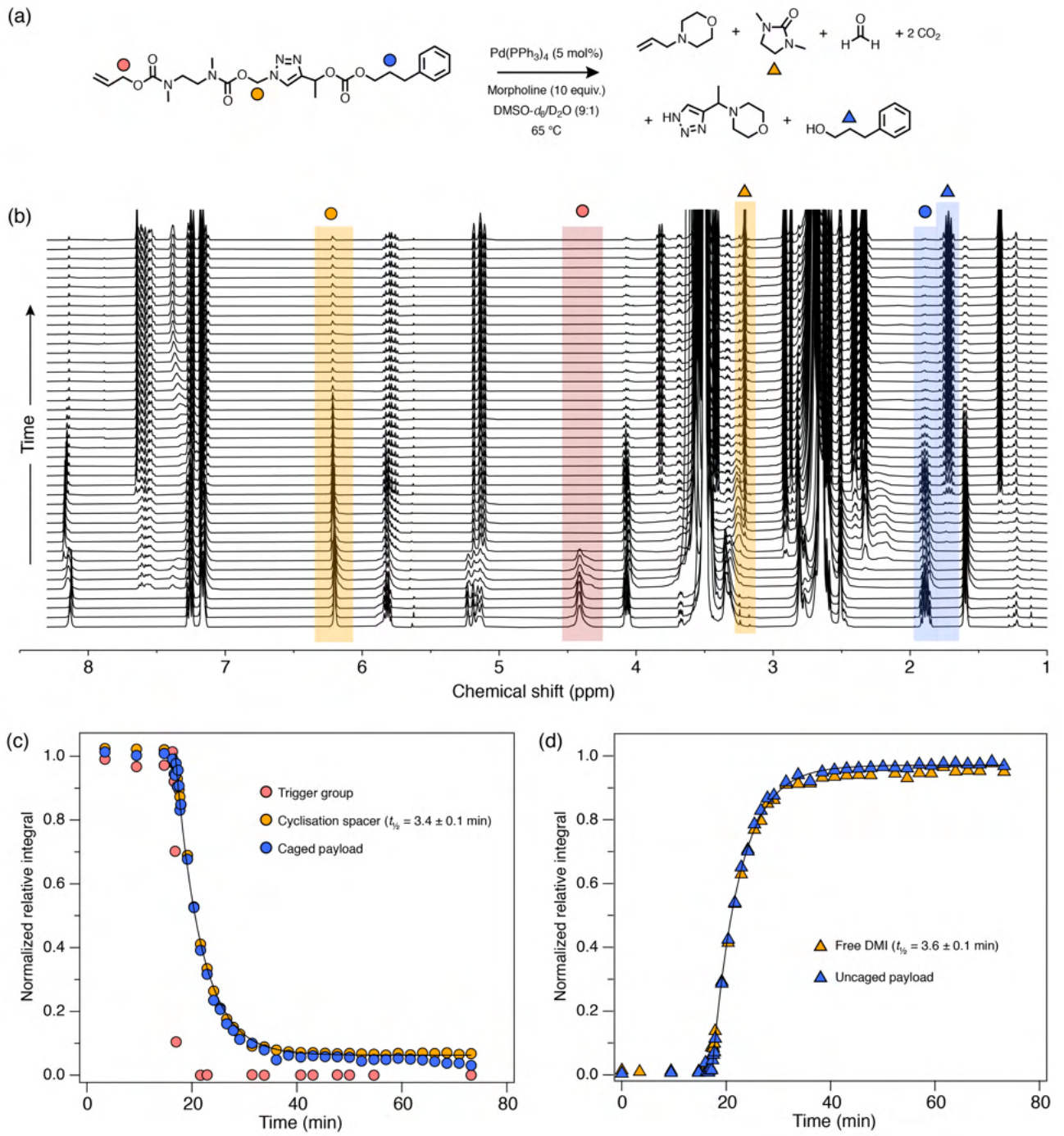

Figure S69. ^{1}H NMR self-immolation analysis of carbonate model **2b** (25 mM in DMSO-d_6/D_2O = 9:1, 400 MHz, 338 K) in the presence of morpholine (10 equiv.). Samples were equilibrated at 65 °C for ~18 min, then $Pd(PPh_3)_4$ was added to initiate self-immolation. **(a)** Reaction scheme showing degradation products. Proton environments used for kinetics analysis are highlighted with markers. **(b)** Stacked NMR spectra. Markers denote proton environments whose normalized integrals were monitored to generate the kinetics plots. **(c)** Kinetics plot showing the three key degradation stages of the self-immolation cascade. Fitted curves are monoexponential decay models used to estimate the degradation half-lives. **(d)** Kinetics plot showing formation of cyclization product DMI and the alcohol payload (3-phenylpropan-1-ol). Fitted curves are monoexponential decay models used to estimate the degradation half-lives. Identical rates of cyclization and 1,4-elimination indicate cyclization is the rate-determining step of payload release for this compound.

S9.4. Kinetics III: *o*NB-capped carbonate-bridged polymer 5

Self-immolation procedure

Polymer **P5** (32 mg, 5.7 µmol) was dissolved in DMSO-d_6 (395 µL) and D_2O (45 µL) and added to a 5 mm NMR tube. An NMR spectrum of the sample was recorded, then the tube was irradiated[†] at 365 nm (100% power setting; cooling fan speed 2000 rpm to maintain sample >30 °C) for 30 min. Another NMR spectrum was recorded, then the sample heated to 65 °C within the NMR spectrometer and the degradation reaction monitored using the same method described for alloc-capped molecules (see Section S9.1).

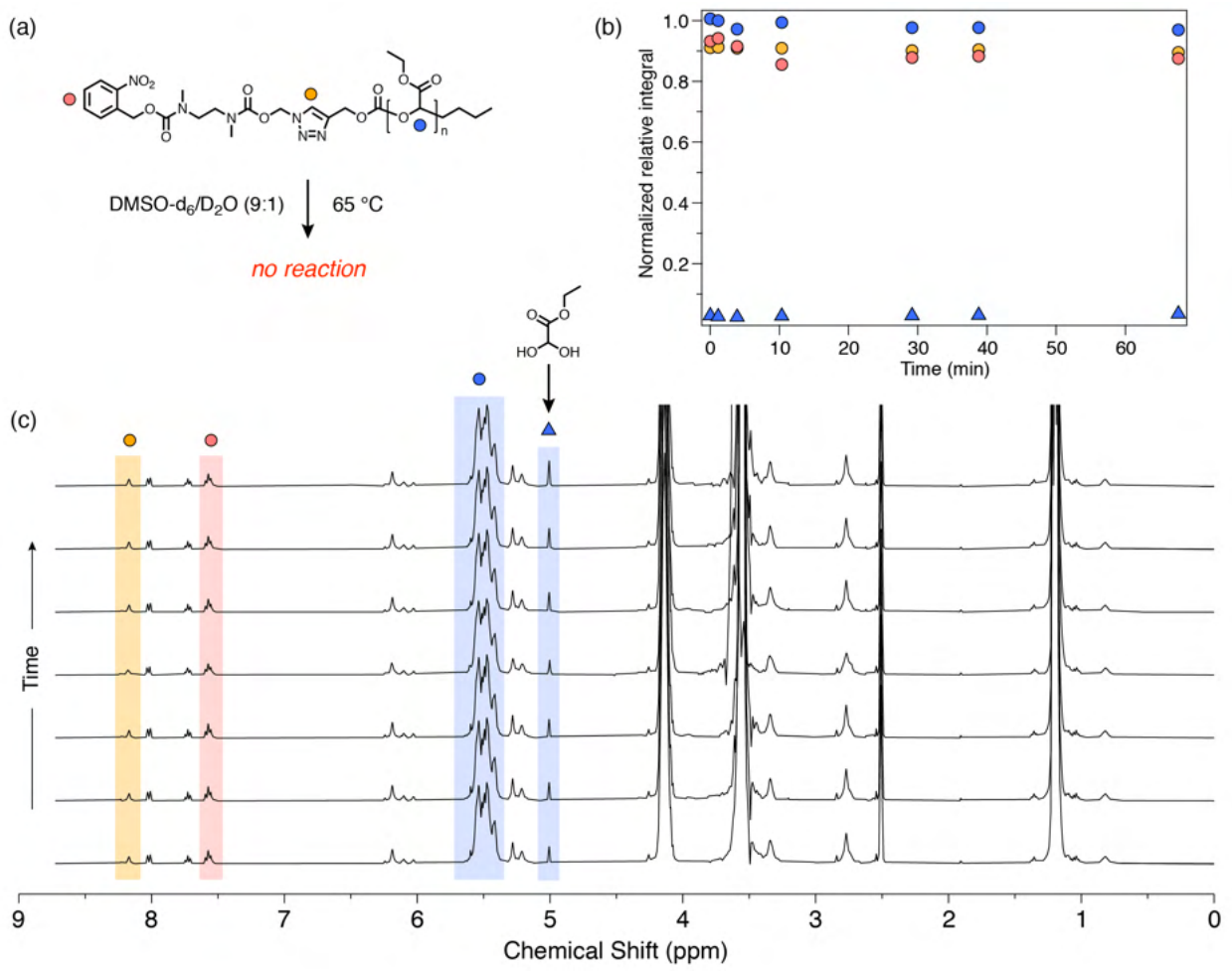

Figure S70. ^{1}H NMR control experiment (25 mM in DMSO-d_6/D_2O = 9:1, 400 MHz, 338 K) confirming the stability of polymer **P5** at 65 °C without prior photoirradiation. (a) Reaction scheme. Proton environments used for kinetics plot are highlighted with markers. (b) Kinetics plot showing no appreciable degradation over at least 60 min. (c) NMR spectra used to generate the kinetics plot. A small amount of residual EtGH was present in the reaction sample from t = 0 min, but did not increase over time.

[†] Samples were irradiated using a Penn PhD Photoreactor M2 fitted with a 365 nm LED light source.

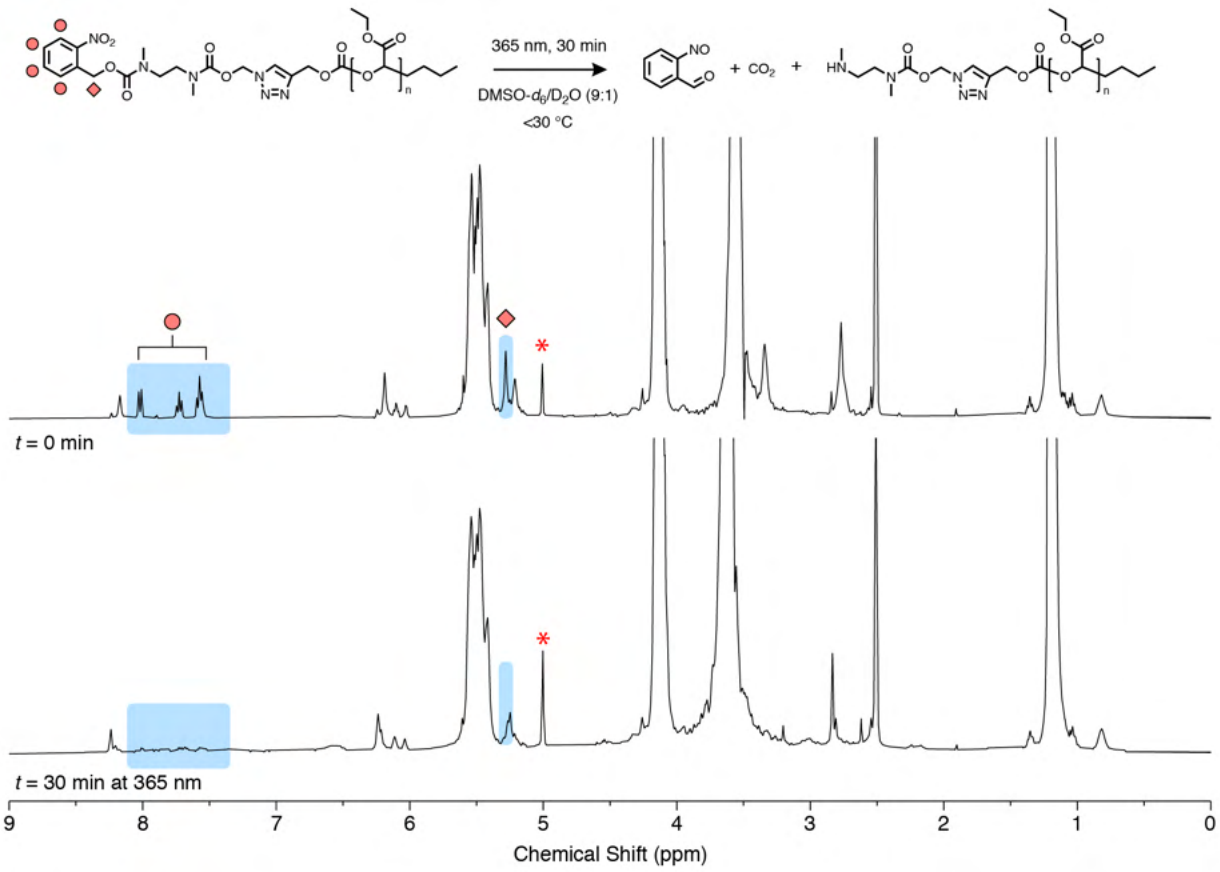

Figure S71. ^{1}H NMR spectra (25 mM in DMSO-d_6/D_2O = 9:1, 400 MHz, 338 K) showing successful cleavage of the *o*-nitrobenzyl end-group following irradiation at 365 nm for 30 min prior to heating at 65 °C. Regions of interested are highlighted in blue, and signals of the *o*-nitrobenzyl group are indicated with markers. Asterisk denotes a small amount of EtGH that is in initially present in the sample and increases slightly following irradiation most likely due to initiation of the depolymerization cascade.

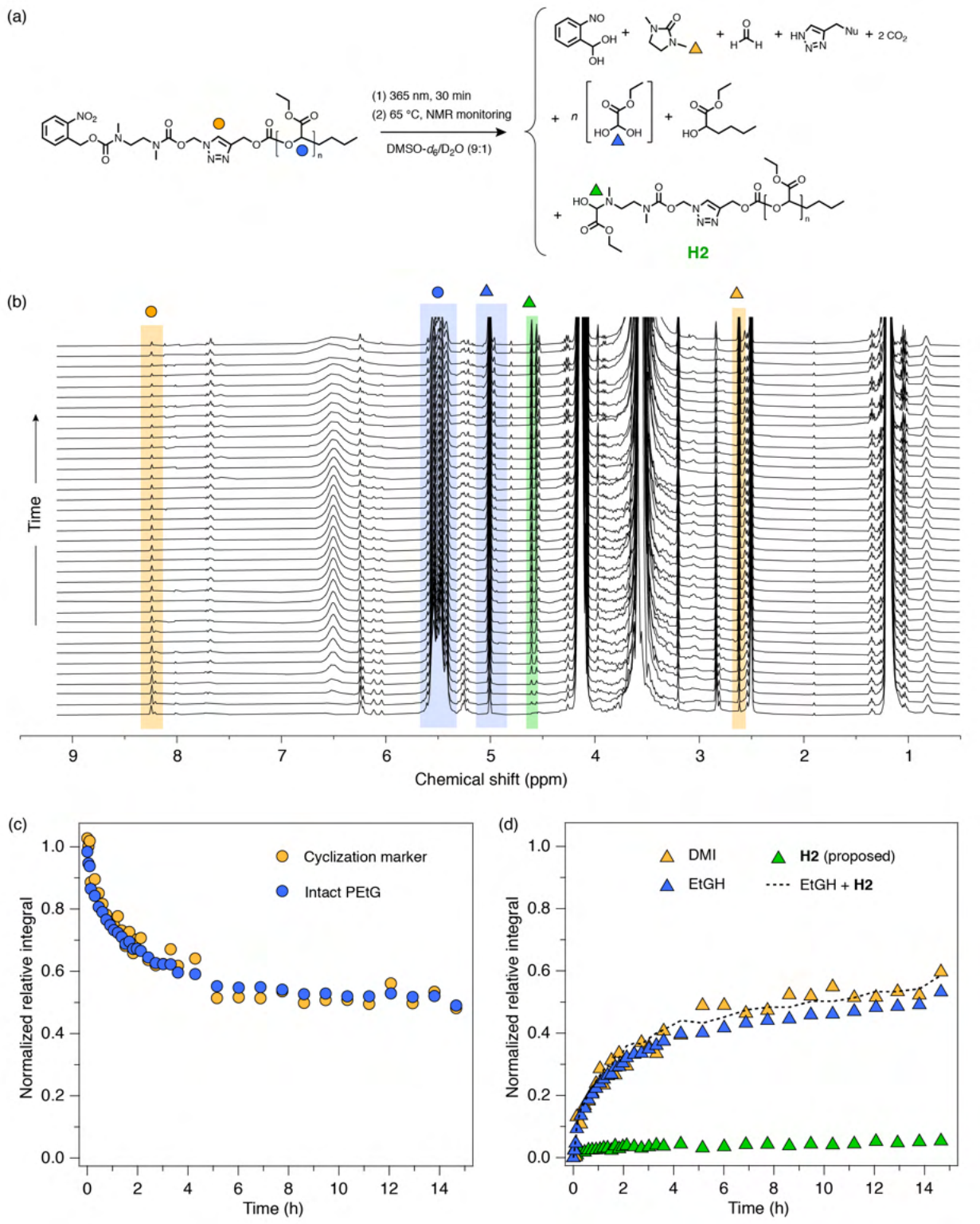

Figure S72. ^{1}H NMR self-immolation analysis of polymer **5** (25 mM in DMSO-d_6/D_2O = 9:1, 400 MHz, 338 K) following irradiation at 365 nm for 30 min. **(a)** Reaction scheme showing degradation products, including the proposed formation of hemiaminal **H2**. Proton monitored for kinetics analysis are marked. **(b)** Stacked NMR spectra, with monitored proton environments highlighted. **(c)** Kinetics plot showing degradation of the cyclization spacer and PEtG backbone. **(d)** Kinetics plot showing formation of DMI, EtGH and putative hemiaminal **H2**. Normalized relative integrals of EtGH and **H2** were computed by subtracting integral values at $t = 0$ (time that *in situ* NMR heating was started) to zero the datasets, then dividing both sets of raw integrals by 50 (i.e., the DP of the PEtG backbone) to allow direct comparison with the amount of DMI formed (whose raw integral was divided by 4 for normalization). The sum of EtGH and **H2** relative integrals agrees with the integrals of DMI, indicating that EtG liberated during depolymerization is converted predominantly into these products.

S10. Auxiliary Discussion: Hemiaminal Formation

Self-immolation data of polymers **P4a-b** and **P5** revealed that diamine cyclization was slow relative to the model compounds, and that depolymerization was incomplete for **P5**. To explain these observations, we propose that the deprotected cyclization spacer (a secondary amine) can react with ethyl glyoxylate liberated from depolymerization, forming a hemiaminal-capped polymer, **H2**, that cannot undergo diamine cyclization (Figure S73). In the case of **P4a-b**, which were depolymerized under basic conditions (morpholine, 10 equiv.), morpholine competes with the deprotected diamine spacer to form **H1**. This results in reversible end-group passivation that slows depolymerization but does not halt it completely. In the case of **P5**, which was depolymerized without morpholine present, hemiaminal formation would be irreversible and thereby prevent complete depolymerization.

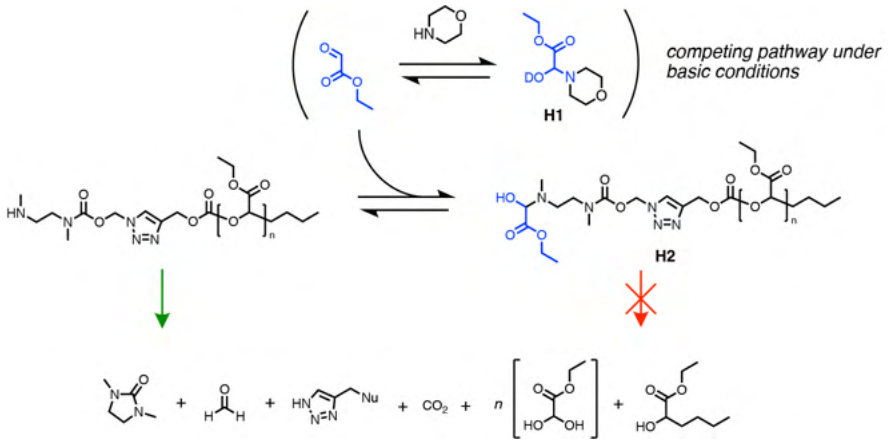

Figure S73. Proposed passivation mechanism whereby the deprotected diamine spacer is converted to a hemiaminal species (**H2**) that cannot self-immolate. For **P4a-b**, morpholine competes with the deprotected diamine for ethyl glyoxylate, forming hemiaminal **H1**. By contrast, self-immolation data for **P5** demonstrates that passivation is non-reversible in the absence of base, resulting in more substantial rate attenuation and incomplete depolymerization.

S10.1. Characterization of hemiaminal H1

Following self-immolation, NMR spectra of **P4a-b** showed a consistent peak at 4.5 ppm that we have ascribed to hemiaminal **H1**. To confirm this assignment, oligo(ethyl glyoxylate)[‡] (32 mg, 0.32 µmol) was equilibrated in DMSO-d_6/D_2O (9:1 *v*/*v*, 450 µL) at 65 °C for 15 min, then was treated with morpholine (28 mg, 0.32 µmol) and the reaction mixture heated at 65 °C for 1 h. NMR analysis of the reaction mixture revealed a presence of a peak 4.5 ppm (Figure S74b) in perfect agreement with the peak assigned to **H1** in the self-immolation experiments (Figure S74c). 1D selective NOESY experiments further support the assignment of **H1** (Figure S75). Attempts to further analyze **H1** by mass spectrometry were unsuccessful due to difficulty extracting it from the reaction mixture.

[‡] Oligo(ethyl glyoxylate) was obtained by removal of toluene from commercially available ethyl glyoxylate in toluene (50 wt% solution) by rotary evaporation. The resulting colorless liquid was used without further purification.

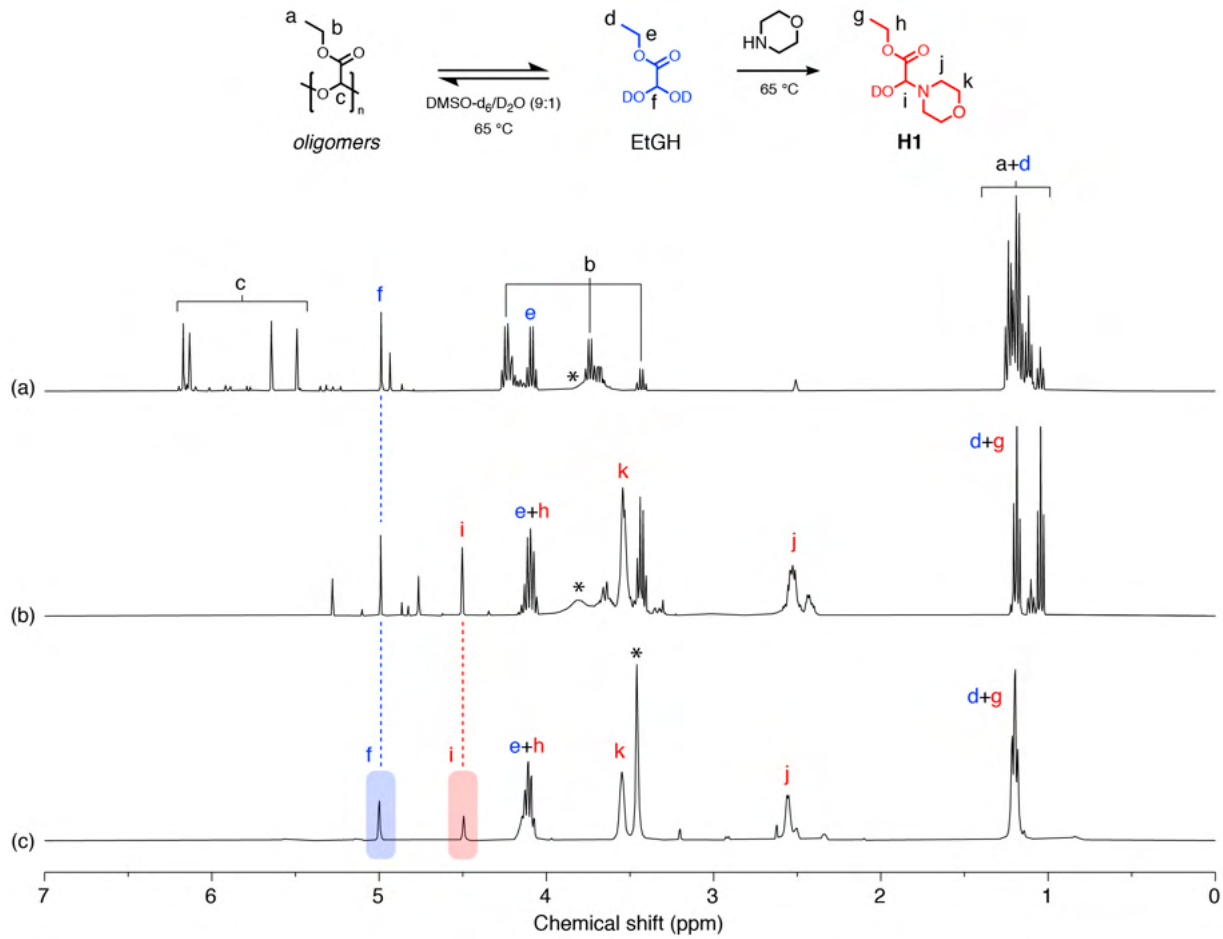

Figure S74. ^{1}H NMR spectra showing formation of hemiaminal **H1** during self-immolation of **P4a-b** (400 MHz, DMSO-d_6/D_2O = 9:1, 300 K). Scheme summarizes the reaction conditions corresponding to spectra (a) and (b). Critically, the presence of H_i in spectra (b) and (c) supports the formation of **H1** as a common species; **(a)** Spectrum of oligo(ethyl glyoxylate) in DMSO-d_6/D_2O following heating at 65 °C for 15 min; **(b)** Spectrum of the same reaction mixture after addition of morpholine and heating at 65 °C for 1 h. Key environments are labelled on the spectrum; **(c)** Representative spectrum of **P4a** following self-immolation (10 h timepoint).

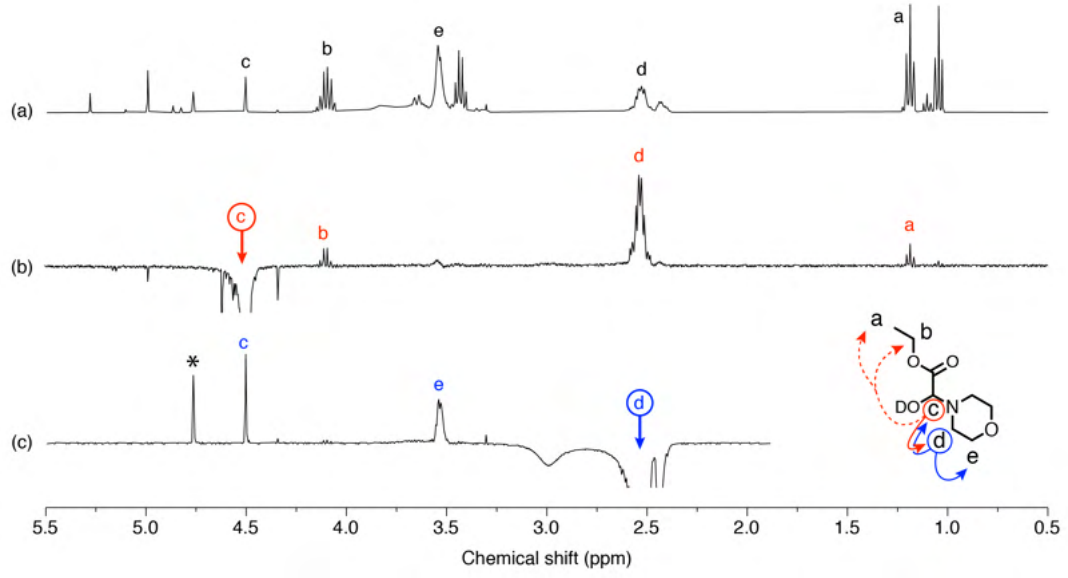

Figure S75. 1D selective ^{1}H NOESY analysis (400 MHz, DMSO-d_6/D_2O = 9:1, 300 K; T_{mix} = 400 ms) of the reaction mixture shown in Figure S74b, which supports the assignment of hemiaminal **H1**. Encircled letters denote the selectively irradiated peaks; **(a)** ^{1}H NMR spectrum of the reaction mixture; **(b)** and **(c)** 1D selective NOESY spectra.

S10.2. Characterization of hemiaminal H2

The NMR spectrum of self-immolated **P5** also showed small peaks ~4.55 ppm, which are ascribed to the formation of hemiaminal **H2**. To test this hypothesis, a sample of oligo(ethyl glyoxylate) (38 mg, 0.37 µmol) was equilibrated in DMSO-d_6/D_2O (9:1 *v*/*v*, 450 µL) at 65 °C for 15 min, then *N*,*N*′-dimethylethylene diamine (19 mg, 0.21 µmol) was added and the reaction mixture heated at 65 °C for 1 h. NMR analysis of the reaction mixture revealed a presence of a peak ~4.55 ppm (Figure S76b) that was also present in the spectrum of fully self-immolated **P5** (Figure S76c). This supports the formation of putative hemiaminal **H2**. Attempts to further analyze **H2** by mass spectrometry were unsuccessful due to difficulty extracting it from the reaction mixture.

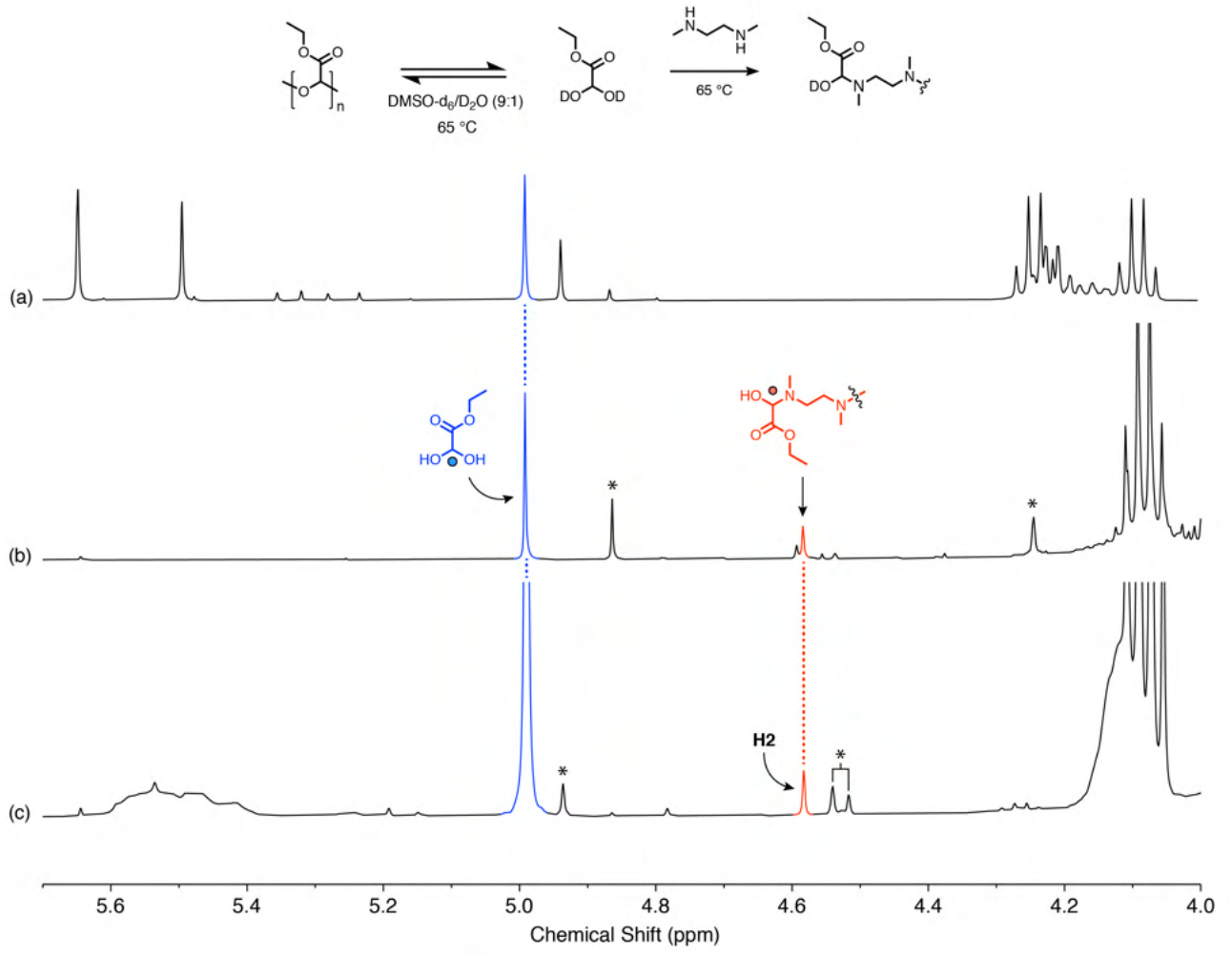

Figure S76. ^{1}H NMR data showing the proposed passivation of the unprotected diamine spacer with ethyl glyoxylate (400 MHz, DMSO-d_6/D_2O = 9:1, 300 K). Scheme shows the expected reaction between oligo(ethyl glyoxylate)/ethyl glyoxylate hydrate and *N*,*N*′-dimethylethylene diamine; **(a)** Spectrum of oligo(ethyl glyoxylate) in DMSO-d_6/D_2O following heating at 65 °C for 15 min; **(b)** Spectrum of the same reaction mixture after addition of *N*,*N*′-dimethylethylene diamine and heating at 65 °C for 1 h; **(c)** Representative spectrum of **P5** following self-immolation (>12 h timepoint). Asterisks denote unidentified peaks that might correspond to related aldehyde hydrate and hemiaminal species.

S11. References

[1] A. Rabiee Kenaree, E. R. Gillies, *Macromolecules* **2018**, *51*, 5501-5510.

[2] W. L. F. Armarego, C. Chai, *Purification of Laboratory Chemicals*, 6th ed., Butterworth-Heinemann, Oxford, UK, **2009**.

[3] D. A. Roberts, B. S. Pilgrim, T. N. Dell, M. M. Stevens, *Chem. Sci.* **2020**, *11*, 3713-3718.

[4] E. Tayama, R. Hashimoto, *Tetrahedron Letters* **2007**, *48*, 7950-7952.

[5] T. N. Forder, P. G. Maschmeyer, H. Zeng, D. A. Roberts, *Chem. Asian J.* **2021**, *16*, 287-291.

[6] a) Y. Ma, X. Jiang, R. Zhuo, *J. Polym. Sci. A.* **2013**, *51*, 3917-3924; b) G. Zhang, Y. Zhang, Y. Chu, Y. Ma, R. Zhuo, X. Jiang, *J. Polym. Sci. A.* **2015**, *53*, 1296-1303.

[7] A. Warnecke, F. Kratz, *J. Org. Chem.* **2008**, *73*, 1546-1552.